DEGRADATION STUDIES OF CARBAMAZEPINE AND ESCHERICHIA COLI IN WASTEWATER USING A NON-THERMAL ELECTRICAL DISCHARGE REACTOR

By

Emmanuel Gwanzura

Bachelor of Engineering (Honours)(Chemical)

National University of Science and Technology, Zimbabwe

Submitted in fulfilment of the academic requirements for the degree of Master of Science in Engineering (Chemical) in the School of Engineering; College of Agriculture, Engineering and Science; University of KwaZulu-Natal, Durban, South Africa.

April 2021

Supervisor: Dr. S. A. Iwarere

Co-supervisor: Professor D. Ramjugernath

DECLARATION

This dissertation constitutes my master's research, undertaken in the Thermodynamics Research Unit, School of Engineering, at the University of KwaZulu-Natal, Durban from August 2018 to November 2020 under the supervision of Dr. S. A. Iwarere and Professor D. Ramjugernath.

I declare that:

i. This dissertation, except where otherwise indicated, is my original work.
ii. This thesis has not been submitted for any degree or examination at any other university.
iii. This thesis does not contain other persons' data, pictures, graphs or other information, unless specifically acknowledged as being sourced from other persons.
iv. The written expressions are in my own words, and where other written sources have been quoted, then:
(a) their words have been re-written, but the general information attributed to them has been referenced;
(b) where their exact words have been used, their writing has been placed inside quotation marks, and referenced.

_____ _____

E. Gwanzura Date

As the candidate's supervisors, we approved this thesis for submission.

_____ _____

Dr. S. A. Iwarere Date

_____ _____

Professor D. Ramjugernath Date

ACKNOWLEDGEMENT

This work is a product of the input of several individuals, departments, and institutions. Many thanks to the following:

- The Water Research Commission for funding the research project.
- My supervisor, Dr. S. A. Iwarere. Thank you for the effort and support you put into this work and for sharing knowledge and opportunities with me. Working with you positively changed my perspective on many things.
- My co-supervisor, Professor D. Ramjugernath. Every time we discussed my work, you always had that 'constructive expert perspective,' which made my work much better. Thank you so much.
- The laboratory technician, Ayanda Khanyile. Ayanda, your help and patience in the fourth-floor laboratory was invaluable.
- The department technical staff, Danny Padayachee and Sanjay Deeraj. Thank you for the work you put in the machining, modifications, and troubleshooting of my equipment.
- The Microscopy and Microanalysis Unit (MMU), Vishal Bharuth. Thank you for the analysis of my samples and input on how to better my experimental procedure to provide better results through visual imaging.
- The Institute of Water and Wastewater Technology staff members, Dr. O. O. Awolusi and Dr. S. Kumari Pillai. Thank you for the invaluable expert knowledge of the microbiology aspects of my work.
- Dr. Adeyinka, your assistance with GC-MS was priceless.
- Family and friends, your support and encouragement gave me the strength to push to the end.

LIST OF CONFERENCES

Parts of this work were presented at the following formal meetings and conferences:

Gwanzura, E., Iwarere, S. A., Ramjugernath, D. Inactivation of pathogens in treated wastewater using non-thermal plasma. Young Water Professional Conference 2019, Durban ICC, (SOUTH AFRICA), 20 – 22 October 2019.

Gwanzura, E., Iwarere, S. A., Ramjugernath, D. Plasma: A novel way of water disinfection. College of Agriculture, Engineering, and Science Postgraduate Research Innovation Symposium (PRIS), UKZN, Westville Campus, Durban, (SOUTH AFRICA), 17 October 2019.

Gwanzura, E., Iwarere, S. A., Awolusi, O., Kumari, S., Ramjugernath, D. Plasma: A novel way of water disinfection. South African Institute of Chemical Engineers KZN Research Day, Mangosuthu University of Technology (MUT), (SOUTH AFRICA), 28 August 2019.

Gwanzura, E., Iwarere, S. A., Awolusi, O., Kumari, S., Ramjugernath, D. Point-to-plane liquid phase plasma discharge with copper electrode for Escherichia coli inactivation in water [3 pages]. Proceedings of the 24th International Symposium on Plasma Chemistry (ISPC 24), Naples (ITALY), June 9 – June 14, 2019. [Full-manuscript, peer reviewed].

ABSTRACT

Over the last 30 years, there has been increasing detection of emerging chemical pollutants and biological contaminants in the aquatic environment. As Wastewater Treatment Plants (WWTP) are considered the primary gateway for chemical and biological contaminants into water bodies, it can be inferred that WWTP in their current configuration are ineffective against the emerging contaminants. Therefore, it is imperative to investigate new technologies capable of removing emerging chemical and biological contaminants. With this background, Advanced Oxidation Processes (AOP) are a candidate technology that can be utilised for wastewater remediation.

This study explores the potential application of an AOP electrohydraulic discharge as a non-conventional tertiary stage technology for the inactivation of *Escherichia coli* (ATCC 25922) (*E. coli*) and degradation of carbamazepine (CBZ) as representative contaminants in wastewater. A reactor geometry with vertical copper electrodes with a 2 mm electrode gap in a point-to-plane configuration, connected in negative polarity to a high voltage direct current power supply, was utilised. Separate semi-batch studies were conducted for *E. coli* and CBZ. All the experiments were conducted using synthetic wastewater.

For the *E. coli* studies, the effects of the electrode gap on the electric discharge, the influence of initial bacterial density, copper electrode material on bacterial inactivation were investigated. The target treatment criterion in the study was the total bacterial inactivation of *E. coli*. For an electrode gap of 2 mm, total inactivation for *E. coli* cell density ranging from 3.96×10^4 to 2.5×10^7 CFU/mL was achieved in 180 seconds. Short inactivation times can probably be attributed to the synergy of shockwaves, radicals, and Ultraviolet radiation within the reactor. Control reactor experiments confirmed the anti-bacterial properties of the copper ions in solution. However, bacteria inactivation can be attributed primarily to plasma discharges in water due to the observed higher inactivation in plasma-treated cells. For example, at 3.96×10^4 CFU/mL initial *E. coli* density, 4.5 log reduction by plasma treatment was observed at 180 seconds compared to 1.7 log reduction in 300 seconds for copper control. The bacterial cell walls were damaged by plasma treatment as observed for plasma-treated cells through the Scanning Electron Microscope imaging. Thus, the destruction of the cell wall can be proposed as one of the possibly numerous contributing mechanisms resulting in *E. coli* inactivation by plasma. In preliminary benchmarking against chlorination and ozonation, the electrohydraulic discharge reactor used in this study had considerably higher treatment costs per cubic metre of wastewater.

For CBZ degradation, discharge current, air flow rate, and initial concentration were investigated, with removal efficiency and energy consumption being the response variables. CBZ degradation experiments utilised Liquid-liquid chromatography for extraction followed by GC-FID and GC-MS for quantitative

and qualitative analysis, respectively. Discharge current, air flow rate, and initial concentration all influenced the removal efficiency to different degrees. However, for energy consumption, only current and air flow rate were significant variables. The highest removal efficiency obtained was 93% ± 4% for 10 and 40 mg/L initial CBZ concentration after 10 minutes of plasma treatment at a current of 0.45 A and no air flow rate. The high removal efficiency could be attributed to higher currents (0.45 A), resulting in an improved generation of highly reactive and high energy species and UV generation. Additionally, no air could also improve discharge stability resulting in an uninterrupted discharge. The experimental setup and plasma reactor used in this study show a prospect for sectors where the concentration level of the contaminants in the effluent is above 10 mg/L based on the investigations carried out within the context of this research. Treatment cost per cubic metre benchmarking of the reactor against established technologies revealed that the reactor still requires significant optimisation.

The research on the reactor demonstrated its capability to treat high chemical and biological contaminants in wastewater with possible applications being in pre-concentrated wastewater remediation. However, there is still room for optimisation. One key area of focus being reducing treatment cost, which may be achieved theoretically, pending further experimental investigation, by the introduction of an AC power supply.

Contents

LIST OF FIGURES

LIST OF TABLES

NOMENCLATURE

Abbreviations

AC	Alternating Current
CBZ	Carbamazepine
DBD	Dielectric Barrier Discharge
DC	Direct Current
E. coli	*Escherichia coli* (ATCC 25922)
ESSWW	*E. coli* spiked synthetic wastewater
ETEC	Enterotoxigenic *Escherichia coli*
GC	Gas Chromatograph
GC-FID	Gas Chromatograph-Flame Ionisation Detector
GC-MS	Gas Chromatograph-Mass Spectrometer
LB	Luria-Bertani broth
NF	Nano Filtration
NTP	Non-Thermal Plasma
PBS	Phosphate-buffered saline
R&D	Research and Development
RO	Reverse Osmosis
SEM	Scanning Electron Microscope
STEC	Shiga toxin-producing *Escherichia coli*
NG	No growth
TRU	Thermodynamics Research Unit
UKZN	University of KwaZulu Natal
UV	Ultraviolet
WRF	White Rot Fungi
WWTP	Wastewater Treatment Plant

Symbols

A	Ampere
E_a	Activation energy
eV	Electron volt
K	Kelvin
E_{EO}	Electrical energy per order
^oC	Degrees Celsius

Chapter One

Introduction

1.1 Research background

Globally, partially treated wastewater is a major cause in polluting aquatic water as 80% of wastewater is released to the environment partially treated (Guppy and Anderson, 2017). In South Africa, less than 10% of the more than 800 wastewater treatment plants (WWTP) comply with international benchmarks and standards in terms of the WWTP effluent they discharge into the environment (Batmen, 2010, Mema, 2010, Herbig and Meissner, 2019). This 'unhealthy situation' is in contravention of the South African regulatory framework (Department of Water Affairs, 2013). To add to this already unsustainable situation, the majority of conventional WWTP are not fully equipped to deal with emerging recalcitrant chemical pollutants and waterborne pathogens (Alvarino et al., 2018).

The utilisation of Non-Thermal Plasma (NTP) technology to complement conventional WWTP might be a viable solution for the treatment of emerging recalcitrant chemical pollutants and waterborne pathogens in wastewater, especially in the tertiary treatment stage. Additionally, NTP wastewater treatment systems have the potential to operate economically for very concentrated wastewater streams if optimised (Krause et al., 2011). In the context of wastewater treatment, NTP is generated by strong electric fields between electrodes, which initiate electrical discharges in the water (direct/electrohydraulic discharge) or on the water surface (indirect discharge). The NTP produces oxidising radicals, active species, ultraviolet (UV) radiation, and shockwaves, which inactivate pathogens and degrade chemical pollutants (Jiang et al., 2014).

This research work focuses on the application of atmospheric pressure NTP for wastewater treatment. It should be emphasised from the onset that this research work does not propose replacing the existing WWTP, but rather retrofitting NTP units, especially in the tertiary stage of treatment, to complement existing WWTPs' shortcomings.

1.2 Research problem

Based on existing literature at the time of this writing, the development of a single plasma unit that is capable of treating waterborne pathogens and recalcitrant chemical pollutants in wastewater is yet to be pursued.

There has been considerable research work on the use of NTP for wastewater treatment. Commercial NTP units are already on the market, for example, the Flowrox Corona launched by Flowrox^{TM} in

November 2019. However, the laboratory scale and commercial units are reported to be able to treat either chemical or biological pollutants but not both.

1.3 Wastewater contaminants

In the aquatic environment, partially treated sewage water poses a threat to public health as the water may be used for recreational or agricultural purposes. Industrial wastewater is characterised to contain chemical pollutants which are associated with non-communicable diseases. On the other hand, urban wastewater, usually treated at the municipal level, is associated with infectious diseases due to the presence of pathogens (Xiao et al., 2018). Conventional pollutants are wastewater contaminants which can effectively be treated by a municipal WWTP, for example, oil and grease, total suspended solids and faecal coliforms (Department of Water Affairs, 2013).

A brief discussion of the wastewater contaminants, showing how the choice of the specific representative contaminants used in this study was derived, is given herein.

1.3.1 Chemical contaminants

Conventional pollutants have a strong and enforceable regulatory framework; hence WWTPs have been optimised to treat wastewater with conventional pollutants. However, micropollutants are poorly regulated (Hai et al., 2018). Micropollutant specific literature in wastewater in the environment is incongruent as it spans numerous and unrelated disciplines (Daughton, 2001). The literature on micropollutants is, therefore, more challenging to locate and critique holistically as compared to conventional pollutant literature. Additionally, although the occurrence of micropollutants is in the µg/L – ng/L range, there is a general lack of information about the toxicity of micropollutants to the environment, human and aquatic health, hence the lack of a robust regulation framework (Verlicchi et al., 2010, Wardenier et al., 2016).

Population growth and improved standards of living have resulted in increased industrial production of anthropogenic inorganic pesticides, plasticisers, pharmaceuticals. The increasing numbers of publications on micropollutants show that researchers have been paying increasing attention to these emerging pollutants as they are being detected in WWTPs effluent, surface water, drinking water, and groundwater (Juhler and Felding, 2003, Schwarzenbach et al., 2006, Kong et al., 2016). The micropollutants and their bioactive metabolites can be continually introduced to the aquatic environment as complex mixtures via several routes but primarily through both untreated and treated sewage.

Carbamazepine (CBZ) was selected as a representative micropollutant in the experimental work in this study. CBZ is widely used in the medical field as an orally administered drug to manage epilepsy, bipolar disorders and stabilise moods (Arye et al., 2011). CBZ is mainly introduced into wastewater by the excretions of individuals who use CBZ to manage various medical conditions. It is essential to ensure that the presence of CBZ in the aquatic environment is minimised as CBZ is a recalcitrant pollutant and the unregulated consumption of CBZ has the potential to disrupt the production of red blood cells and platelets (Wanda et al., 2017). CBZ has an interestingly odd characteristic of higher concentration in WWTP effluent than in the influent in some WWTP (Clara et al., 2004, Vieno et al., 2007). This property of increased concentration in the WWTP effluent exhibits the general ineffectiveness of conventional WWTP to degrade CBZ. There is, therefore, the need for complementary treatment technologies for CBZ in wastewater.

1.3.2 Microbiological contaminants

Water is a perfect medium for the growth of a wide range of species of microorganisms. Some of these microorganisms may be found naturally in the water supply. The majority of microorganisms in the water are not problematic for humans, as some can be harnessed. An excellent example of the beneficial utilisation of microorganisms is the use of certain strains of yeasts to produce beer and bread (Bokulich and Bamforth, 2013, Ijah et al., 2014). Furthermore, the growth of specific bacterial strains in contaminated water can treat the water as they help degrade the contaminants in the wastewater. Nevertheless, the presence of other disease-causing microbes, commonly referred to as pathogens, is harmful and in some instances, life-threatening. Waterborne pathogens can be viruses, bacteria, protozoa, algae and parasitic worms.

Pathogens in wastewater are a concern as the wastewater, if not adequately treated, will, in turn, introduce the pathogens into fresh and drinking water sources. Ultimately, this presents the risk of exposure to other living organisms.

In this study, *Escherichia coli* (ATCC 25922) was selected as the representative waterborne pathogen utilised in all experimental work. Going forward in this work, *Escherichia coli* (ATCC 25922) will be shortened to *E. coli*, *Escherichia coli* will mean the broad bacterial *Escherichia coli* family, while specific *Escherichia coli* bacterial strains will be specified. *E. coli* was chosen for safety and health reasons in the research. *E. coli* is classified as Biosafety Level 1 Agent meaning it does not cause disease in healthy humans. The decontamination of surfaces and workspaces with bleach (cheap and readily available) is sufficient. The choice of *E. coli* as a waterborne microorganism in this study is also supported but the fact that even in the 21st century, *Escherichia coli* related outbreaks are being reported, the most recent being the 2015 United States *E. coli* O157:H7 outbreak and the 2011 German

E. coli O104:H4 outbreak. *Escherichia coli* is a high health significance pathogen (heath significance relates to the severity and frequency with outbreaks). *Escherichia coli* are microbes of interest.

1.4 Aim and objectives

Based on the background above, there is an impetus to create a hybrid prototype plasma reactor which utilises the synergy of the chemically active species, shock waves and UV light produced by NTP to inactivate waterborne pathogens and degrade chemical pollutants in wastewater. Within the application area of wastewater, this research aims to modify a non-thermal electrical discharge reactor for CBZ degradation and *E. coli* inactivation as model contaminants in wastewater at atmospheric pressure.

The objectives of the study, which will enable accomplishment of the aim are detailed below as:

1.4.1 Reactor modification

In the context of this work, the first electrical discharge NTP prototype for wastewater treatment was designed and built in the Thermodynamics Research Unit (TRU) in 2017. This reactor unit was utilised for phenol spiked wastewater treatment investigations in 2018. Based on the recommendation of work with the first prototype, the starting point of this work was the modification of the certain accessories and electrode configuration for a new reactor design to a make a larger reactor for the treatment of chemical and biological synthetic wastewater.

1.4.2 System assessment for recalcitrant CBZ degradation

The reactor system was assessed using removal efficiency and electrical energy consumption in treating CBZ spiked synthetic wastewater. System optimisation based on the experimental results was carried out to assess the capabilities of the reactor within the specified operational limitations.

1.4.3 Evaluation of *E. coli* inactivation

The reactor was evaluated in terms of its inactivation ability against *E. coli* as a representative waterborne pathogen in *E. coli* spiked synthetic wastewater (ESSWW). Total inactivation of the *E. coli* bacteria was the acceptable treatment criteria set for the study.

1.5 Scope and limitations

NTP in the context of wastewater treatment is a multidisciplinary specialist subject. This work focused on NTP in wastewater treatment from a Chemical Engineering perspective, focusing on the design, construction, and operation of processes.

The in-depth analysis of the following will not be part of this work:

- The microbiology of the *E. coli*;
- The physics of the plasma propagation;
- The chemistry of CBZ and CBZ degradation.

However, relevant aspects and core concepts from other fields were discussed where applicable.

1.6 Dissertation structure

The dissertation is structured as chapters. Below is a summary of the chapter content.

Chapter one introduces the thesis by giving a background of the field of study and justification for the contaminants selected for the study. The aim and objectives of the study are then presented and expanded.

Chapter two discusses the literature related to atmospheric pressure NTP technology in relation to the objectives. The review will focus on the treatment of the chosen contaminants, namely CBZ and *E. coli* in the larger context of wastewater then specifically in relation to atmospheric pressure NTP technology.

Chapter three details the first NTP prototype and the modifications incorporated into the NTP reactor utilised in this work. The experimental setup and procedure for CBZ degradation and the *E. coli* inactivation are detailed separately in this chapter.

The results and discussion of this work are divided into chapters four and five. Chapter four presents the result and discussion of the experimental results of CBZ wastewater treatment and the system optimisation for CBZ discussion. Chapter five presents the result and discussion of the experimental results of the E. coli inactivation.

Chapter six provides a conclusion of the work as it links the contribution of the experimental work and the results towards attaining the research objectives. The recommendations of the study are also included in this chapter.

1.7 Conclusion

There is an emerging class of chemical and biological wastewater contaminants which cannot be effectively treated by conventional WWTPs. While these emerging biological and chemical pollutants may not be regulated at the moments, it is imperative to invest in technologies which complement existing WWTPs to treat the contaminants. In this regard, the aim of this work is the utilisation of plasma technology in investigating the degradation of a recalcitrant chemical pollutant (CBZ) and a common pathogen responsible for disease outbreaks (*Escherichia coli*) as a possible alternative technology which can complement conventional WWTP in addressing the problematic contaminants of the 21st century.

The next chapter discusses literature central to this work and presents background information on key aspects that informed this study.

Chapter Two

Literature review

2.1 Introduction

Plasma describes a fully or partially ionised gas system consisting of a concentration of free positively and negatively charged species, for example, positive ions, negative ions, and electrons (Piel, 2017). If a plasma system is partially ionised it will contain molecules, neutral atoms, radicals and excited species. The charged particles in plasma systems are responsible for the electrical conductivity properties. Classical/thermal plasma systems are characterised by the higher mean kinetic energy of the charged particles (1 - 10^5 eV) compared to the NTP system. Plasmas on earth can be generated by the input of vast amounts of energy (thermal, beams, radiation and electric field). In nature, lightning and the stars are the most visible and everyday examples of plasmas.

Plasma systems can be categorised into thermal plasma and NTP. Thermal plasmas, as the name implies, operates at high temperatures of 10^3 - 10^4 K and are characterised by a thermal equilibrium of the gas and the ions of the plasma. However, NTP is characterised by charged particles (ions and electrons) at temperatures of more than 10^4 K and gas at less than 10^2 K, the charged particles and the gas are not in thermal equilibrium.

The motivation to utilise NTP is the high ion temperature of 10^4 – 10^5 K (approximately 1–10 eV mean energy); therefore, reaction with high activation energy (E_a) can be realised. For example, the effective ozone generation process is possible only under NTP conditions (Malik et al., 2001b). Additionally, because the bulk of the operation liquid maintains a relatively low temperature, there is little need for specialised materials of construction and very advanced process control for NTP application.

NTP reactors are often operated at low pressure conditions which require expensive vacuum techniques. The current trend globally is to develop atmospheric pressure NTP systems to enhance economic feasibility (Mechsner et al., 2013).

2.2 Electric discharges in relation to wastewater treatment

The intuitive first step when discussing technology is to present its merits. The summarised key merit points for the NTP electrohydraulic discharge (discharges that occur within the water body) in the wastewater field are:

- Electrical discharges produce multiple types of high energy and highly reactive chemical species *in situ;* thus, the need for chemical addition and specialised dosing equipment is eliminated. Additionally, UV light and shock waves are produced during the electrical discharge. The synergy of the UV, shockwaves, supercritical conditions and the produced highly reactive chemical species enhance wastewater treatment (Mozgina et al., 2009);
- The control of the produced reactive species can be achieved through the adjustment of gas/liquid flow rates, and applied energy, which enhances process control as the quantity of the reactive species produced can be adjusted to fit the wastewater contaminant concentration fluctuations and;
- Electrode materials can be selected to catalyse the treatment process; for example, silver electrodes can assist in pathogen inactivation since silver is known to have anti-microbial properties (Adnan, 2019).

2.2.1 Electric discharge reactor types

In wastewater treatment, there are numerous NTP reactor configurations. However, three NTP reactor configurations are repeatedly reported, namely the glow discharge, pulsed corona discharge and dielectric barrier discharge (DBD).

2.2.1.1 Glow discharge

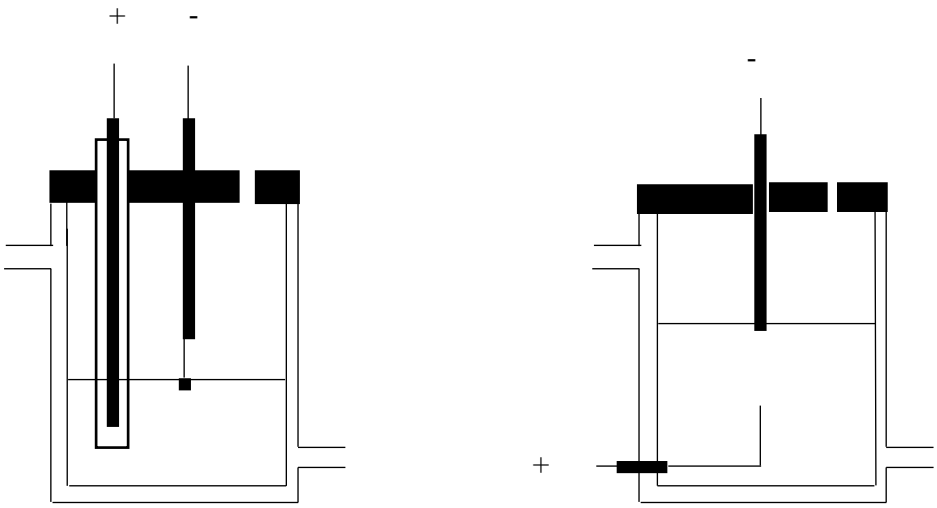

Figure 2.1 Glow discharge reactor configurations at atmospheric pressure (extracted from Gao, 2006)

Figure 2.1 illustrates two common glow discharge geometries showing different electrode configurations. One electrode usually just touches the water surface while the other electrode is submerged in the water.

The reactor gets its name from the glow which appears when the reactor is operational. The glow is the plasma. The glow discharge has predominately been utilised for chemical contaminant degradation. The contact glow discharge has been reported to be effective in the treatment of aromatics, trichloroacetic acid, alkyl benzene sulfonates, ionic liquids and dyes (Amano and Tezuka, 2006, Gupta, 2017). Pathogen related research using the contact glow, though limited, has been reported (Motyka et al., 2018).

The glow discharge uses continuous direct current (DC). The anode is usually a wire positioned to just touch the wastewater surface. The DC voltage is usually less than 1 kV. The cathode will be submerged and enclosed in a porous glass (Gao, 2006). When the circuit is completed, vapour forms at the anode. The current flows from the anode through the conductive vapour to the cathode. All the charged species in the plasma vapour are accelerated by the potential difference between the electrodes and impart kinetic energy which can be as high as 100 eV (Malik et al., 2001b).

The key distinguishing characteristic between glow discharges and DBD and pulsed corona discharges is the heating characteristic of the glow discharge hence it can be termed hot plasma. The DBD and pulsed corona discharges do not exhibit the heating characteristic because only the free electrons gain high energy and all other heavier ions maintain close to ambient air temperature hence the name cold plasma.

2.2.1.2 Dielectric Barrier Discharges

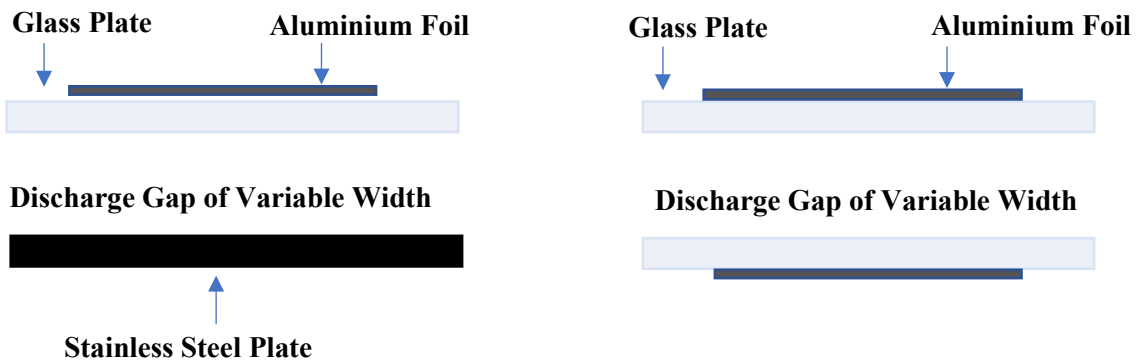

Figure 2.2 Possible DBD electrode configuration showing possible electrode material (Adapted from Yehai, 2016)

Figure 2.2 shows a 2D representation of two possible DBD configuration comprises of parallel electrodes using glass as a possible dielectric. The electrodes can be fabricated of the same material or different material can be used as the electrode material.

The electric plasma discharge occurs between the parallel electrodes. One or both electrodes is usually covered by a thin dielectric material, such as quartz (Eliasson et al., 1987, Mouele et al., 2015). DBD

utilise AC power supply. DBD dominantly produce electrons as the charged particles due to the short AC induced micro-discharges. The electrons which are accelerated under the potential difference ionise the ambient gas. The result is a chain reaction which produces more charged particles, radicals and ions which are responsible for pollutant degradation (Malik et al., 2001b). Streamers may be produced if there is repeated electron-induced ionisation of the gas (Yehia, 2016).

One limitation which the DBD shares with the glow discharge configuration are that the electrical discharges are in the gas phase or close to the water surface hence there is low diffusion of the active species into the water bulk (Foster, 2017).

The merit of the DBD electric discharge is that it is safer to work with as the configuration averts the development of localised spark or arc discharges and it has a large plasma zone. However, there are still a lot of technical and economic challenges, for example, higher energy input which has not yet been satisfactorily solved.

2.2.1.3 Pulsed Corona Discharges

There are various types of corona discharges; however, the dominant type in wastewater treatment is the pulsed corona discharge.

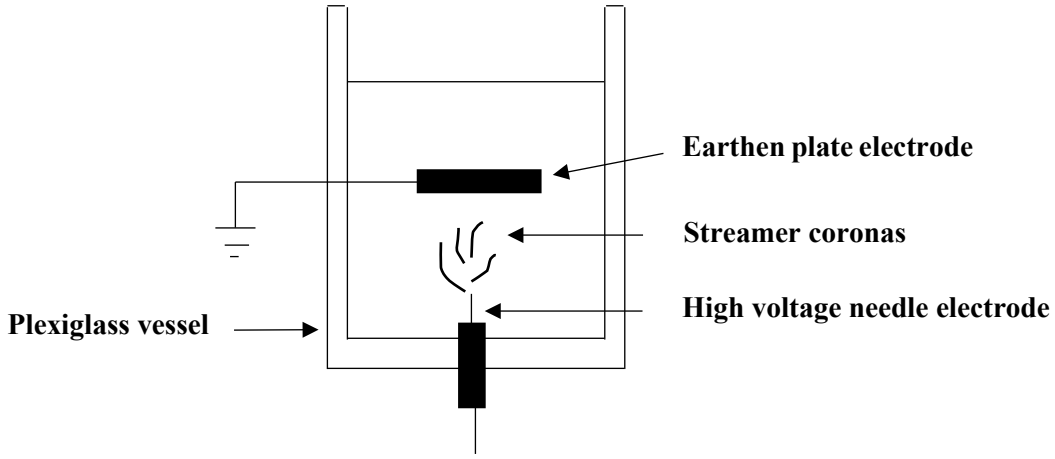

Figure 2.3 Pulsed Corona needle and plate type reactor

Figure 2.3 shows the dominant reactor configuration, a needle–plate arrangement where the plate is grounded, and the needle is attached to the high-voltage terminal.

Pulsed corona discharges are electrohydraulic discharges, thus differentiating them from glow and DBD discharges (Locke et al., 2006). Pulsed corona discharge reactor utilises a pulse generator based on the discharge of a capacitor on a low-inductance circuit through a spark gap switch (Grekhov et al., 1997, Smulders et al., 1998). To increase the intensity of the electric field in a needle-plate configuration, only the tip of the needle is exposed. A variant configuration is the wire–cylinder (or coaxial) which has the

advantage that larger volumes of water can be exposed to the electric discharge and hence the wire-cylinder configuration is easier to scale up (Sunka et al., 1999).

Similar to the DBD, the pulsed corona electric discharge predominantly produces electrons which are accelerated by the potential difference between the electrodes. The accelerating free electrons ionise neutral gas molecules. Free electrons can repeat the process to create an electron avalanche.

The plasma channel temperature can reach 50 000 K and produce UV light and shockwaves. The formation of transient supercritical water characterises pulsed corona discharges due to high pressure and steam in the steam bubbles formed (Locke and Thagard, 2012).

2.2.2 Electrode material of construction

At the core of the NTP unit is the electrode system. Various electrode materials have been used in different systems including copper (Wang, 2017), stainless steel (Gao et al., 2020), silver (Vukusic et al., 2016, Bi Jeon et al., 2020)**.** The electrodes are subjected to extreme temperatures during operation. There are qualifying criteria for the electrode system, namely:

- The electrode system should be able to withstand high temperatures as they are subjected to extreme temperatures.
- The electrodes should resist wear. Electrode wear should be avoided as it adds further contamination, in the form of metal ions, to the wastewater during treatment, and this will defeat the purpose of the treatment process.
- A catalytic electrode material is desirable. An example of electrode catalysis is the enhanced performance of silver electrodes plasmas (Vukusic et al., 2016). More research into electrode catalysis in wastewater should be done as a limited number of studies have investigated the positive or negative contribution of the electrodes in wastewater treatment NTP systems.

2.2.3 NTP discharge chemical species generation

Electrons produced by the electrical discharges are accelerated by the potential difference are which eventually involved in collisions with less energised molecules, species and ions. The main reactions in water which are induced by electrical discharges are listed below (Jiang et al., 2014, Khlyustova et al., 2016, Gharagozalian et al., 2017):

$$e^- + H_2O \rightarrow OH^\bullet + H^\bullet + e^- \qquad Equation\ 2.1$$

$$H_2O \rightarrow OH^\bullet + H^\bullet \qquad Equation\ 2.2$$

$$H_2O \rightarrow \tfrac{1}{2}H_2O_2 + \tfrac{1}{2}H_2 \qquad Equation\ 2.3$$

$$2H_2O \rightarrow H_3O^* + e_{eq}^- + OH^\bullet \qquad Equation\ 2.4$$

$$H^\bullet + O_2 \rightarrow HO_2^\bullet \qquad Equation\ 2.5$$

$$H^\bullet + H_2O_2 \rightarrow H_2O + OH^\bullet \qquad Equation\ 2.6$$

$$OH^\bullet + H_2O_2 \rightarrow H_2O + HO_2^\bullet \qquad Equation\ 2.7$$

$$e_{eq}^- + OH^\bullet \rightarrow OH^- \qquad Equation\ 2.8$$

$$e_{eq}^- + H^\bullet + H_2O \rightarrow OH^- + H_2 \qquad Equation\ 2.9$$

$$e_{eq}^- + H_2O_2 \rightarrow OH^\cdot + OH^- \qquad Equation\ 2.10$$

$$H^\bullet + OH^\bullet \rightarrow H_2O \qquad Equation\ 2.11$$

$$2OH^\bullet \rightarrow H_2O_2 \qquad Equation\ 2.12$$

$$2HO_2^\bullet \rightarrow H_2O_2 + O_2 \qquad Equation\ 2.13$$

$$H^\cdot + HO_2^\bullet \rightarrow H_2O_2 \qquad Equation\ 2.14$$

$$H_3O^+ + OH^- \rightarrow 2H_2O \qquad Equation\ 2.15$$

Where

* denotes a high energy state

$^\bullet$ denotes a radical

The hydroxyl free radical ($OH^\bullet$) plays a dominant in pollutant degradation. Hydrogen peroxide and ozone can oxidize some organic compounds, but their rates of reaction are much slower than that of hydroxyl free radical. The transport mechanisms for the active species depend on where in the plasma system they are produced as depicted in Figure 2.4.

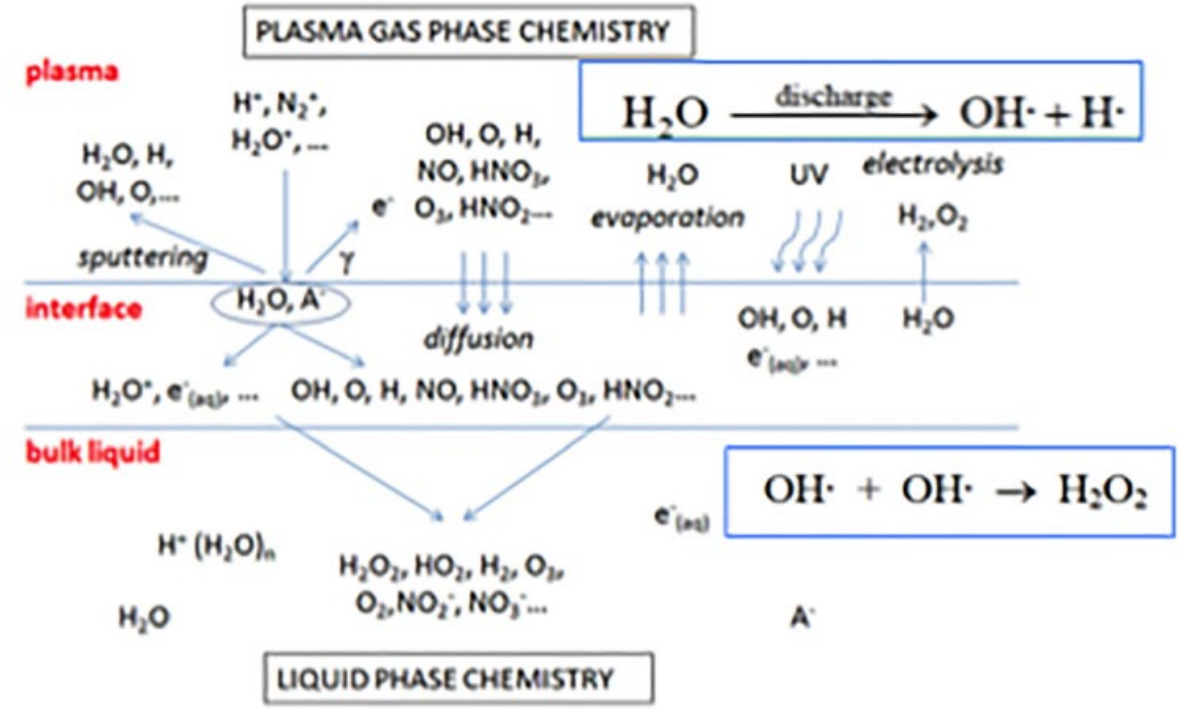

Figure 2.4 Plasma-liquid reactions and phase interactions (Adapted from (Foster et al., 2012))

Figure 2.4 depicts the reactions, species and transport mechanisms of the species. Bulk liquid reactions involve fewer species as the species in the plasma and interface zone have low diffusivities, and some species have short life half-lives in the liquid (Foster et al., 2012).

2.2.4 Electric discharge system comparison

Table 2.1 gives a compressed comparison of different plasma efficiencies to degrade different wastewater contaminants. Table 2.1 can be used as a guide on the various type of Advanced Oxidation Processes (AOPs) to use for a specific contaminant.

Pulsed spark, pulsed arc and gamma-ray plasmas are effective for the treatment of *E. coli* (microorganisms) and CBZ (a compound introduced into wastewater mainly through the urine). However, real wastewater contains numerous other compounds, for example, inorganics. As research is on-going, the ideal plasma unit should be able to degrade other contaminants as real wastewater contains a matrix of contaminants. The best plasma technologies, in terms of removal efficiency, are pulsed spark and arc plasmas as they have the best average score based on their ability to treat a wider variety of contaminants that are present in sewage and industrial wastewater.

Plasma system comparison for chemical pollutants is not limited to removal efficiency only but should consider energy consumption and the degradation by-products for chemical pollutant degradation.

However, evaluating energy consumption is complicated as it has to account for initial contaminant level, water volume treated and set removal efficiency. Different approaches have been proposed by different authors to effectively compare NTP reactor energy consumption, for instance, the Figures of merit and the energy yield (Bolton et al., 1996, Magureanu et al., 2015).

The advantage of the Figure of merit is that they have specific formulas for different contaminant concentration range, making it more specific and accurate as degradation dynamics change with concentration; hence it has been adopted by the International Union of Pure and Applied Chemistry (IUPAC)(Bolton et al., 2001). For CBZ in wastewater (CBZ concentrations less than 100 mg/L), the Figure of merit is used as the electrical energy per order (E_{EO}). E_{EO} is defined as the electrical energy in kWh required to degrade a contaminant by one order of magnitude in 1 m^3 of contaminated water with units of kWh per order per m^3. However, the difficulty with the use of the EEO values is that often, reports lack important details that affect the parameter, making its interpretation misleading and application difficult.

Table 2.1 Comparison of various AOPs for wastewater treatment (Dors, 2013)

Legend	Good	Adequate	Partial	None
	1	2	3	4

	Radiolysis		Gas Discharge		Electrohydraulic Discharges	
	e-beam	Gamma-ray	Corona	Barrier	Pulsed spark	Pulsed arc
Micro-organism	2	1	2	2	1	1
Urine compounds destruction	1	1	3	3	1	1
Oxidising power	1	1	1	1	1	1
Algae destruction	4	4	4	4	3	1
VOCs Destruction	1	2	3	3	1	2
Removal of inorganics	3	3	3	3	2	2

2.3 CBZ and its treatment in wastewater

2.3.1 CBZ characterisation

CBZ and its metabolites micropollutants have low degradability which puts them among the most recalcitrant pharmaceuticals. Several studies even reported higher CBZ concentrations in WWTP effluents than in the influent (Zuehlke et al., 2004, Vieno et al., 2007), this odd CBZ characteristic can be explained by the cleavage of the conjugate CBZ-N-glucuronide (Bahlmann et al., 2014). More than thirty metabolites of CBZ have been identified from human and rat urine (Lertratanangkoon and Horning, 1982), and these are introduced into sewage water.

Table 2.2 details the physicochemical and pharmacological properties of carbamazepine.

Table 2.2 Physicochemical and pharmacological properties of CBZ

Title	Detail	Reference
Structure	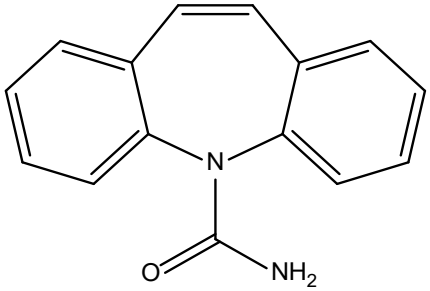	
Chemical formula (CAS No.)	$C_{15}H_{12}N_2O$ (298-46-4)	
Molecular weight	236.2686 g mol^{-1}	
Water solubility	215 mg/L (25 °C)	(Murphy et al., 2002, Borisover et al., 2011)
Log P	2.45	(Yu et al., 2008)
Excretion	72% urine and 28% faeces	(Hai et al., 2018)

2.3.2 Occurrence of CBZ in wastewater

CBZ is universally present in raw wastewater and has been reported to be present in a wide range of concentrations from the high ng/L to low µg/L. The concentration of CBZ in WWTP effluent is highly variable and covers the 30–6300 ng/L range (Petrovic et al., 2009, Jelić et al., 2012, Luo et al., 2014). The fluctuation in the concentration of CBZ in wastewater can be attributed to different drug usage in an area. Conventional WWTP cannot effectively remove CBZ from wastewater or degrade CBZ (Wick et al., 2009, Alvarino et al., 2014). The majority of wastewater treatment technologies applied to CBZ degradation have not performed to satisfaction (Siegrist and Joss, 2012, Zhou et al., 2016).

In South Africa (SA), as in many other countries on different continents, there is no regulation specific to micropollutants, CBZ included, in wastewater effluent which can be discharged despite the fact that wastewater is the source of micropollutants in the aquatic environment. The regulatory framework in place is for micropollutant source, for example, there is regulation for pharmaceutical and pesticide use and disposal but there is no regulation on safe WWTP effluent levels and there is no information on the long-term effect of the micropollutants on the environmental and on the health of humans.

Judging by the increasing number of micropollutant related publications, there has been increasing academic interest on the occurrence of micropollutants in environmental systems such as wastewater (Deblonde et al., 2011), surface water (Luo et al., 2014) and groundwater (Lapworth et al., 2012). An equal increase in interest has been on the performance of conventional treatment technologies for the removal of micropollutants (Bolong et al., 2009, Alexander et al., 2012, Verlicchi et al., 2012).

2.3.3 Existing CBZ treatment technology

Several technologies have been proposed for the treatment and degradation of CBZ in wastewater. CBZ removal in conventional WWTP is usually reported to be less than 20 % (Wardenier et al., 2016). Below are selected technologies and a discussion of why they fail to treat CBZ as well as why effective technologies have not been commercialised.

2.3.3.1 Conventional Activated Sludge

Removal of CBZ by Conventional Activated Sludge (CAS) form WWTP influent ranging from 10 to 1850 ng/L in both aerobic and anaerobic digesters shows negligible removal (Clara et al., 2005, Yan et al., 2014, Subedi and Kannan, 2015). The integration of ultrafiltration or a microfiltration membrane to a CAS process to give MBR also show negligible removal (Hai et al., 2011, Tadkaew et al., 2011). The inadequate removal of CBZ in wastewater is possibly due to its physicochemical properties and the structure induced hydrophobicity which limits removal by sorption to a maximum of 20% (Zhang et al., 2008, Wijekoon et al., 2013). Additionally, the stable structure of CBZ (primary amine) makes it resistant to biodegradation (Wardenier et al., 2016).

2.3.3.2 White Rot Fungi

White Rot Fungi (WRF) has been reported to be effective in degrading recalcitrant micropollutants (Hai et al., 2006, Yang et al., 2013, Asif et al., 2017). The extra and intracellular enzymes of the WRF are the reason WRF is effective in recalcitrant micropollutants, CBZ included. (Golan-Rozen et al., 2011, Margot et al., 2013, Asif et al., 2017). *P. ostreatus* (PC9), a WRF strain, achieved the highest CBZ degradation of 99%, while moderate degradation of around 55% has also been reported (Golan-Rozen et al., 2011, Nguyen et al., 2015). However, WRF operates efficiently under bacteria free sterile

conditions only (Yang et al., 2013, Nguyen et al., 2014). The challenge of maintaining the reactor sterility, particularly in wastewater applications, reduce the feasibility of WRF as a viable technology for CBZ degradation.

Additionally, for all biodegradation process in the WWTP, it was concluded that multi-ring organic compounds, especially those with -withdrawing groups, such as halogens, are extremely difficult for micro-organism to degrade effectively.

2.3.3.3 Reverse osmosis and Nanofiltration

Reverse osmosis (RO) and Nanofiltration (NF) membranes have been reported to retain CBZ effectively, as shown in Table 2.3. A combination of membrane fouling and scaling and expensive operation expenses makes the application of membrane technology not feasible in CBZ removal from wastewater. Also, there is the question of safe disposal of the CBZ cake after it is retained on the membrane. The problem of a safe, viable disposal option for the retained contaminants is also applicable to adsorption on activated carbon (AC).

Table 2.3 CBZ removal from wastewater by RO and NF

Membrane type (pore size)	Removal efficiency (%)	Reference
NF (0.34 nm)	98	(Radjenović et al., 2008)
NF (0.27 nm)	97	(Comerton et al., 2008)
NF (0.84 nm)	74	(Gur-Reznik et al., 2011)
RO (0.34 nm)	98	(Radjenović et al., 2008)
RO	99	(Beier et al., 2010)

2.3.3.4 CBZ Degradation by Advanced Oxidation Processes

AOPs produce highly reactive species, for example, hydroxyl free radical and ozone radicals. Due to the highly reactive species they produce, AOPs are able to degrade CBZ. Ozonation has been shown to be very effective with some researchers reporting 99% degradation (Ternes et al., 2002), however UV systems are only effective in clear water as any turbidity reduces transmittance of the UV radiation. UV system without any complementing system have been reported to be ineffective in CBZ degradation recording degradation as low as less than 5 % (Im et al., 2012, Shirazi et al., 2013, Alharbi et al., 2017).

The addition of hydrogen peroxide or a photocatalyst such as titanium oxide (TiO_2) has been reported to significantly improve the degradation of CBZ (Miklos et al., 2018). The addition of chemicals to improve the degradation efficiency can be problematic specifically in the case of the Fenton's reagent which requires acidic conditions which can only be provided by the addition of more chemicals (Dai et al., 2012). It then becomes a case of adding multiple dangerous pollutants to remove one chemical hence it is not economically and environmentally feasible.

2.3.4 CBZ degradation mechanism by electrical discharge

The interaction of the CBZ and the NTP produced ozone, UV, hydrogen peroxide, highly reactive and oxidising is important as it determines the mechanism of degradation. Generally, it is thought that NTP degrades CBZ by an oxidation mechanism (Miklos et al., 2018).

Possible mechanisms for the degradation pathways for the degradation of CBZ by electric discharges could be initiated by the hydroxylation of the benzene ring by the $OH^{\bullet}$ radical. (Joshi et al., 1995, Sun et al., 1999, Sun et al., 2000). Further oxidation results in oxidative ring cleavage producing acidic intermediate by-products, for example, oxalic and malic acid. Further oxidation of the acidic intermediates produces simple compounds, for example, carbon dioxide and water depending on the conditions. CBZ degradation by electric discharge has been reported to follow first-order kinetics (Tezuka and Iwasaki, 1997, Tezuka and Iwasaki, 1999). The first oxidative step is the rate determining step.

Further investigation on the contribution of other plasma species in wastewater contaminants treatment should be conducted as this is not yet fully understood.

2.3.5 CBZ treatment by-products

A sustainable treatment option should not produce more harmful by-products. A key question in the use of electric discharges concerns the identity and toxicity of the CBZ degradation by-products.

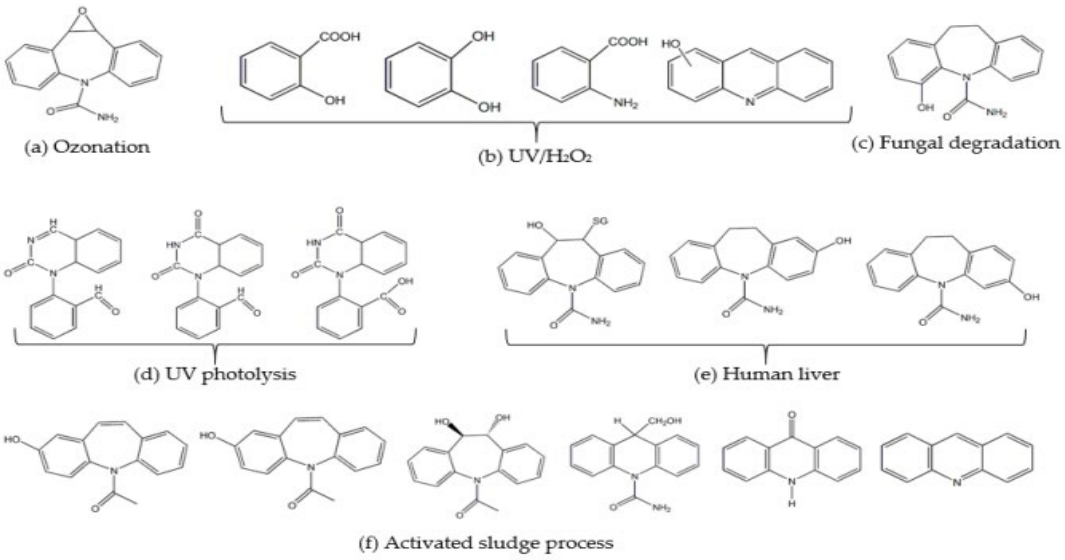

Figure 2.5 Metabolites/degradation products formed following CBZ degradation by different processes

CBZ degradation by a ring cleavage by ozone forms the metabolite epoxy-carbamazepine (Figure 2.5 (a)) (Huerta-Fontela et al., 2011). CBZ degradation produces different by-products based on the technology and operation conditions, for example, UV alone (Mcdowell et al., 2005) and UV/H_2O_2 (Vogna et al., 2004) give different degradation products demonstrating that the presence of H_2O_2 changes the degradation mechanism (Figure 2.5 (b) and (d)). In biological systems (human liver and WRF), CBZ degradation products usually contain the azepine structure if degradation is through biological systems (Figure 2.5 (c) and (d)).

CBZ, CBZ degradation intermediates and CBZ by-products showed no estrogenic activity (Mohapatra et al., 2013). There are conflicting reports on the toxicity of CBZ degradation by-products, some researchers report that CBZ by-products are non-toxic (Leclercq et al., 2009, Li et al., 2011, Vom Eyser et al., 2013) while researchers noted that CBZ degradation by AOPs does not automatically result in mineralization. Incomplete mineralisation results in intermediates that may be harmful in the aquatic environment (Wiegman et al., 2003, Kosjek et al., 2009), for example, acridine.

2.3.6 Analysis of CBZ in wastewater

Key area to the discussion on CBZ NTP treatment is the analysis of CBZ in wastewater. CBZ quantitative analysis in wastewater is either done by the High-Performance Liquid Chromatography (HPLC) with a mass spectrometer (MS) or variable wavelength detector and the Gas Chromatography (GC) with a MS detector (GC-MS). CBZ is non-volatile and contains polar functional groups; therefore, HPLC offers direct injection (Durán-Alvarez et al., 2009). GC analysis of CBZ in wastewater requires additional extraction and derivatization depending on the method. Qualitative analysis mostly uses GC-

MS. GC, however, has the potential disadvantage that the CBZ may degrade into several components in the injection port, making quantitative analysis challenging (Lajeunesse, 2007). Additionally, false positives have been reported for CBZ using GC-MS; hence extreme care must be taken when utilising the GC-MS for quantitative and qualitative work (Lewis et al., 2014). GC techniques favour use of MS as a detector due to its high sensitivity, however, the use of Gas Chromatography–Flame Ionisation Detection (GC-FID) has been reported for concentration down to 1 mg/L (Kadioglu and Demirkaya, 2007).

2.3.7 CBZ in wastewater conclusion

The occurrence of CBZ in wastewater and the subsequent release of CBZ in the aquatic environment due to ineffective treatment might not present an immediate health hazard to human and aquatic ecosystems. However, it is imperative to invest in Research and Development (R&D) for systems that can effectively remove CBZ from wastewater for reuse purposes and from surface water for drinking purposes.

2.4 *Escherichia coli* and its treatment in wastewater

2.4.1 *Escherichia coli* characterisation

Escherichia coli are rod-shaped bacteria (see Figure 2.6) found naturally in the environment, foods, and intestines of warm-blooded life forms (Woodward, 2015). *Escherichia coli* are a large and diverse group of bacteria. The harmless strains in the intestines are beneficial to the host as they produce vitamin K_2, which is essential for blood clotting.

However, of concern are the pathogenic strains of *Escherichia coli* which are categorised into five classifications. However, only two are clinically more prevalent and important, namely Shiga toxin-producing *Escherichia coli* (STEC) and Enterotoxigenic *Escherichia coli* (ETEC) (Bhavsar and Krilov, 2015).

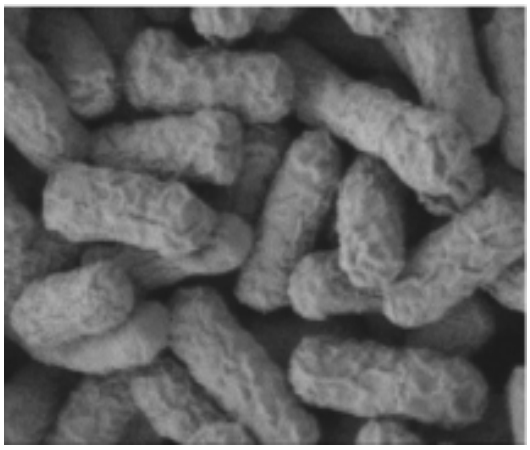

Figure 2.6 3D Scanning Electron Microscope (SEM) *Escherichia coli* imaging at x25000 magnification (Estifaee et al., 2019).

2.4.2 Escherichia Coli occurrence in wastewater

All countries have WWTP microorganism effluent guidelines for discharge into the aquatic environment. In SA, total coliforms, including *Escherichia coli,* should be zero for wastewater effluent to be discharged (Department of Water Affairs, 2013).

WWTPs in their current configuration are not always effective in treating bacteria, including *Escherichia coli*. Below are sample reported cases of *Escherichia coli* populations in the WWTP effluent which was discharged to the aquatic environment:

- A study of 6 WWTP in SA show 2.67 x 10^0 CFU/100mL up to 7.15 x 10^4 CFU/100mL *Escherichia coli* population in the tertiary WTTP effluent to be discharged (Omar and Bernard, 2010);
- In Austria, an average of three WWTP reported 10^2 CFU/mL WWTP effluent reaches the receiving environment (Reinthaler et al., 2003);
- In a study involving hospital and municipal sewage, 2.7×10^3 CFU/mL *Escherichia coli* was reported as being the bacterial density reaching the aquatic environment (Korzeniewska et al., 2013).

Escherichia coli is unique in that it has one of the lowest infective doses of 10 (Schmid-Hempel and Frank, 2007). Hence it is essential to target total *Escherichia coli* inactivation.

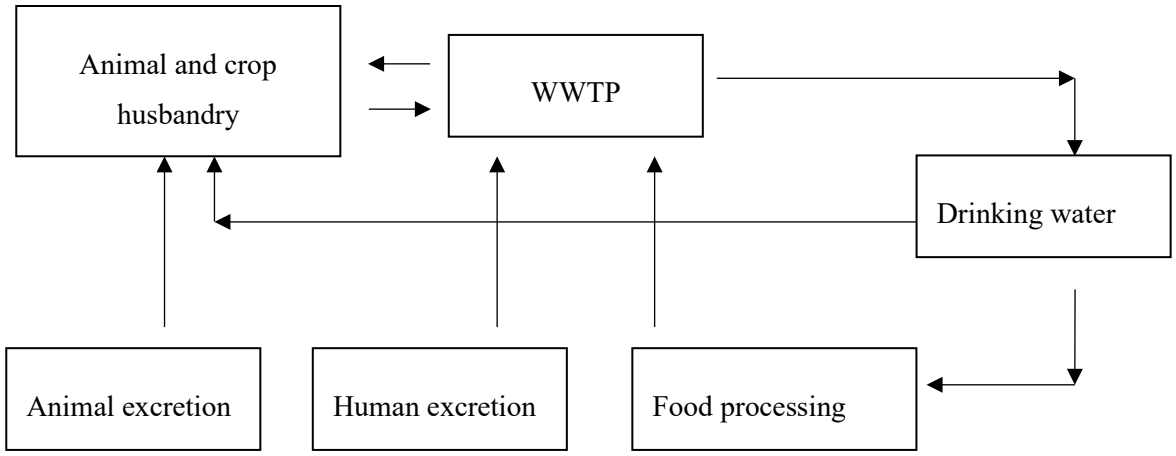

Figure 2.7 *Escherichia coli* cycle showing *Escherichia coli* transmission

Figure 2.7 shows the two primary sources of *Escherichia coli* in water are sewage water and black water from the meat and vegetative processing. However, the occurrence of *Escherichia coli* in wastewater is more complicated as it is an interrelated 'cycle' involving animal and crop husbandry and water reuse. Figure 2.7 details the cycle.

The natural starting point for the cycle description is the animal and human stomachs, where *Escherichia coli* occurs naturally (Bélanger et al., 2011). Human excretion in serviced facilities introduces the *Escherichia coli* into sewage water which is treated at WWTP. At the WWTP the release to the environment of ineffectively or incompletely treatment of the sewage water can then contaminate drinking water sources while bush defecation results in *Escherichia coli* entering fresh and drinking water sources. Additional human defecation into pit latrines can introduce the *Escherichia coli* into underground water and thus into wells. Once the *Escherichia coli* is in freshwater sources, the *Escherichia coli* can then be ingested by humans again, thus perpetuating the cycle.

Animal excretion can introduce *Escherichia coli* into freshwater and drinking water sources as the dung is carried by surface runoff. Additionally, *Escherichia coli* in animal excretion can be introduced into/onto plants through the use of organic fertiliser. Also, some animal excretion can be used as food for other animals, thus spreading the *Escherichia coli*; for example, broiler excretion can be used as an ingredient as supplementary feed for cattle feed. *Escherichia coli* can also be introduced into/onto food through watering with the water infected with *Escherichia coli* from surface runoff or the release of untreated sewage. When the infected animal and vegetative food are processed the *Escherichia coli* in the processing wastewater then enters the WWTP were if there is ineffective inactivation, *Escherichia coli* enters the environment, and the cycle continues.

2.4.2.1 Chemical-resistant *Escherichia coli* in wastewater

Escherichia coli chlorine resistance has been reported (Zeng et al., 2020). Given that chlorine and chlorine-based compounds are the most common and cost-effective waterborne pathogen inactivation, chlorine resistant bacteria could have catastrophic health implications.

However, antibiotic-resistant in bacteria can be potentially much more dangerous. Micropollutants, specifically antibiotics, in wastewater play a pivotal role in the evolution and mutation of microbes in wastewater and the environment in general (Zumstein and Helbling, 2019). WWTPs are a significant source of antibiotic-resistant *Escherichia coli* which can spread further in the environment by reaching rivers together with effluents discharged from WWTPs. *Escherichia coli* has been reported to be resistant to include ampicillin, cephalothin, nalidixic acid, piperacillin, sulfafurazole, gentamicin, trimethoprim and tetracycline (Watkinson et al., 2007, Reinthaler et al., 2003).

WWTPs are not capable of the effective inactivation of antibiotic and chlorine resistant *Escherichia coli* (Osińska et al., 2020). The antibiotic and chlorine resistant *Escherichia coli* in the effluent enters the water ecosystems together with discharged wastewater (Rizzo et al., 2013, Guan et al., 2018, Bondarczuk and Piotrowska-Seget, 2019).

Interestingly, it has been reported that UV treatment at a dose of 40 mJ/cm^2 can induce mutations that enhance *Escherichia coli* ampicillin resistance (Pang et al., 2016). This illustrates the dynamics and complexities of *Escherichia coli* treatment and the need for multiple technologies to complement each other.

2.4.3 A review of *Escherichia coli* inactivation technologies

Chlorine chemical-based treatment is generally cost-effective in *Escherichia coli* inactivation, but an alarming development has been the reported existence of chlorine tolerant *Escherichia coli* and chlorine based inactivation may produce harmful by-products (Farkas-Himsley, 1964, Ryu and Beuchat, 2005, Schwering et al., 2013). UV treatment is also popular in pathogen inactivation. UV causes inactivation by disrupting normal cellular functions (Cho et al., 2010) and has the merit of not producing disinfection by-products (Zyara et al., 2016). However, UV is rarely used in wastewater treatment for inactivation as its effectiveness is significantly reduced by turbidity and UV systems have high operational expenses (Werschkun et al., 2012). Additionally, there is the possibility of increasing antibiotic resistance due to UV induced mutation (Pang et al., 2016). *Escherichia coli* cellular repair has been reported if low-pressure UV radiation in lower-dose is utilised for disinfection (Zimmer and Slawson, 2002). *Escherichia coli* inactivation is effective. The only drawback of using ozone is that it decomposes rapidly, and it requires the use of specialised generation and dosing equipment (Werschkun et al., 2012, Zhong et al., 2017).

2.4.3.1 Sterilisation by electrical discharge

In relation to this study, sterilization by electrical discharges can be attributed to the synergistic effect of the intense electric fields, ozone, shock waves, UV radiation and hydrogen peroxide (Cui et al., 2018). The inactivation of *Escherichia coli,* in particular by plasma, has been primarily attributed to physical cell wall damage (Vukusic et al., 2016, Estifaee et al., 2019). However, the waterborne pathogen inactivation mechanism is complex, and there may be other physiochemical phenomena contributing to the inactivation.

2.4.4 *Escherichia Coli* in wastewater conclusion

While most WWTP and NTP have been effective in treating *Escherichia coli* in wastewater, it should be remembered that bacterial pathogens are unusually adaptive and are continuous exposed to chemical agents that cause mutations, the treatment technology needs to keep improving to remain relevant.

2.5 Effect of plasma on wastewater quality parameters

Water treatment is much more than the treatment of contaminants. Wastewater has to comply with specific wastewater quality parameters. Below are reported findings on the effect of plasma on wastewater qualities irrespective of the contaminant type.

2.5.1 pH

Plasma treatment reduces wastewater pH values (Vukusic, 2016). The addition of oxidising gases such as air, oxygen, nitrogen and argon, further reduce the final treated wastewater pH (Wardenier, 2016).

2.5.2 Conductivity

NTP treatment of wastewater has been reported to increase electrical conductivity (Van Nguyen, 2018). The increase in electrical conductivity is possibly due to electrode wear, causing the introduction of electrode metal ions into the treated wastewater. Several other NTP produced ions contribute to the solution conductivity. One possible source of the ions is the self-decomposition of ozone or other ions, present in the liquid sample.

2.5.3 Metal ions content

Electrode wear has been reported in some NTP experiments (Potocký et al., 2009); however, some researchers have reported that they hardly had any electrode wear. Electrode wear can be a result of the high electron temperatures. The problem is more prevalent in NTP utilising DC power sources as

compared to AC powered reactors. After NTP treatment, it is important to test for electrode metal ions in the treated wastewater to determine electrode wear. Switching the power supply on and off is reported to be a viable way of reducing electrode wear as electrode temperature is regulated (Niels, 2016).

2.6 Conclusion

R&D has demonstrated that plasma-based wastewater treatment is a promising technology, as excellent results have been reported with lab-scale NTP units. Scale-up and economic viability still pose significant challenges. A possible avenue which may assist with the economic viability of NTP is the production of one unit capable of treatment of recalcitrant micropollutants and antibiotic and chlorine resistant pathogens instead of having separate reactors for each pollutant class.

Published reports indicate variation in the removal and or inactivation efficiencies of different plasma techniques. The source of the efficiency variation could be the differences in design configuration, the material of reactor construction as some material add catalytic properties to the process, type of plasma produced as different active species concentration may be produced, physical and chemical properties of chemical pollutants and the physical and genetic makeup of the pathogen.

The next chapter presents the experimental setup and procedures utilised in the study.

Chapter Three

Experimental setup and procedure

3.1 Introduction

Chapter three details the equipment, chemical, and methods utilised in this study. Section 3.2 presents configuration details of the first atmospheric pressure NTP prototype designed and developed by in 2017 by the TRU. Section 3.3 and 3.4 details and justifies the design modifications on the new reactor and the reactor auxiliary equipment, respectively. The experimental procedure for CBZ and *E. coli* experiments are presented separately. Section 3.5 details the CBZ materials and methods employed in this study from the calibration to the data analysis methods. Section 3.6 focus on the *E. coli* inactivation experimental procedure.

3.2 2017 NTP reactor prototype review

There are technical details and theoretical understanding that is required to be able to effectively generate and sustain any form of electrical discharge in water as there are multiple dynamics at play.

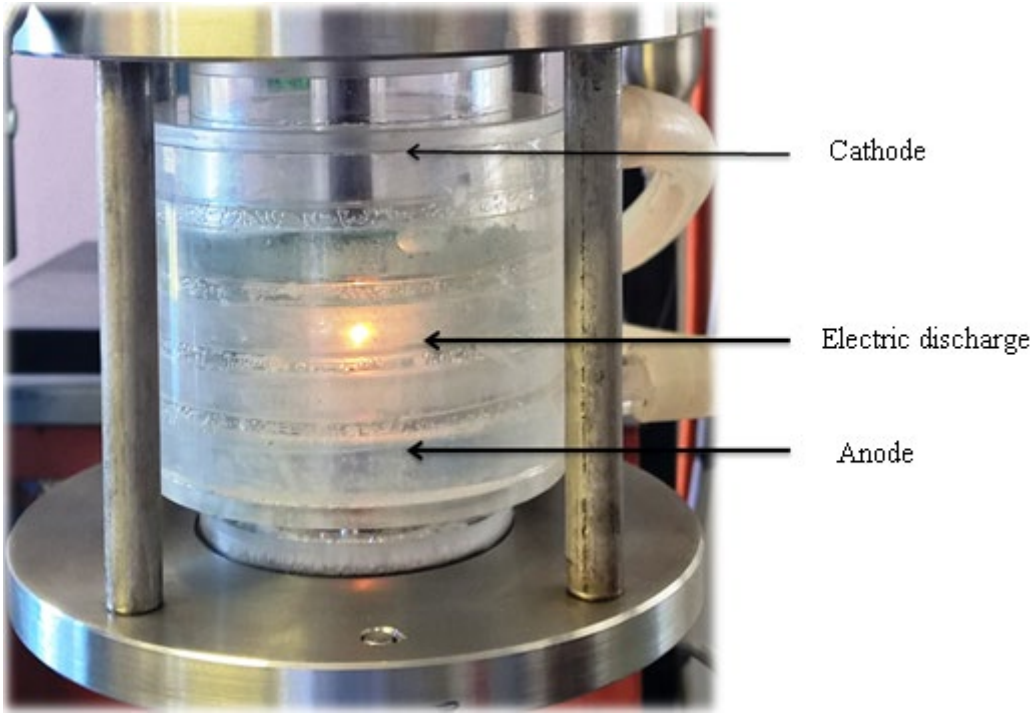

Figure 3.1 The first NTP reactor in operation showing the electrical discharge generated between the electrodes

Figure 3.1 shows the first prototype, which was a Perspex hollow cylindrical vessel pressed between the bottom and top 316 stainless steel plates. The reactor utilised a vertical point to a plane electrode configuration. The electrodes were made of copper and had a 6 mm diameter. The electrode gap could be varied as the anode could be moved up and down, thus reducing or increasing the electrode gap, respectively. The electrodes were connected in negative polarity to a direct current power supply. The cathode was the top fixed electrode. Figure 3.1 also shows a discharge generated between the electrodes in a wastewater treatment application. The type of discharge generated was an arc discharge. The drainage port was at the bottom of the reactor. The reactor had a Perspex cooling jacket which circulated water at room temperature. Air was introduced into the reactor from the top. The reactor was open to the atmosphere and operated at a low current as it is intended to treat wastewater using low-energy and non-thermal processes.

Figure 3.2 shows a cross-section rendering of the reactor showing the key aspects which were to be modified.

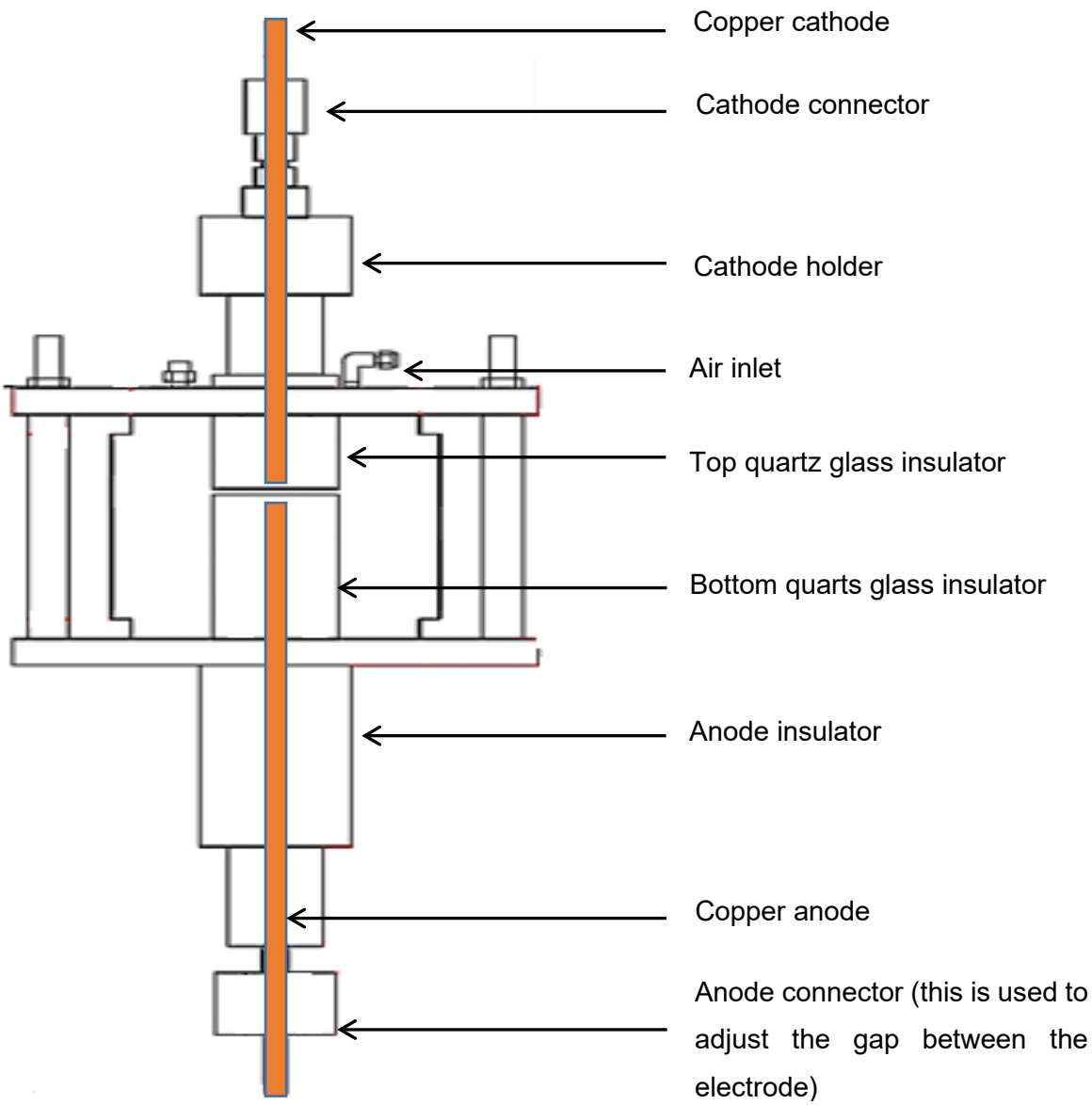

Figure 3.2 Reactor cross-section showing key aspects subject to modifications

3.3 Experimental setup

The modified reactor system description is based on the key components of the system, namely: the plasma reactor, flow system, data acquisition and electrical circuit architecture.

3.3.1 Modified reactor description

The modified reactor produces an electric discharge in the liquid at atmospheric pressure as it has an opening at the top. The modified reactor total volume was 0.5 L. In this work, the reactor was operated at a volume of 0.3 L to ensured that during treatment the water is contained in the reactor and there is a

very low probability of the water coming out from the opening at the top especially if air is bubbled from the bottom of the reactor.

The reactor was a hollow cylindrical quartz glass positioned between the top and bottom 316 stainless steel plates. Below are the detailed design modifications to the reactor system, which resulted in the reactor utilised in this work.

3.3.1.1 Gas inlet port

The first prototype reactor had a gas inlet port at the top, a modification on the reactor used in this work positioned the air inlet at the bottom of the reactor. Having the gas inlet port at the bottom has three advantages, namely:

- The addition of the gas into the water aids in providing the plasma gas in the liquid. The gases utilised in plasma treatment are expensive (nitrogen, argon, helium). The positioning the air inlet at the bottom of the reactor increases contact time and allows for maximum absorption of the air into the liquid.
- Previous work cited possible wastewater concentration inconsistencies hence the addition of a stirrer was recommended (Mohan, 2018b). The introduction of gas at the bottom aids in the mixing of the wastewater and ensures consistent wastewater composition. As the gas is fed to the reactor from the bottom, it has a stirring effect on the water in the reactor. This method of mixing has an economic and operational advantage of zero in-reactor maintenance as there are no moving mixer parts. Furthermore, the liquid would continue to move in the reactor after the gas bubble reaches the surface.
- Additionally, as a function of the reactor volume, the plasma volume is extremely small; hence there is a need to disperse the active species. This dispersion can be aided by the mixing effect of the gas as it is fed from the bottom.

3.3.1.2. Simpler electrode holders and connectors

The initial reactor electrode holders were bulky and with many parts (see Figure 3.2 and the dimension in Appendix C). The electrode holder and connectors were modified to achieve the following:

- Simplicity: the new design had fewer parts, ensuring easier troubleshooting and maintenance.
- The modified reactor had a greater height than the first prototype reactor, so it would require longer electrodes. There was a need to redesign the electrode holders to reduce excessive electrode length and use shorter electrodes. Shorter electrodes are beneficial as the electrode material is expensive and requires constant sharpening. Additionally, shorter electrodes result

in less resistive heating during treatment as electrical resistance is directly proportional to the length of a conductor.

3.3.1.3 Electrode configuration

The electrode configuration was maintained as a vertical point to plane as the literature on arc stability; the vertical configuration was demonstrated to improve the volume of fluid treatment by the discharge. However, the anode had a cylindrical head (8 mm diameter and 2 mm height) attached to the end of the 6 mm diameter electrode. The cathode maintained the 60^{o} angle top (see Appendix B).

In the first prototype reactor, the electrode gap was positioned equal distance from the top and bottom plates. The modification was to shift the electrode gap position down to a distance of ¼ of the reactor height from the bottom plate. This modification was done to ensure better temperature control of the reactor system as the electric discharge occurs in a zone with colder water as cold water has a higher density and moves to the bottom of the reactor where the electrode gap is positioned, and the discharge occurs. Additionally, the position was selected as it aids mixing. During plasma treatment, bubbles are formed in the wastewater, and as the bubbles move up the reactor, they aid in the mixing of the water in the reactor and dispersing of the reactive plasma species.

3.3.1.4 Insulating quartz glass modification

The first prototype reactor had an open quartz insulator on the bottom and top electrodes, as shown in Figure 3.3. Water tended to accumulate in the bottom quartz tube, which made cleaning the reactor challenging. Also, there were increased chances of cross-contamination of different batch contents; therefore, the new reactor did not have the bottom quartz tube. The reason for the bottom quartz covering the anode on the first prototype reactor was to reduce the chance of a short circuit. To prevent the chance of a short circuit on the anode, the surface area of the bottom electrode was increased by inserting an 8 mm diameter and 2 mm cylindrical height head attached to the end of the 4 mm electrode (as shown in Figure 3.3).

Additionally, the top electrode was tapered at the end to expose only the tip of the sharpened cathode as this intensified the electric field (Malik et al., 2001a).

3.3.1.5 Temperature probe

The temperature probe inlet was moved from the bottom plate to enter the reactor from the side at the same level as the electrode gap. The temperature probe was positioned at 4 cm from the electrodes to reduce the possibility of a short circuit as the probe is metallic. Also, a 4 cm distance from the discharge zone ensures that the bulk water temperature is measured.

3.4 Auxiliary reactor systems

3.4.1 The gas flow system

The flow system is responsible for delivering the gas at the correct flow rate. Gas from the cylinder was fed to the reactor to supply the plasma gas. The flow system consists of a dual-stage low-pressure regulator, tubing and fittings, as well as a flow controller. The pressure regulator allows for the control of the flow pressure. The gas (air in this study) was fed from the bottom of the reactor through the gas inlet port. The flow controller regulates the flow of the gas to ensure that the gas flow rate commensurate with the set flow rate value.

3.4.2 The data acquisition

An Agilent 34972A data acquisition instrument is connected to a computer system and set up to view and record the temperature in the reactor during the treatment process. The stored data can be collected for processing by a memory stick. The data acquisition and measuring instrument was arranged in such a way as to protect them from any unanticipated surges in the power supply system.

3.4.3 The electrical circuit

A plasma discharge was generated between the electrodes at atmospheric pressure by applying a high voltage to the cathode using a direct current (DC) power supply unit. The cathode was connected to the negative polarity and the anode to the neutral point on the power supply. The power supply is a Technix-SR-10R 5000 with a maximum output voltage and current of 10 kV and 0.5 A, respectively. The current in the circuit was set on the power supply. The high voltage probe had a voltage rating of up to 20 kV, a bandwidth of up to 30 MHz, and an offset of 0.2 mV. The high voltage probes were connected directly to the cathode through the cathode holder. A BNC connector from the high voltage probes was used as a connection to the LeCroy Wavejet 354A 4-channel digital oscilloscope with a bandwidth of 500 MHz and a real-time sampling rates of up to 2 GS/s. The voltage reading was logged into the oscilloscope and collected using a memory stick for the electrical power consumption, which is need for the reactor performance analysis.

This setup connected the reactor and ballast resistors (two kilo-Ohm ballast resistors) installed in series between the power supply and the discharge reactor in order to limit and regulate the amount of current flowing in the electrical circuit to the power supply. The series connection of the reactor and the ballast implies that the load current will always be equal to the current supplied, whereas the voltage is maintained in a parallel network.

Figure 3.3 shows the schematic of the reactor and the auxiliary equipment.

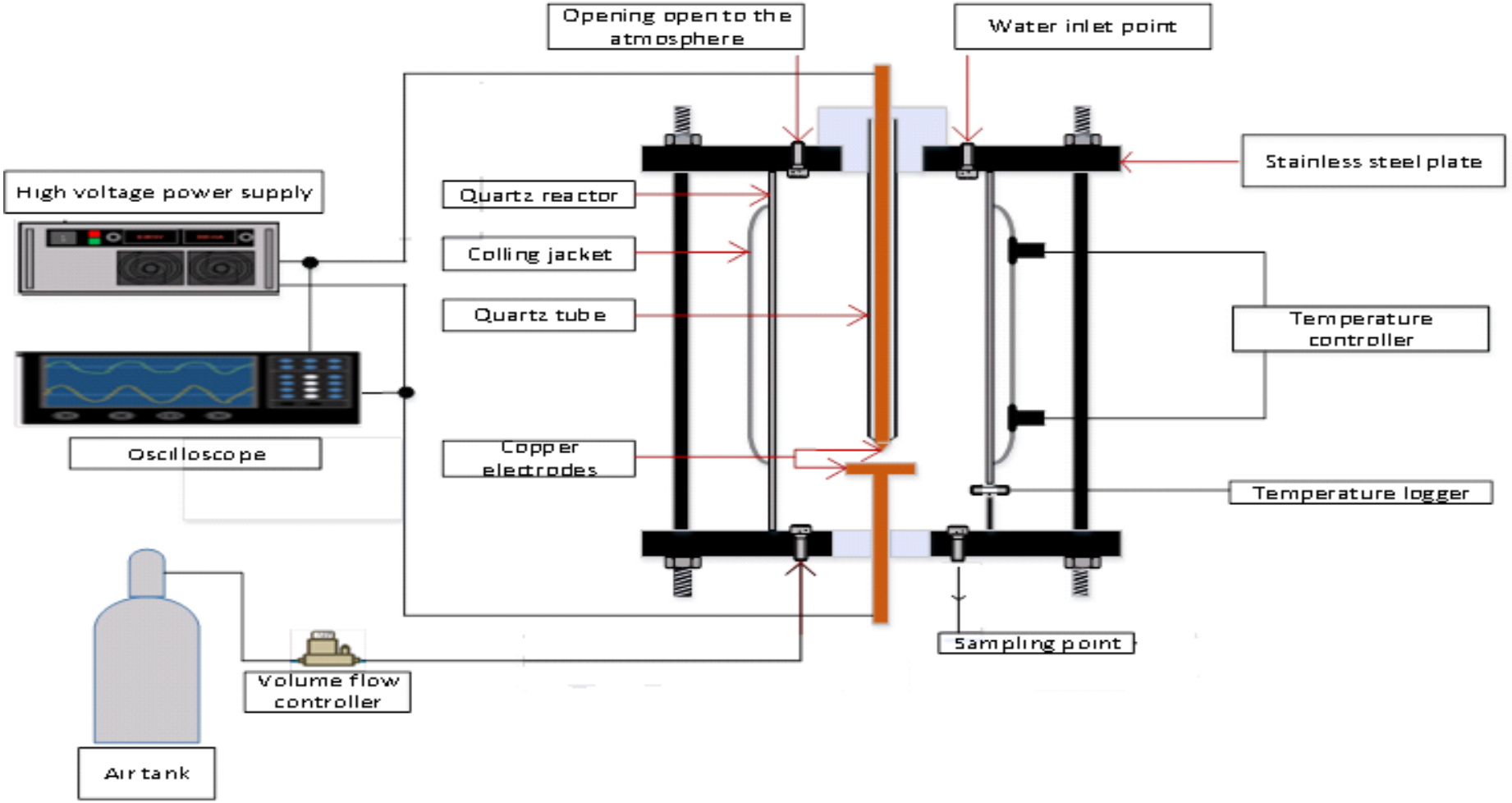

Figure 3.3 Schematic of arc discharge reactor and auxiliary equipment

3.5 Carbamazepine materials and method

3.5.1. Chemical and reagents

Table 3.1 gives the list of all applied reagents throughout this work. All chemicals were used without any further purifications.

Table 3.1 Chemicals applied in this work

Name	Chemical formula	Purity	Supplier/Manufacturer
Acetone	C_3H_6O	>95.5	Merck
Carbamazepine	$C_{15}H_{15}N_2O$	99.4	DLD scientific
Dichloromethane (DCM)	CH_2Cl_2	99	Merck

3.5.2 Design of Experiments

CBZ is a recalcitrant pollutant so literature suggests long treatment times for effective CBZ degradation, in some instances up to 60 minutes (Krause et al., 2011, Wardenier et al., 2019) therefore cost and efficiency considerations are crucial. The design of experiments (DoE) was done with optimisation in mind.

The Central Composite Design and the Box-Behnken are powerful optimisation analysis techniques. This work did not utilise the Central Composite Design or the Box-Behnken due to the need for more experimental runs, a challenge compounded by the need to repeat the runs to determine reproducibility and the addition of centre runs in the design. This study utilised a factorial design with 3 factors at two levels for the theoretical examination of experimental space. The factorial design can be utilised on the basis that the model generated is statistically adequate (Rakić et al., 2014).

A factorial design was chosen as it allows the screening of factors and interactions which affect the responses. Central points were incorporated in the design at random intervals in the design providing estimation of pure error and curvature. Additionally, the centre points permit the user to check the goodness-of-fit of the planar two-level factorial model.

The central points were conducted in replicates while non-centre points were conducted in duplicate to measure repeatability. The key performance criteria/response factors are contaminant removal efficiency (Y_1) and energy consumption (Y_2). Numerous process variables affect the key performance criteria namely electrode gap, electrode material of construction, operation volume, gas flow rate,

treatment time, current and initial concentration. For this work, the electrode gap and electrode material had already been investigated and optimised from work on the first prototype reactor (Mohan, 2018a), these findings are in agreement with the literature (Cheng et al., 2012), and the recommendations were adopted in this work.

The key factors affecting the response factors are the discharge current (current) (X_1), gas flow rate (flow rate) (X_2) and initial contaminant concentration (concentration) (X_3) as they have been identified as the three most critical independent parameters.

There is no general agreement on which one is the most effective gas (Hijosa-Valsero et al., 2014, Xiao et al., 2016, López et al., 2019), so air was utilised in this study after cost considerations. The maximum gas flow rate was determined experimentally. The maximum gas flow rate was a flow rate that maintained arc stability and did not push the water through the opening at the top. Experimental results show that 3 L/min was the maximum acceptable gas flow rate. The current was limited to the operating current range of the power supply (0 - 0.5 A). Applying the demarcation by (Bolton et al., 1996) for qualitative concentration levels in plasma AOP applications, low concentration levels were used in this study. Initial concentration levels in the mg/L range were selected based on initial CBZ concentration levels reported in the literature (Krause et al., 2011, Liu et al., 2012, Magureanu et al., 2015) to enable system comparison as functions of contaminant removal efficiency (Y_1) and energy consumption (Y_2). Additionally, analytic complications at the µg/L and equipment availability considerations were taken into count when deciding the concentration range.

Each independent factor two different levels, which are coded as –1 (low) and +1 (high), centre points are designated as (0) as shown in Table 3.2.

Table 3.2 Design factors and their level values

Factor	Code	Low (-1)	Centre point (0)	High (1)	Unit
Current	A	0.250	0.350	0.450	A
Flow rate	B	0	1	3	L/min
Concentration	C	10	20	40	ppm

Running the full complement of all possible factor combinations means that the main and interaction effects can be estimated. There are three main effects, three two-factor interactions and a three-factor interaction, all of which appear in the full model as shown in Equation 3.1.

$$Response\ factor\ (Y)$$
$$= C_0 + C_1A + C_2B + C_3C + C_4AB + C_5AC + C_6BC + \varepsilon \ldots\ldots\ldots Equation\ 3.1$$

Where C_i are constants and ε is an error term,

A factorial design with a minimum resolution of 5 allows for the estimation of all the eight-factor coefficients (however, three-factor interactions are ignored as they are insignificant for categorical factors). Factorial models in Design Expert do not produce polynomials, thus excluding curvature from the Lack-of-Fit test and the residuals, thus providing more precise information about the fit of the model (The software does a separate test for the curvature). One benefit of this procedure is that the assumptions concerning normality and constant variance can be checked even in the presence of curvature. This allows for the identification of any problems in the data analysis that might otherwise be obscured by curvature inflating the residuals. Table 3.3 depicts the full list of random experimental runs.

Table 3.3 List of possible randomised experimental runs generated by Design Expert

Run #	Current	Airflow rate	Concentration
1	1	1	-1
2	1	-1	1
3	-1	-1	-1
4	1	1	-1
5	-1	1	1
6	-1	1	-1
7	0	0	0
8	1	-1	1
9	-1	1	-1
10	1	-1	-1
11	1	1	1
12	-1	-1	-1
13	-1	-1	1
14	1	1	1
15	0	0	0
16	-1	-1	1
17	-1	1	1
18	0	0	0
19	1	-1	1

3.5.2.1 Experimental validation

Experimental validation entails testing a system at the conditions used by other researchers and comparing the obtained results to ensure that the system produces consistent results or trends. Experimental validation is essential as it can alert the investigator of any potential faults in the equipment or the need to adjust to the experimental procedure.

This work did not do experimental validation as the equipment used in this work was a modified design; hence, there was no prior work on the system to replicate and compare results. Additionally, the reactor

system could not replicate other researchers' work due to critical design differences, for example, power supply and discharge type, which would make a validation attempt futile.

3.5.3 Stock, standards, and quality control solutions

The stock solution of CBZ was prepared to 50 mg/L concentration in DCM in a 50 mL flask (The stock solution was stored at 4 ºC when not in use. The working solutions (1, 2, 3, 4, 5, 10, 20, 30, 40 and 50 mg/L) of CBZ concentrations were prepared by serial dilution of the stock solution. The quality control (QC) solutions of 1.5, 15 and 35 mg/L were also prepared by serial dilution of the stock solution. Fresh QA solutions were prepared for every analysis. Liquid measurements for serial dilutions were performed using micro pipets with new tips for every measurement to ensure exact measurements.

3.5.4 Calibrations

A calibration range of 10 data points was prepared for standards at 1, 2, 3, 4, 5, 10, 20, 30, 40 and 50 mg/L. Quantitative analysis was done by GC-FID. All the analysis were done in triplicates by GC-FID in random order. The calibration curve was established by plotting the peak areas of CBZ versus the concentrations of CBZ standard samples. GC-2010 Shimadzu GC-FID equipment was used to analyse the samples for quantitative analysis. All work with GC-FID involved manual injection with a Shimadzu 5 µL syringe (accuracy and reproducibility: ± 2%). The separation of the components in the injected sample was achieved using ZB-5MS capillary column (30 m × 0.3 mm × 25 µm). The ZB-5MS is suitable for polycyclic aromatic hydrocarbon, has a low column bleed, and has a high maximum temperature (350 ºC) especially given the high boiling point of CBZ. The split mode (5:1) was used with nitrogen carrier gas at 2 mL/min flow rate. Hydrogen and synthetic air were used as auxiliary gases for the detector (FID). The injector port and detector temperatures were set at 270 ºC. 5 µL of the sample was manually injected into the GC-FID system to ensure clear peak resolution and reduce variance. Table 3.4 details the GC-FID oven program. The GC-FID program was optimised to have short run time.

Table 3.4 GC-FID oven program for quantitative analysis

Ramp (ºC/min)	Set temp (ºC)	Hold time (min)
	100	1.7
100	220	1
10	270	0

Before the application of an analytical method for the analysis of wastewater samples, the analytical procedure should be investigated to confirm its suitability. In this work, the validation of the GC-MS procedure was restricted to an investigation of the parameters: (i) linearity, (ii) accuracy, (iii) precision (iv) limit of detection (LOD) and limit of quantification (LOQ) and v) recovery studies.

Precision, measured as intraday precision was evaluated by assessing three replicate QA samples at 1.5, 15 and 35 mg/L CBZ concentration levels. Precision was reported as relative standard deviation (RSD%).

$$RSD\ (\%) = \frac{s}{x} \times 100 \ldots\ldots\ldots\ldots\ldots\ldots\ldots\ldots\ldots\ldots\ldots\ldots Equation\ 3.2$$

Where s is the standard deviation and x is the average concentration. Both statistic parameters were calculated for each concentration level. The reported RSD% value was determined as the RSD% value calculated from three concentration levels.

Both accuracy and precision should fall within the proposed criteria of RSD% <15% (Kadioglu and Demirkaya, 2007). Intra-day (repeatability) during the same day and inter-day (intermediate precision) on different days were also conducted with the three replicate of QA samples for precision.

A prescribed approach for determining the LOD and LOQ for water samples was proposed by the United States of America Environmental Protection Agency (EPA) and Corley (Corley, 2002). Limit of detection (LOD) and Limit of Quantification (LOQ) were calculated as follows:

$$LOD = \frac{3 \times S_m}{b} \ldots\ldots\ldots\ldots\ldots\ldots\ldots\ldots\ldots\ldots\ldots\ldots Equation\ 3.3$$

$$LOQ = \frac{10\ \times\ S_m}{b} \ldots\ldots\ldots\ldots\ldots\ldots\ldots\ldots\ldots\ldots\ldots\ldots Equation\ 3.4$$

Where $\frac{S_m}{b}$represents the signal of the background noise of the 1 µg/L standard

The $\frac{S_m}{b}$ was calculated according to equation 3.5:

$$\frac{S_m}{b} = \sqrt{\frac{\sum(C_i - C_p)^2}{n-2}} \ldots\ldots\ldots\ldots\ldots\ldots\ldots\ldots\ldots\ldots\ldots\ldots Equation 3.5$$

Where $\frac{S_m}{b}$ represents the root mean square standard error on the calibration curve, C_i the concentration of the calibration standards (mg/L), C_p the concentration predicted from the calibration curve, and n the number of calibration standards (10).

3.5.5 Extraction and recovery studies

Determination of micropollutants in wastewater and other environmental samples is often a challenging task. For extraction, solid-phase extraction (SPE) and liquid-liquid extraction (LLE) were the available option, however in this study LLE using DCM was the chosen method for CBZ extraction from the CBZ spiked synthetic wastewater. The LLE was preferred after the following considerations, i) simple operational procedure and ii) chemical and equipment cost considerations. SPE was also another viable option which could have been utilised as the equipment was available, however with the use of SPE, the possibility of SPE plastic cartridges dissolving into DCM; thus introducing extraneous peaks in analysis (Zhao et al., 2018). Additionally, it has been utilised in previous studies involving CBZ extraction from aqueous samples (Wardenier et al., 2019).

Based on the recommendations of the EPA and extraction optimisation, extraction was performed on a 5.00 mL water sample in two steps of 1.5 mL dichloromethane per extraction step. The extraction efficiency, as measured by the percentage recovery (Section 3.5.6), was measure after the final extraction as this was the extraction which produced the sample to be analysed. After adding the dichloromethane to the water, there was adequately shaking for 5 minutes, followed by settling for 10 minutes. After extraction, the organic phase was removed and transferred into the GC vial and analysed using GC-FID. GC-FID analysis was then performed with the GC-FID method, described in section 3.4.4.

3.5.6 Percentage recoveries

In order to test the effectiveness and validate the sample preparation and determination protocols for CBZ, an extraction of 5 mL of the synthetic wastewater at 1, 2, 10, 20, 40 mg/L spiked CBZ concentration was performed.

After the extraction, the samples were analysed on a GC-FID, and the peak areas were compared to the peak areas of the standard 1, 2, 10, 20, 40 mg/L.

The accuracy of the optimized extraction procedure was determined by calculating the recovery percentage as the ratio between the individual micropollutant concentrations in dichloromethane before and after extraction.

$$Percentage\ recovery\ (R) = \frac{y}{x} \times 100 \ldots\ldots\ldots\ldots Equation\ 3.6$$

Where y is the concentration of CBZ extracted found the aqueous after equilibrium was reached, and x is the concentration of CBZ spiked in the aqueous solution (Arshad et al., 2017). QA samples were extracted in duplicates. Based on the literature, for this study 80% was the set acceptable minimum

recovery (Miao and Metcalfe, 2003, Krause et al., 2011, Böger et al., 2018). The percentage recoveries in this study were in the range of 83.1% for 1.2 mg/L to 88.1 % for 40 mg/L.

3.5.7 Experimental procedure

3.5.7.1 Reactor cleaning

Before and after every experimental run, the reactor was thoroughly cleaned to ensure no cross-contamination between runs. Cleaning entailed washing the reactor with soap water, rinsing with distilled water then filling the reactor with acetone for 10 minutes to dissolve any CBZ or CBZ by-products into the acetone followed by thorough rinsing of the reactor with distilled water.

3.5.7.2 Quality Assurance

The calibration is central to the quantitative analysis of this work. For quality assurance purposes, before every experimental run, the applicability of the analytical method for the calibration analysis of the QA samples was investigated. The validation of the GC-FID procedure was restricted to an investigation of the parameters: (i) linearity, (ii) accuracy and (iii) precision.

3.5.7.3 Synthetic wastewater preparation

A fresh 0.5 L CBZ spiked synthetic wastewater sample was prepared for every experimental run. In a typical experiment, 0.3 L of the CBZ spiked synthetic wastewater at either 10, 20, or 40 mg/L CBZ concentration spiked was feed into the reactor for treatment. The remaining 0.2 L was set aside for pre-treatment recovery studies, pH, conductivity measurements.

To prepare either a 10, 20, or 40 mg/L of CBZ spiked synthetic wastewater, 5, 10 or 20 mg of CBZ were weighed, respectively, on an analytical balance, measuring in grams up to 4 decimal places. The weighed CBZ was added to a 0.5 L flask half-filled with distilled water. The flask was shaken to homogenise and filled up to the mark, then allowed to equilibrate.

3.5.7.4 Pre-treatment wastewater characterisation

The wastewater parameters (temperature, pH, conductivity and initial CBZ concentration) were determined before every experimental run. It is crucial to ensure that the CBZ spiked synthetic wastewater is at the prescribed initial CBZ concentration. Before every experiment, the concentration of the CBZ in the wastewater is determined by LLE (section 3.5.5) followed by GC-FID analysis (section 3.5.4). Only synthetic wastewater within a 10% deviation from the target CBZ concentration was used for experimental runs. Conductivity and pH were measured using a portable pH/conductivity meter (Orion 4 star, Thermo Scientific).

3.5.7.5 Plasma treatment

Plasma treatment was conducted in semi-batch operations. The initial step of all plasma treatment runs was to set the current and airflow rate values to the predetermined DoE levels. 0.3 L of the characterised influent was fed in the plasma reactor manually. To minimise electrode wear and avoid excessive gas and liquid temperatures, the voltage applied to the reactor was operated in 30 seconds on and off cycles (Petrik et al., 2015, Wardenier et al., 2016, Mohan, 2018b). Plasma treatment time was regarded as the total time which the voltage was applied to the reactor. At plasma treatment time intervals of 2.5, 5, 7.5 and 10 min, approximately 5 mL reactor effluent samples were taken and put into 10 mL vial for sample preparation and sampling.

3.5.7.6 Post-treatment sample preparation and analysis

After plasma treatment, 5 mL of each sample was measured using a micro pipet. Micropollutant extractions were performed through an optimized LLE method in section 3.5.5. After extraction, micropollutant concentrations of the plasma-treated samples were analysed using the optimised GC-FID quantitative analysis, as described in section 3.5.4.

Equally crucial to the removal efficiency are the products of the CBZ degradation process. Ideally, a treatment process should not produce by-products more harmful than the parent compound. The qualitative analysis utilised the GC-MS technique. Agilent GC-MS equipment was utilised to analyse the samples. The separation was achieved using ZB-5MS, 30 m, capillary column (30 m × 0.3 mm × 25 μm,) with helium as the carrier gas. The MS detector was set in scan mode. The column temperature was set at 80 ºC with an injection temperature at 250 ºC using split injection mode. Table 3.5 shows the GC-MS oven program for qualitative analysis. The pressure was set at 37.2 kPa with a total flow of 4.4 mL/min and a column flow of 0.69 mL/min with a linear velocity of 30.6 cm/sec at purge flow of 3.0 mL/min using a split ratio of 100.0. The ion source temperature was set at 240 ºC with an interfacial temperature of 280 ºC and solvent delay set at 4.00 min to prevent oversaturation of the column and maintain the long lifespan of the column, detector gain was set at 0.94 kV. The total run time was 20.28 minutes, and the scan speed was 1428 with m/z range from 35 to 500.

Table 3.5 GC-MS oven program for qualitative analysis

Ramp (°C/min)	Set temp (°C)	Hold (min)
	80	1
30	225	1
4	231	1
14	280	1
45	300	6

3.5.8 Data analysis

All the data was entered and analysed on Microsoft Excel. Significant differences between runs were determined by using the t-test at the 0.05 significance level. Error bars indicating standard deviations from the means are displayed on graphs.

Calibration data were subjected to regression analysis. Accuracy, precision, Intra-day (repeatability) and inter-day (intermediate precision) of the QA samples should fall within the proposed criteria of RSD% <15% (Kadioglu and Demirkaya, 2007).

Electrical characterisation to determine the voltage and power usage of the reactor was conducted using the data from the power supply. The power supply was a high voltage DC hence power was calculated using formula 3.7.

$$P = V \times I \ldots\ldots\ldots\ldots\ldots\ldots\ldots\ldots\ldots\ldots\ldots\ldots\ldots Equation\ 3.7$$

Optimisation process involved i) model analysis; ii) mathematical modelling of the effect of the parameters on removal efficiency; iii) mathematical modelling of the effect of the parameters on energy consumption; and iv) process optimisation within the selected constraints of power consumption minimisation and removal efficiency maximisation.

3.6 *E. coli* inactivation experimental procedure

3.6.1 Experimental design

The experimental design factored in three key aspects, namely i) electrode gap determination; ii) effect of increasing initial *E. coli* cell density on treatment effectiveness; and iii) the investigation of the contribution of copper to *E. coli* inactivation. All runs were done in duplicate due to economic and time constraints of the post-treatment analysis. Total inactivation was designated if the results of all the samples from the duplicate runs showed no bacterial growth

In all the *E. coli* experimental runs, the current was set to 0.45 A and with no gas being fed into the reactor.

3.6.1.1 Discharge Gap determination

The optimum electrode gap had to be determined as these experiments with *E. coli* were the first biological contaminant conducted with the plasma unit.

The gap was varied between 2 mm and 4 mm while the concentration remained constant. Table 3.6 shows the two experimental runs to determine the most suitable electrode gap. The gap which resulted in the most stable electrical discharge was determined as the optimum gap and was used for all experimental investigation after.

Table 3.6 Electrode gap determination experiments

Run	Electrode gap (mm)
1	2
2	4

3.6.1.2 Effect of initial *E. coli* Density

E. coli cell density in sewage and the aquatic environment has been reported to vary over a wide range and can be as high as 2×10^7 CFU/mL (Huijbers et al., 2020). The *E. coli* concentration in was increased to determine the limits of the system can treat the most *E. coli* dense wastewater. Table 3.7 shows the experimental runs and the *E. coli* density in the ESSWW used in each of the experimental runs.

Table 3.7 Experimental runs to determine the effect of initial cell density

Experiment	Procedure Description
3	ESSWW with 3.96×10^4 CFU/mL initial *E. coli* cell density exposed to plasma.
4	ESSWW with 1.3×10^5 CFU/mL initial *E. coli* cell density exposed to plasma treatment.
5	ESSWW with 2.5×10^7 CFU/mL initial *E. coli* cell density exposed to plasma.

After experiments three, four and five, the remaining treated wastewater in the reactor was drained, decontaminated in the autoclave set at 120 ºC for 30 minutes. The decontaminated wastewater samples were put in plastic vials and analysed by a Perkin Elmer Optima DV5300 by an Inductively Coupled Plasma Optical Emission Spectrometer (ICP-OES) to determine the concentration of copper ions that were released into the water during treatment. Cu 213.597 and Cu 224.700 were considered. Parameters for the ICP-OES axial analysis were set to power 1.5 kW, nitrogen as the auxiliary gas at 0.2 L/min, and Argon as the nubuliser gas at 0.8 L/min. The ICP-OES was calibrated with standards prepared from 1000 mg/L solutions. The concentration of copper released into the treated wastewater were in the range of 0.4 to 0.7 mg/L of copper, depending on the initial *E. coli* concentration.

3.6.1.3 Investigation of the contribution of copper to *E. coli* inactivation

The rationale for the second factor is that the electrode material, copper, is a well-known antimicrobial agent and investigating its contribution to the inactivation process was key and therefore prompted using control reactors. Below is Table 3.8, depicting the experimental runs.

Table 3.8 Experimental runs to establish the contribution of copper to *E. coli* inactivation

Experiment	Procedure Description
6	ESSWW with 2.5×10^7CFU/mL initial *E. coli* cell density sample exposure to plasma.
7	Copper control with 0.4 mg/L copper ion concentration and ESSWW with 2.5×10^7CFU/mL initial *E. coli* cell density (control for Experiment 6).
8	Copper control with 0.7 mg/L copper ion concentration and ESSWW with 2.5×10^7CFU/mL initial *E. coli* cell density (control for Experiment 6)

The copper ion stock (1000 mg/L) solution was prepared form cupric sulphate (99.5 % purity supplied by Rochelle chemicals) and autoclaved distilled water. Adequate volumes of the stock were added to make the target copper ion concentration in the 0.3 L volumes used in the respective runs.

3.6.2 Experimental procedure

3.6.2.2 Inoculum Preparation

E. coli was obtained from the Institute for Water and Wastewater Technology, Durban University of Technology. Before each experiment, *E. coli* were inoculated into 250 mL Schott bottles containing sterilized Luria-Bertani (LB) broth and grown overnight at 37 °C (16 h) in a shaking incubator (150 rpm). The cells were harvested by centrifugation at 15000 rpm for 10 min at room temperature. The supernatant was washed twice with sterile phosphate-buffered saline (PBS, pH: 7.4). The pellet was then resuspended in PBS, its absorbance was measured at OD600 and the bacterial concentration was adjusted to 10^8 CFU/mL and used as the stock.

3.6.2.3 Reactor disinfection

The reactor was thoroughly cleaned before each run, after and in-between runs to ensure no carryover of viable *E. coli* cells. The cleaning procedure entailed an initial cleaning with autoclaved distilled water, then filling the reactor with 0.5% hypochlorite for 15 minutes, followed by thorough rinsing with autoclaved distilled water three times.

3.6.2.4 Synthetic *E. coli* wastewater preparation

E. coli stock was always mixed by shaking before use. *E. coli* spiked synthetic wastewater (ESSWW) was prepared by adding measured volumes of *E. coli* stock to 0.3 L beakers then adding autoclaved distilled water to the mark. Table 3.7 shows the volumes of *E. coli* stock and the corresponding autoclaved distilled water utilised. The contents of the beakers were thoroughly mixed for one minute before pre-treatment sampling and being added to the reactor.

Table 3.9 ESSWW composition

Target *E. coli* density	Amount of *E. coli* stock added (mL)	Autoclaved distilled water added (mL)
3.96×10^4 CFU/mL	0.12	299.88
1.3×10^5 CFU/mL	0.4	299.6
2.5×10^7 CFU/mL	75	225

3.6.2.5 Pre-treatment water sampling

The wastewater qualities were determined before every experimental run. It is important to ensure that the ESSWW is at the prescribed initial *E. coli* cell density. Before every experiment, a 5 mL sample

was taken from the 0.3 L ESSWW and stored at 4 ºC for analysis together with treatment samples. Conductivity and pH of the synthetic ESSWW were measured before each experiment using a portable pH/conductivity meter (Orion 4 star, Thermo Scientific).

3.6.2.6 Plasma treatment

For *E. coli* Plasma treatment, the current was set to 0.45 A and the airflow rate set to 0 L/min. 0.3 L of the characterised ESSWW was fed in the plasma reactor manually. To minimise electrode wear, excessive gas and liquid temperatures, the voltage applied to the reactor was operated in 30 seconds on and off cycles (Petrik et al., 2015, Mohan, 2018b). Plasma treatment time was regarded as the time in which the voltage was applied to the reactor. *E. coli* plasma treatment was conducted in semi-batch mode with samples being withdrawn every 30 seconds of treatment. Different *E. coli* cell density in the wastewater was achieved by dilution of the stock concentrated *E. coli* water to the desired density.

3.6.2.7 Control Experiments

The copper control experiments were conducted in 0.3 L beakers covered at the top by parafilm. Copper control experiments are conducted with copper ion concentration at 0.4 mg/L and 0.7 mg/L to cover the upper and lower limits of the copper ions concentration in the water at 180 seconds after plasma treatment. To make a 0.4 mg/L and 0.7 mg/L copper solution, 120 and 210 microliters of a 1000 mg/L copper ion stock solution were added to the beakers used for the control run respectively. The copper ion stock solution was prepared by dissolving copper sulphate in distilled water. Approximately 0.3 L of the ESSWW was measured into the beakers with the copper solution and the contents thoroughly mixed. The sampling of copper control runs was done before introducing the ESSWW into the beaker with the copper solution. Another sample was taken after 300 seconds from the mixture of ESSWW and copper and the copper solution.

For the non-treated, non-copper controls, 0.3 L of the ESSWW was added into the beakers. The sampling of control runs was done at 0 sec and 300 seconds.

3.6.2.8 Post *E. coli* treatment enumeration

For microbial enumeration, the samples were taken before and after plasma treatment, stored at 4˚C in sterile tubes and analysis were carried out within 16 hours of sampling. Control and treated samples were collected in sterile tubes after their respective post treatment storage time. A 10-fold serial dilution of the samples taken before and after plasma treatment (for bacteria enumeration) were made and the 0.1 mL of the diluted samples were spread plated on HiCrome™ Coliform Agar (Sigma Aldrich). The plates were incubated at 37 °C for 24 to 48 hours. After incubation, the colonial morphology was noted and the colony count was made and recorded as CFU/mL.

3.6.2.9 Scanning Electron Microscope

Cell imaging was done by SEM. The plasma-treated aqueous solutions were centrifuged, and the supernatant discarded to obtain dense cell pellets for SEM.

The SEM sample preparation followed the protocol described by the UKZN Microscopy and Microanalysis Unit (MMU). Briefly, cell pellets were fixed for 2 hours by 2.5% glutaraldehyde in sodium cacodylate buffer (SCB). The fixed cells were washed three times with SCB, and then three times with deionized water. Dehydration of samples was achieved by washing with increasing concentrations of ethyl alcohol (50, 70, 80, 90, 99.5%). In the last step, all samples were fixed on carbon tape and sputter-coated with gold particles for 2 min. Images were taken by Hitachi S-570.

3.6.3 Data analysis

All data values were entered and analysed on Microsoft Excel. The survival bacterial populations were analysed by independent t-test to test statistical significance among treatment runs. Statistical significance was accepted at $p < 0.05$. All microbial data were pooled and average values and standard deviations determined. Error bars indicating standard deviations from the means are displayed on graphs.

Trends in the bacterial inactivation and the effects of the independent variables on inactivation were also discussed.

Chapter Four

Carbamazepine results and discussion

4.1 Introduction

The experimental procedure with CBZ produced some interesting results, which will be presented and discussed in this chapter in fulfilment of research objective number two. The detailed determination of the influence of the individual operation was determined through Design Expert. Additionally, given the significantly longer treatment times required for CBZ degradation, the results of theoretical optimisation of the process are also presented and discussed. The conclusion summarises all the key findings on CBZ degradation.

4.2 Calibration, recovery and validation procedure

The external standard calibration method was utilised to evaluate the performance of the GC-FID quantitative analytic method. The calibration curve was utilised for the quantification of CBZ. The utilised method was optimised for short run times and showed good separation of the solvent and solute (CBZ) (3.95 minutes retention time). The calibration curve covers the range of concentrations from 1 - 50 mg/L. The reliability of the GC-FID method was assured by a validating protocol whose performance characteristics are listed in Table 4.1 (Guideline, 2005, Moosavi and Ghassabian, 2018).

Table 4.1 Linear regression of the calibration data for GC-FID measurements

Parameter	Value
Calibration range (mg/L)	0 – 50
Slope	2845
Standard error of slope(S_e)	273
Correlation coefficient (R^2)	0.9998
LOD (mg/L)	0.28
LOQ (mg/L)	0.96

An R^2 higher than 0.99 was observed, which demonstrates good linearity. However, the R^2 value alone is not sufficient to confirm the goodness of fit. Additionally, the data was evaluated using the distribution of residuals which revealed randomly placed data points around the horizontal axis, thus

demonstrating the appropriateness of the linear regression model for interpreting the experimental data as the linear model was an adequate description of the data. Thus, the calibration range established the interval between which the highest and lowest concentration of CBZ could be determined with accuracy. The calibration curve, sample GC-FID chromatogram are presented in Appendix A. The standard error of the slope can be interpreted to mean that if the data is normally distributed, the S_e value is acceptable as more than 95% of all the data points fall within $\pm 2S_e$.

At 1 mg/L, comparatively high RSD% (10.6%) was observed. However, CBZ analysis by GC-FID at less than 5 mg/L has been reported with acceptable criteria of RSD% <20 (Statistical Subcommittee of the Analytical Methods Committee, 2004, Kadioglu and Demirkaya, 2007). The cause of the variation is possibly due to the marked breakdown of CBZ at lower concentrations in the injection port and weak and inconsistent sensitivity of the instrument to CBZ as concentrations approached the LOQ and LOD. However, at 2 mg/L, the RSD% drops to below 5%.

The lowest concentration level of an analyte that can be determined and quantified by an analytic method is known as the LOD and LOQ, respectively. The LOD and LOQ were established through the use of the calibration curve, as discussed in Section 3.5.4. The LOD and LOQ are close to the lowest calibration point at approximately double the lowest calibration point. As noted above, at concentrations approximating 1 mg/L, the repeatability as demonstrated by the 10.6% RSD% in the quantification by the GC-FID instrument utilised in the study is comparatively higher, the LOD can be taken to represent the lowest concentration value, which can be quantified within a 95% confidence interval as specified by the regression analysis. Thus, the calibration curve can be used for the quantification of CBZ in the range of 1 – 50 mg/L.

Recovery of the synthetic CBZ wastewater sample was evaluated by extracting in duplicate at every recovery concentration level and analysing in triplicate. The results of the recovery experiments are reported in Table 4.2. Literature shows the acceptable range for the recovery of CBZ in the water at 80 – 120% (Miao and Metcalfe, 2003, Krause et al., 2011, Böger et al., 2018), The results show recoveries in the acceptable range and good repeatability, hence demonstrating a robust method. While additional clean-up steps could have obtained high recoveries, there is a possibility of additional variability in the result.

Table 4.2 Results of the recovery studies (n=3)

Spiked Level(mg/L)	Mean recovery (%)	RSD%
1.2	83.1	10.3
5	83.7	1.8
10	84.0	1.4
20	85.3	1.1
40	88.1	0.7

Tables 4.3 and 4.4 illustrate the intraday and inter-day variations of the analytical method. The values show acceptable inter-day variability. The precision is lower at 1.5 mg/L as generally precision reduces as the LOD (0.28) and LOQ (0.96) is approached.

Table 4.3 GC-FID intraday variability

QC concentration (mg/L)	Measured (n=3)	RSD%
1.5	1.51±0.17	11.51
20	25.10±0.25	0.98
35	35.07±0.13	0.35

Table 4.4 GC-FID inter-day variability

QC concentration (mg/L)	Measured (n=6)	RSD%
1.5	1.49±0.15	10.17
20	25.09±0.19	0.78
35	35.17±0.26	0.74

4.3 Plasma treatment effect on water quality parameters

Micropollutant decomposition dominantly occurs at the plasma-liquid interface and in the bulk liquid. In the bulk liquid, micropollutant decomposition is the result of the production of a wide variety of

aqueous radicals and ions. A series of complex interactions cause the formation of these oxidative species. A complete discussion of all interaction mechanisms between all chemical species with micropollutants is beyond the scope of this work and constitutes an entire high-level ongoing research in the field of NTP and wastewater treatment. The reactor was not optimised to produce a specific set of radicals or reactive species. However, an investigation of the water quality parameters, conductivity and pH, is performed as it may provide insight into the chemical processes taking place in the reactor.

4.3.1 pH

Irrespective of the starting concentration and operating conditions, there was a general decrease in the pH of all the plasma treated CBZ wastewater.

The starting pH of the CBZ wastewater was 6.8±0.3 for the 10 -40 mg/L range. The initial pH value is lower than the value of 7-8 commonly reported in the literature (Magureanu et al., 2011, Liu et al., 2012, Wardenier et al., 2019). The lower pH can possibly be attributed to the carbon dioxide dissolved in the distilled water as the distilled water was kept in clean closed containers, however, the container was not airtight.

Different operational conditions produced different final pH values. A current of 0.45 A and air flow rate of 3 L/min resulted in the highest pH drop after plasma treatment resulting in an average final pH value of 2.9. A current of 0.25 A and air flow rate of 0 L/min resulted in the smallest pH drop after plasma treatment resulting in an average final pH value of 3.7.

The experimental results on pH show that plasma treatment leads to a strong increase in acidity irrespective of the operating conditions. The sharpest decrease in pH after 10 minutes of treatment was observed for plasma discharges at 0.45 A discharge current and 3 L/min air flow rate. The introduction of air into the plasma reactor results in lower final pH values. This can be attributed to the addition and replenishment of nitrogen compounds in the water (Kogelschatz et al., 2003).

The acidification of water, spiked with chemical contaminants, treated with plasma has been extensively studied in the literature ((Brisset et al., 2008). Additionally, strong pH drops in micropollutant solutions have been confirmed by many other researchers. pH drops down to 2.01 have been reported after plasma treatment (Shainsky et al., 2012). Similar results were obtained through experimentations in other reactor types.

Literature suggests that acidification of plasma-treated water plasmas is the result of nitrous acid (HNO_2) and nitric acid (HNO_3) formation in the bulk liquid. The source of the nitric and nitrous acid is the nitrogen in the atmosphere as the reactor is open to the atmosphere.

The first set of possible reaction which causes the acidity is the formation of nitrogen monoxide (NO) due to the plasma. Further reactions of the nitrogen monoxide produce nitrogen dioxide as shown in equation 4.1 and 4.2 (Kogelschatz et al., 2003):

$$2NO + O_2 \rightarrow 2NO_2 \ldots\ldots\ldots\ldots\ldots\ldots\ldots\ldots\ldots\ldots Equation\ 4.1$$

$$NO + O_3 \rightarrow NO_2 + O_2 \ldots\ldots\ldots\ldots\ldots\ldots\ldots\ldots\ldots Equation\ 4.2$$

The nitrogen oxides dissolve into the water, leading to the formation of nitrite and nitrates (Equation 4.3-4.4). According to these reactions, the formation of nitrite and nitrate also results in the production of hydrogen cations (H^+) in the aqueous phase, which describes the experimentally observed pH drop by plasma discharges in air(Lukes et al., 2012):

$$2NO_2 + H_2O \rightarrow NO_2^- + NO_3^- + 2H^+ \ldots\ldots\ldots Equation\ 4.3$$

$$NO + NO_2 + H_2 \rightarrow 2NO_2^- + 2H^+ \ldots\ldots\ldots\ldots\ldots Equation\ 4.4$$

Given the critical role nitrogen based compounds play in determining pH, a possible explanation for a lowest final pH (2.9) with air flow rate at 3 L/min could be the constant addition of air, which contains approximately 78% nitrogen, which acts as an additional supply of nitrogen into the water hence driving reaction to the right side.

Significant pH drops have also been reported in literature in solutions treated in nitrogen-free plasmas. For instance, a final pH value of 2.07 after oxygen DBD plasma treatment of deionized water has been reported (Shainsky et al., 2012). This suggests that other reactive species, formed in the liquid phase, contribute as well to the acidification of deionized water in the plasma chamber. Probably, the self-decomposition of ozone, produced in the plasma discharge, contributes to significant lower pH values. Although ozone decomposition in water is mainly initiated under alkaline conditions, it has also been observed, at a slower rate, under acidic conditions (Ershov and Morozov, 2009). Possibly, the formation of charged species in the gas phase, and the subsequent dissolution in the aqueous phase also contributes to the observed pH drops. Further research is needed to validate these claims.

4.3.2 Conductivity

Electrical conductivity is dependent on the ions in the aqueous phase. The conductivity is important as it affects the chemistry of the plasma in the water. A high conductivity implies an aqueous solution with a higher concentration of charged species which may interact with active species generating complex products instead of hydroxyl radicals available for degradation reactions (Li et al., 2013).

In addition to the pH measurements, also changes in solution conductivity were measured. The initial conductivity was 0.24 ± 0.06 µS/cm. The general trend is for the increase in the initial conductivity due to plasma treatment. The final conductivity is a function of the discharge current and the air flowrate. The highest final conductivity was that of water treated at the highest current (0.45 A) and air flowrate (3 L/min), which produced a final conductivity of 439 µS/cm. Air appears to be the dominant contributor to the conductivity as the conductivity for 0.45 A and 0 L/min is close to the conductivity of 0.25 A and 3 L/min (Figure 4.1). The role of air flowrate in influencing conductivity may be attributed to how air flow rate at 3 L/min resulted in discharge instability hence more marked electrode degradation, thus depositing more copper ions in the solution which contributes to an increase in conductivity since 0.25 A and 3 L/min has conductivity almost equal to 0.45 A and 0 L/min.

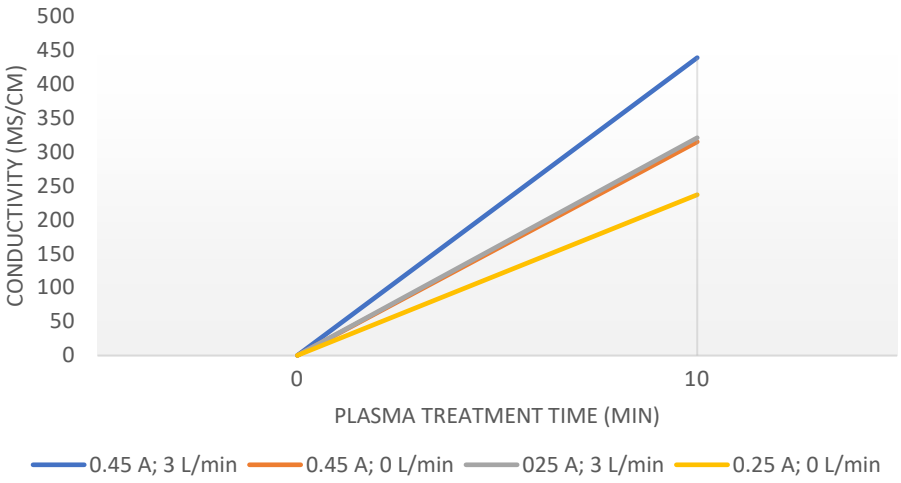

Figure 4.1 Conductivity change due to plasma treatment at different reactor conditions

Together with the pH drop explained in the pH measurements (Section 4.3.1), the increase in conductivity delivers additional experimental evidence about the production of charged species in the treated solution. For discharges in air, the main contribution of the solution conductivity is delivered by the decrease in pH (Magureanu et al., 2015). Moreover, conductivity and pH are closely correlated with each other, as predicted by (Burlica and Locke, 2008):

$$\Lambda = \Lambda_o + 1000([H^+] + 198[OH^-]) \dots\dots\dots\dots Equation\ 4.5$$

With H^+ an OH^- respectively the concentration of hydrogen cations and hydroxyl anions expressed in mol^{-1}. Λ_o is the initial solution conductivity (µS/cm), and Λ the steady-state conductivity, also in µS/cm.

However, Equation 4.5 may not fully explain the increase in conductivity as there are other ions influencing the final conductivity value. One source of ions in the visible electrode wear during plasma treatment since continous DC power supply can cause significant electrode wear. The on and off nature

of powering the reactor only reduces electrode wear. However, electrode wear is not eliminated. Electrode wear deposits CU^{2+} and Cu^{3+} ions in the water which can contribute to the increase in conductivity.

4.4 Electrical characterisation

The focus of the electrical characterisation is to measure the reactor power rating at different current settings. Within the 0.25 – 0.45 A current range, the current has a positive direct relationship with the discharge voltage and power as shown in Figure 4.2.

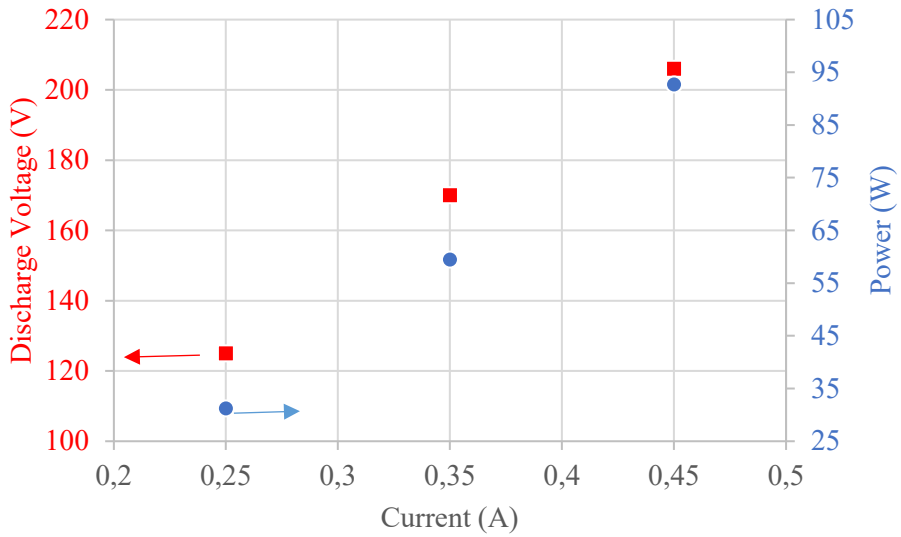

Figure 4.2 Power and Voltage as a function of operating current at atmospheric pressure

The formula for calculating the voltage followed the methodology utilised in previous work which utilised the same power supply (Govender, 2016).

$$V_{rms} = \sqrt{\frac{\sum_1^n (V^2)}{n}} \quad \text{.....(Equation 4.6)}$$

Where V is the voltage obtained from the oscilloscope measurements and n is the number of voltage data points between 10 000 and 60 000.

The power supply utilised in this study was DC hence the power of the plasma discharge was determined by multiplying the voltage by the current as described in section 3.4.4.

4.5 CBZ rates of degradation

The target pollutant, CBZ, was degraded as a single solution mixed with distilled water. The degradation of organic compounds in water by plasma treatment is predominantly an oxidation process by reactive species, for example, free radicals (•OH, O•, H•, O-, HO_2•), oxidants (H_2O_2, O_3), cavitation, shock waves, and UV radiation that can be generated by the plasma gas. The plasma treatment efficiency is driven by highly reactive species with a short half-life. The mechanism for cyclic organic compounds is complex and is dependent on numerous variables, for example, plasma gas makeup, reactor configuration and discharge type. (Jiang et al., 2014).

The extent of CBZ degradation at 10 minutes of plasma treatment, measured by the removal efficiency, is presented in Table 4.5. It can be observed from Table 4.5 that higher removal efficiency is favoured by higher currents and no air flow rate.

Table 4.5 Average removal efficiency of plasma treatment at different reactor conditions after 10 minutes of NTP treatment

10 mg/L initial CBZ concentration			**40 mg/L initial CBZ concentration**		
Current (A)	Flow rate (L/min)	Removal efficiency (%)	Current (A)	Flow rate (L/min)	Removal efficiency (%)
0.45	3	47.9	0.45	3	37.7
0.45	0	89.8	0.45	0	95.8
0.25	3	42.8	0.25	3	42.5
0.25	0	73.6	0.25	0	34.1

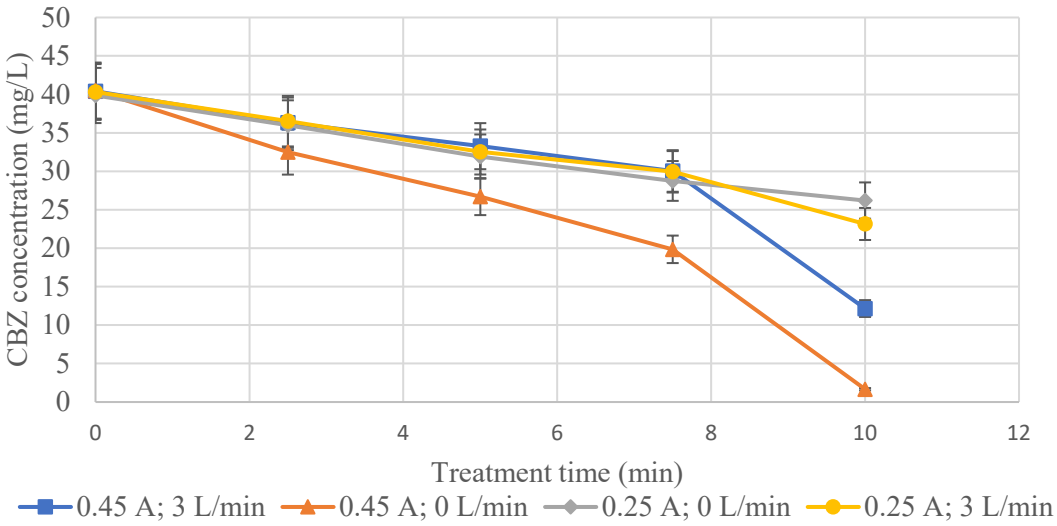

Figure 4.3 Time dependent degradation of CBZ at 40 mg/L starting concentration. **Error bars (vertical):** ±9%

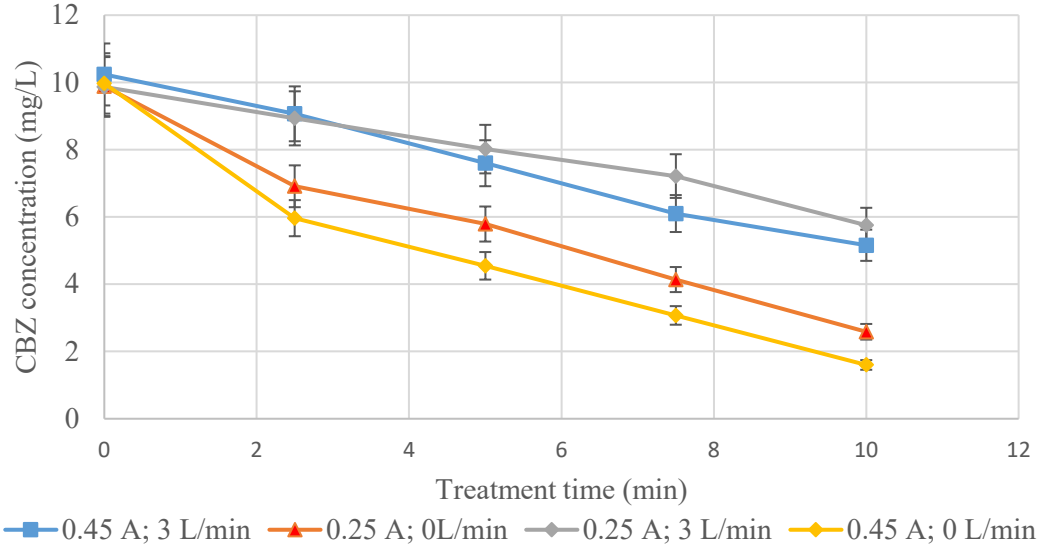

Figure 4.4 Time dependent degradation of CBZ at 10 mg/L starting concentration. **Error bars** (vertical): ±9%.

In Figure 4.3 and 4.4, the lines are not for modeling or to show reaction kinetics/rates but to graphically illustrate the decrease in concentration.

From the experimental results, given in Figure 4.3 and 4.4, it could be seen that steady-state conditions are not obtained within the 10 minutes treatment phase as stationary concentrations are not achieved within the 10 minutes of operation.

A common trend in this study is the detriment of higher gas flow rate on the degradation of CBZ. Better CBZ degradation is obtained with no air flow rate irrespective of the initial concentration; this trend is more evident in Figure 4.4. Lower flow rates may be beneficial as they improve the mass transfer of the reactive species from the gas phase to the liquid phase. However, it should not be concluded that lower flowrates favour higher degradation in all plasma reactor designs and for all operating gasses; for example an increase in pure oxygen flowrate increase oxidising radical and ozone density and consequently degradation (Sun et al., 1997).

Hence, it is an interesting result that support that available information on the low production of ozone in an arc or spark discharge. This is beneficial because high ozone concentration is not good for water quality.

Additionally, the introduction of air, while it is beneficial in terms of adding oxygen and enhancing the radical formation, has a negative side effect of disrupting arc stability due to the formation of bubbles and stirring the water. Thus, the discharge region is constantly under perturbation. This result is in agreement with Krause (2011), who noted an inverse relationship between air flow rate and degradation efficiency, particularly in a single solution as in this study.

There is a direct correlation between the current setting and CBZ degradation. As the current increases, and conclusively power according to Figure 4.2, electrons produced by the plasma discharges gains more electrical energy from the electric field. Therefore, more gas molecules will be ionized through electron. impact ionization (Zhang et al., 2008)(Zhang et al., 2007; Rong and Sun, 2014). Eventually, this will induce a higher production of active species production in the gas and liquid phase and more vigorous micropollutant decomposition.

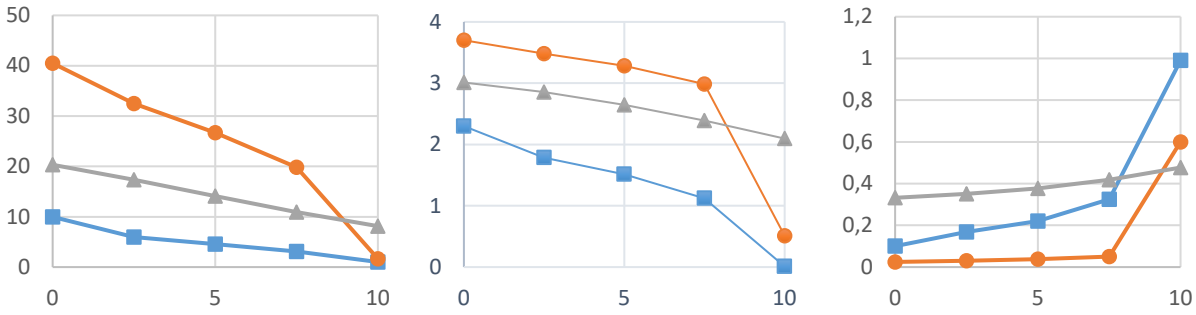

(a) **(b)** **(c)**

Figure 4.5 CBZ degradation plots **(a)** Concentration vs time **(b)** In (Concentration) vs time

(c) I/concentration vs time. Colour Legend: ■ 10 ppm starting concentration; ▲ 20 ppm starting concentration; ● 40 ppm starting concentration

From Figure 4.5, it can be inferred that the degradation of CBZ for 40, 20 and 10 mg/L follow zero order reaction kinetics though the rates for 10 and 40 mg/L appear to significantly change at 7.5 minutes (near straight lines for concentration versus treatment time in Figure 4.5 (a)). The order of the reaction is not dependent on the concentration of CBZ but the rate that active plasma species flux colliding with the surface molecules (Benetoli et al., 2011, Brisset et al., 2008). 10 and 20 mg/L appear to have similar rate constants; however, the kinetics for initial CBZ concentration of 40 mg/L after before and after 7.5 minutes of plasma treatment is very different and difficult to explain. It may be proposed that at 7.5 minutes of plasma treatment, the interaction of the CBZ degradation and by-products may initiate new kinetics.

Electrode wear deposited copper ions in the water. The copper ions may act as catalysts in an oxidation process similar to the Fenton reaction (Marković et al., 2015, Wu et al., 2012), but the electrode wear would be minimal as the reactor utilised low current. However, the catalytic effect of the copper ions in CBZ spiked synthetic wastewater treatment was not investigated in this study. Additionally, while copper ions may have a catalytic effect on pollutant degradation, the wear of the metal electrodes should be minimised as it adds metallic ion contaminants and reduce the life of the system.

Although the dynamics of all these factors noted by Jiang et al. (2014) are complex, an attempt to optimise the treatment process was undertaken.

4.6 CBZ degradation by-products

After determining the effectiveness of technology in treating pollutants in wastewater, key questions then include what is the pollutant being broken down into, and is the by-product more toxic than the parent compound? In this study, an initial qualitative characterisation of a pure CBZ and DCM sample was done to identify the mass to charge ratio (m/z) of the pure CBZ (Figure 4.6).

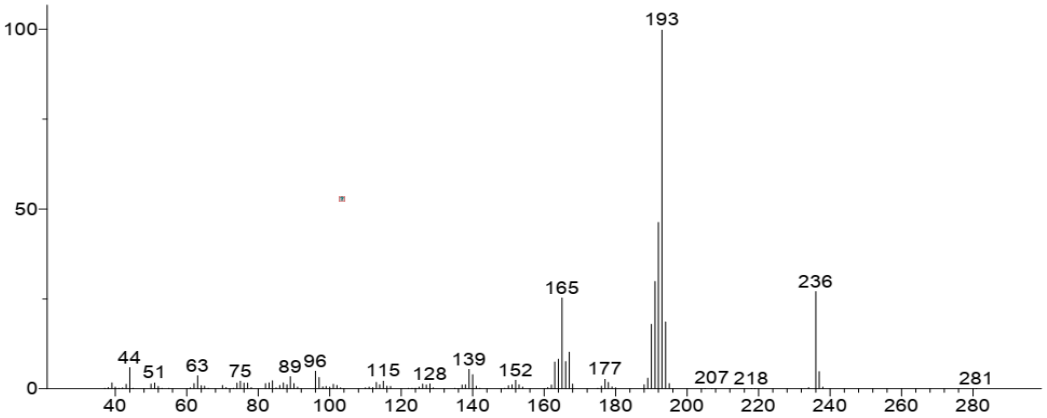

Figure 4.6 Chromatogram of pure CBZ by GC-MS in scan mode characterised by the CBZ m/z base fragments (198, 236 and 165)

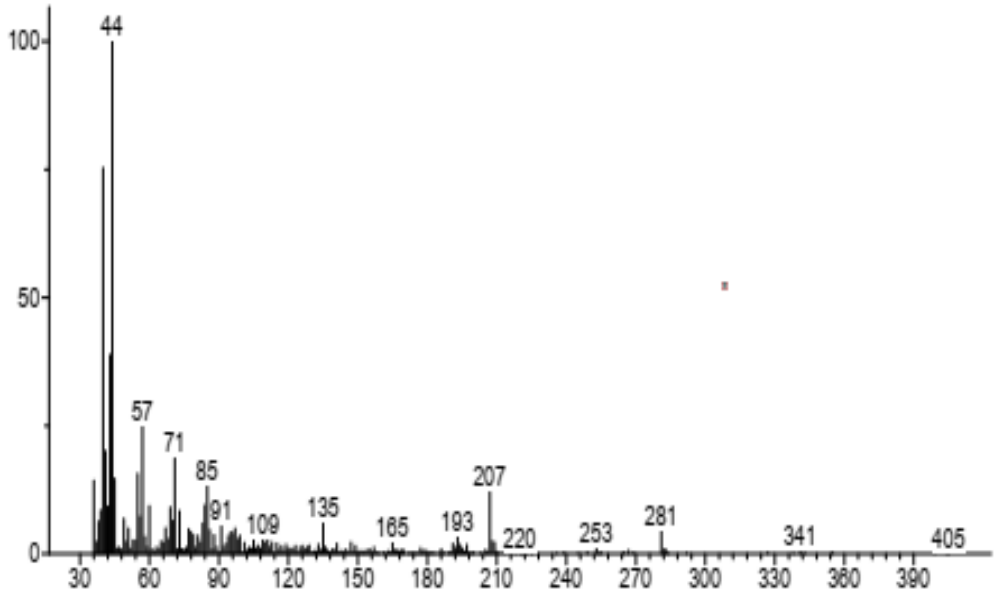

Figure 4.7 Mass spectra fragments CBZ after 10 minutes of plasma treatment at 0.45 A and 0 L/min

To identify possible degradation by-products, a comparison of fragments from the mass spectra and against the mass spectra of CBZ degradation by NTP degradation was conducted. CBZ degradation was confirmed as the CBZ identifier m/z fragments were no longer the base ions.

In all the qualitative results, a 44 m/z fragment present signifying the breaking of the CHON fragment from the nitrogen on the center ring of CBZ. Other key fragments, depending on the operating conditions, are 57, 71,97,121,135. The degradation mechanisms are beyond the scope of this study and numerous intermediates and by-products could be the possible products of CBZ treatment by NTP. Table 4.6 shows 5 possible by-products based on the most abundant m/z fragments.

Table 4.6 Possible CBZ oxidation by-products

Elemental Formula	Molecular Weight	Mass fragments
$C_2H_2O_4$	90	44, 45, 46
$C_{15}H_{12}N_2O_2$	252	44, 180, 207,
$C_{15}H_{10}N_2N_3$	266	44, 109,165
$C_{15}H_{11}C_1N_2O_4$	319	44, 57,71,
$C_{15}H_{12}N_2O_5$	300	107, 193, 257

An interesting result in some of the GC-MS chromatograms involved the identification of silicon-based compounds. It was concluded that the silicon was from the quartz covering the cathode as inspection of the quartz showed damage to the quartz (Appendix B2). The silicon could not be from excessive column bleed as the baseline of the chromatogram was stable and the mass spectra fragments did not show the characteristic column bleed m/z ions.

4.7 Plasma system optimisation

4.7.1 Model analysis

The total number of runs was 19, including three (3) replicates using the processing parameters at the center points. The model is a factorial model with a maximum of 3-factor interactions. Table 4.7 shows the experimental runs and the values for the removal efficiency and energy consumption for the runs.

Table 4.7 Removal efficiency and energy consumption at experimental design values

Run	Factor 1 A: Current (A)	Factor 2 B: Flow rate (L/min)	Factor 3 C: Concentration (mg/L)	Response 1 Removal efficiency (%)	Response 2 Energy consumption (kWh)
1	-1	-1	-1	73.13	0.0049
2	-1	-1	1	34.27	0.0051
3	1	1	-1	46.95	0.0155
4	-1	-1	1	34.78	0.0049
5	1	-1	-1	90.04	0.0152
6	1	-1	1	94.96	0.0149
7	-1	1	-1	42.81	0.0054
8	-1	1	1	42.57	0.0052
9	0	0	0	58.59	0.0123
10	0	0	0	59.96	0.0121
11	1	-1	1	96.84	0.0152
12	-1	-1	-1	74.54	0.0151
13	1	1	1	69.13	0.0156
14	1	-1	-1	89.50	0.0151
15	0	0	0	60.59	0.0120
16	1.	1	1	70.55	0.0157
17	1	1	-1	48.43	0.0153
18	-1	1	-1	42.83	0.0051
19	-1	1	1	42.48	0.0056

The model evaluation revealed that the lack of fit and pure error had 4 degrees of freedom(df) and 10 df, respectively. This is acceptable as the Design Expert recommendation is a minimum of 3 lack of fit df and 4 df for pure error to performa valid lack of fit test for the generated model.

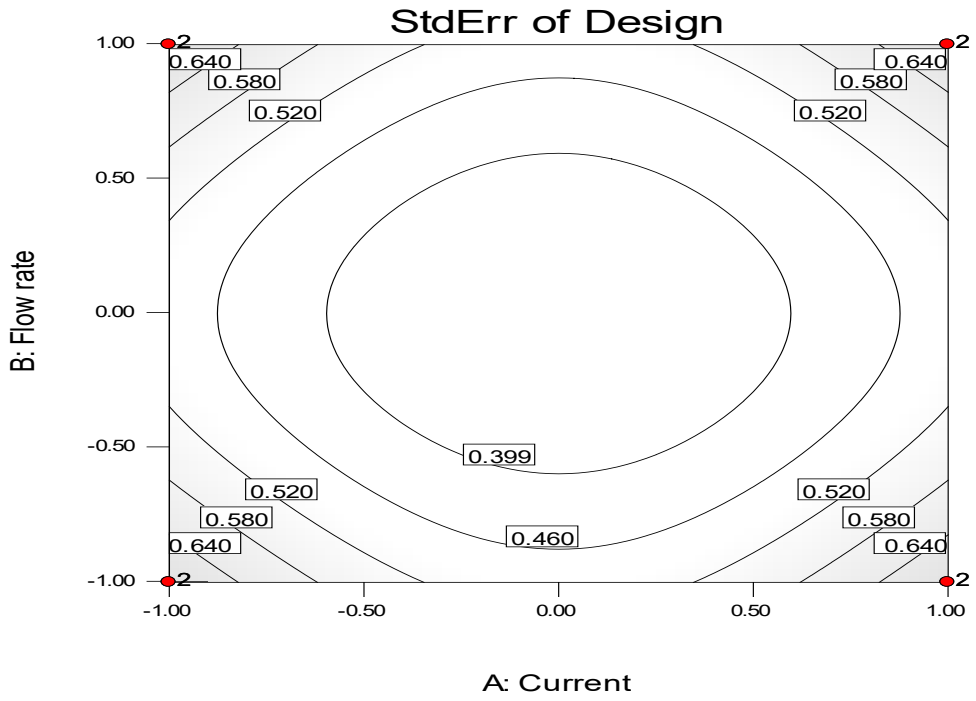

Figure 4.8 Design evaluation graph for standard error at -1level for concentration (10 mg/L) with the design pints marked in red at the corners of the plot.

Figure 4.8 shows the standard error of prediction for areas in the design space. The standard error should be low which is approximately 1.0 or lower. Figure 4.8 shows a maximum standard error across the region of interest of 0.640, which is acceptable. The design evaluation graph for +1 level of concentration (40 mg/L) also show a maximum standard error of 0.64

The ANOVA analysis was performed to determine the significance and adequacy of the regression models for both removal efficiency and energy consumption as represented by Figure 4.9. For both responses, no transform was assigned as the ration of the maximum and the minimum was less than 10, specifically 2.82 for removal efficiency and 3.2 for energy consumption. ANOVA analysis showed that the models were significant and had F values of 1407.29 and 2056.93for removal efficiency (Table 4.8) and energy consumption (Table 4.9), respectively. The values of the respective R^2 values are comparable. Additionally, the Adequate precision which measures the signal to noise are above the recommended minimum of 4. The conclusion from the ANOVA is that this model can be used to navigate the design space.

Table 4.8 Results of ANOVA for the factorial model for the removal efficiency

Source	Sum of Squares	df	Mean Square	F Value	p-Value Prob>F	Comment
Model	7620.59	7	1088.66	1407.29	<0.0001	Significant
A-Current	2971.07	1	2971.07	3840.66	<0.0001	
B-Flow rate	2055.49	1	2055.49	2657.11	<0.0001	
C-Concentration	34.84	1	34.84	45.04	<0.0001	
AB	519.95	1	519.958	672.14	<0.0001	
AC	1198.44	1	1168.44	1510.43	<0.0001	
BC	744.06	1	744.06	961.84	<0.0001	
ABC	126.73		12.73	163.82		
Curvature	15.29	1	15.29	19.76	0.0012	Significant
Pure error	7.74	10	0.77			
Cor Total	7643.61	18				

R^2 0.9990; Adjusted R^2 0.9983; Predicted R^2 0.9964, Adq pression 101.39

Table 4.9 Results of ANOVA for the factorial model of the energy consumption

Source	Sum of Squares	Df	Mean Square	F Value	p-Value Prob>F	Comment
Model	4.128E-004	7	5.897E-005	2056.93	<0.0001	Significant
A-Current	4.121E-004	1	4.121E-004	14375.23	<0.0001	
B-Flow rate	5.625E-007	1	5.625E-007	19.62	0.0013	
C-Concentration	2.250E-008	1	2.250E-008	0.78	0.3965	
AB	1.000E-008	1	1.000E-008	0.35	0.5679	
AC	0.000	1	0.000	0.000	1.000	

BC	6.250*E-008	1	6.250E-008	2.18	0.1706	
ABC	1.000E-008	1	1.000E-008	0.35	0.5679	
Curvature	9.080E-006	1	9.080E-006	316.75	<0.0001	Significant
Pure error	2.867E-007	10	2.867E-008			
Cor Total	4.221E-004	18				

R^2 0.9993; Adjusted R^2 0.9988; Predicted R^2 0.9978, Adeq Precision 91.394

Equation4.7 and 4.8 are determined by ANOVA as the equations which describe the relationship between the response factors and the significant independent variable.

$$Energy\ consumption = 0.010 + (0.005075 * Current) + (0.0001855 * flowrate) .. Equation\ 4.7$$

$$Removal\ efficiency = 62.17 + (13.63 * Current) - (11.33 * Flow\ rate) - (1.48 * Concentration) - (5.7 * Current * Flowrate) + (8.55 * Current * Concentration) - (6.82 * Flow\ rate * Concentration) + (2.84 * \text{Current} * \text{Flow rate} * \text{Concentration}) \ldots\ldots\ldots\ldots\ldots\ldots\ldots\ldots Equation\ 4.8$$

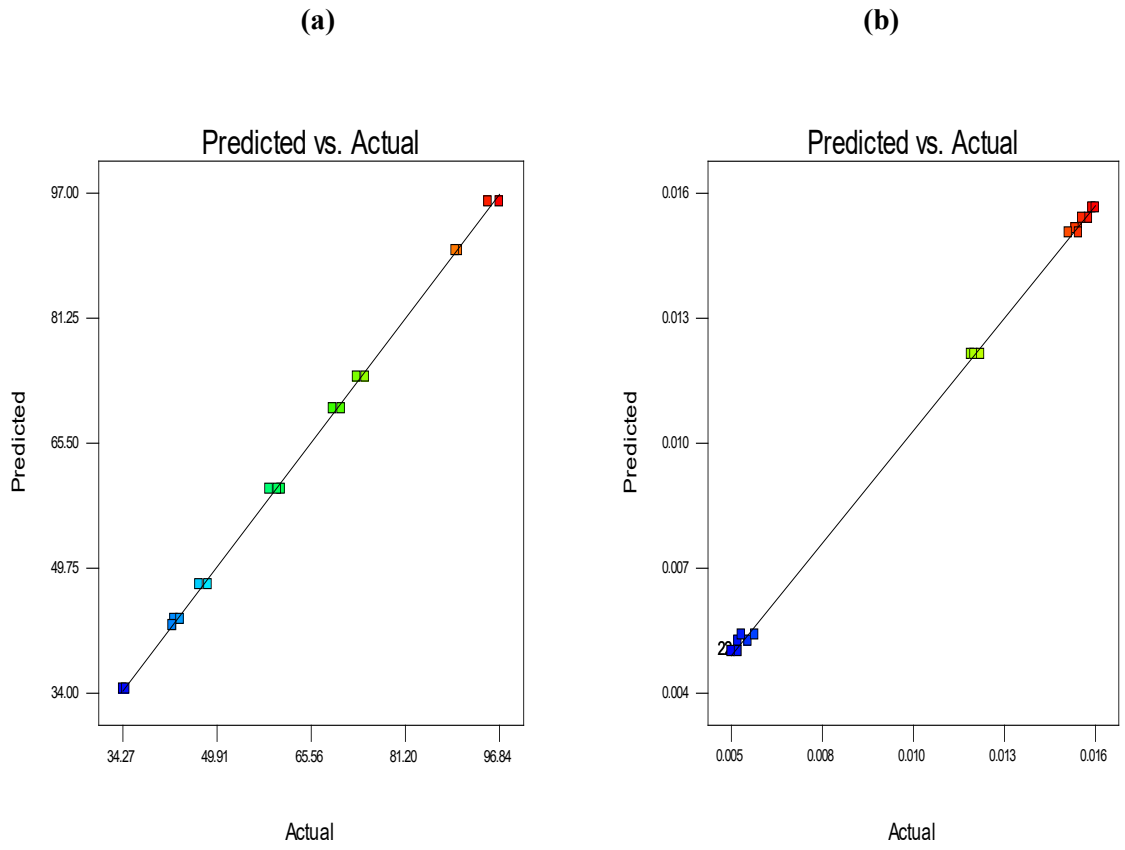

Figure 4.9 Experimental versus predicted results **(a)** Removal efficiency; **(b)** Energy consumption.

Figure 4.9 shows the comparison between the predicted values from the model generated by equation 4.7 and 4.8 against the actual experimental values.

4.7.2 Effect of process parameters on removal efficiency

The process parameters or interactions with p-values below the critical value of 0.05 are considered to have a significant impact on the removal efficiency (refer to Table 4.8). Current, flow rate, concentration, current-flow rate interaction, current concentration interaction and the flow rate-concentration interaction are the significant terms. Among the significant terms, the current, flow rate and current-concentration interaction are the most significant as they have the largest F value. The current and the current-flow rate-concentration interaction are the least significant terms as they have the smallest F (refer to Table 4.8). The effects of process parameters and their interactions in influencing CBZ degradation are presented in Figures 4.11 to 4.13. The discussion will focus on the effect of the two factor interactions on removal efficiency. Discus the effect of one factor, for example, current on

removal efficiency does not give much information as it would just determine if the factor and removal efficiency have a positive or negative relationship.

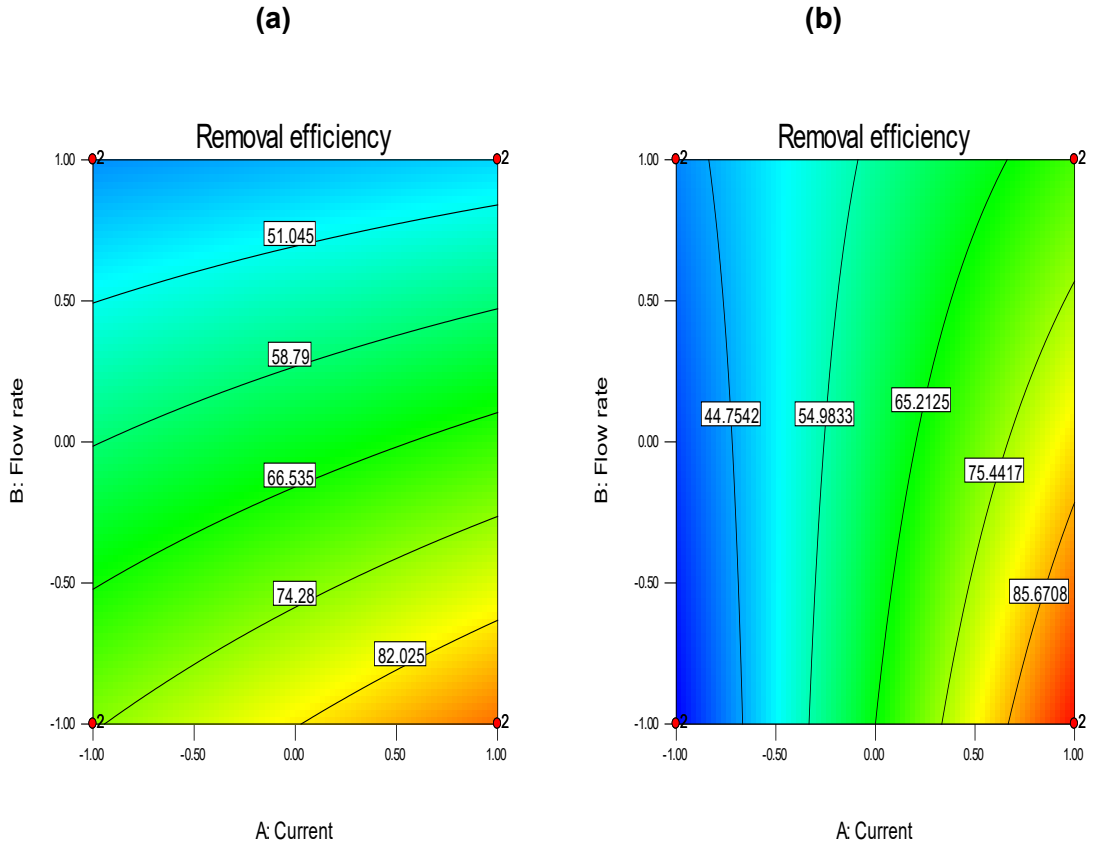

Figure 4.10 Effect of current and flowrate and their interaction on removal efficiency at **(a)** 10 mg/L; **(b)** 40 mg/L

Figure 4.10 (a) and (b) shows the effects of the current and flow rate on CBZ degradation at concentrations of 10 and 40 mg/L respectively. Irrespective of the starting concentration, an increase on current increases removal efficiency while an increase in air flow rate up to values less than 1 L/min increase the removal efficiency. Increasing the air flow rate above 1 L/min starts to reduce the removal efficiency. The current- flow rate interaction for the 10 – 40 mg/L has a maximum removal efficiency of 82 – 85 % respectively. Lower flow rates appear to favour enhanced removal efficiency for 10 mg/L starting concentration across the whole current range according to Figure 4.10 (a). Figure 4.10 (b) suggests that the effect of the air on removal efficiency for 40 mg/L is minimal as the contours are almost vertical (small angle to the horizontal), the effect of air increasing slightly as the current increases past 0.35 A.

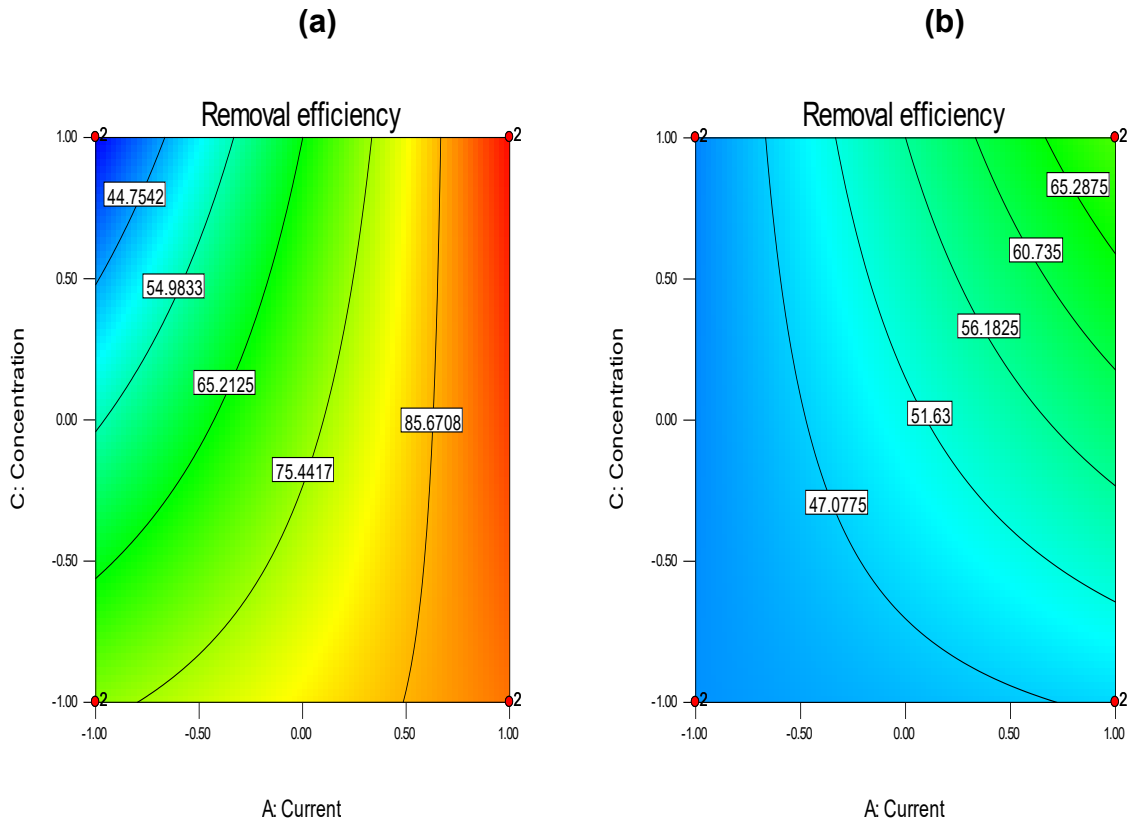

Figure 4.11 The effect of current-concentration interaction on removal efficiency at **(a)** 0 L/min; **(b)** 3 L/min

According to Figure 4.11, lower flowrate results in higher removal efficiency irrespective of the starting concentration or current result. The highest removal efficiency at 0 L/min is 85.67% (Figure 4.11 (a)) as compared to the highest removal efficiency of 65.29% at 3 L/min. Figure 4.11 (a) show that at 0 L/min, as the current nears 0.45 A, removal efficiency becomes independent of the initial concentration. Flow rate of 3 L/min cause an interaction of the current and concentration for any current or concentration range.

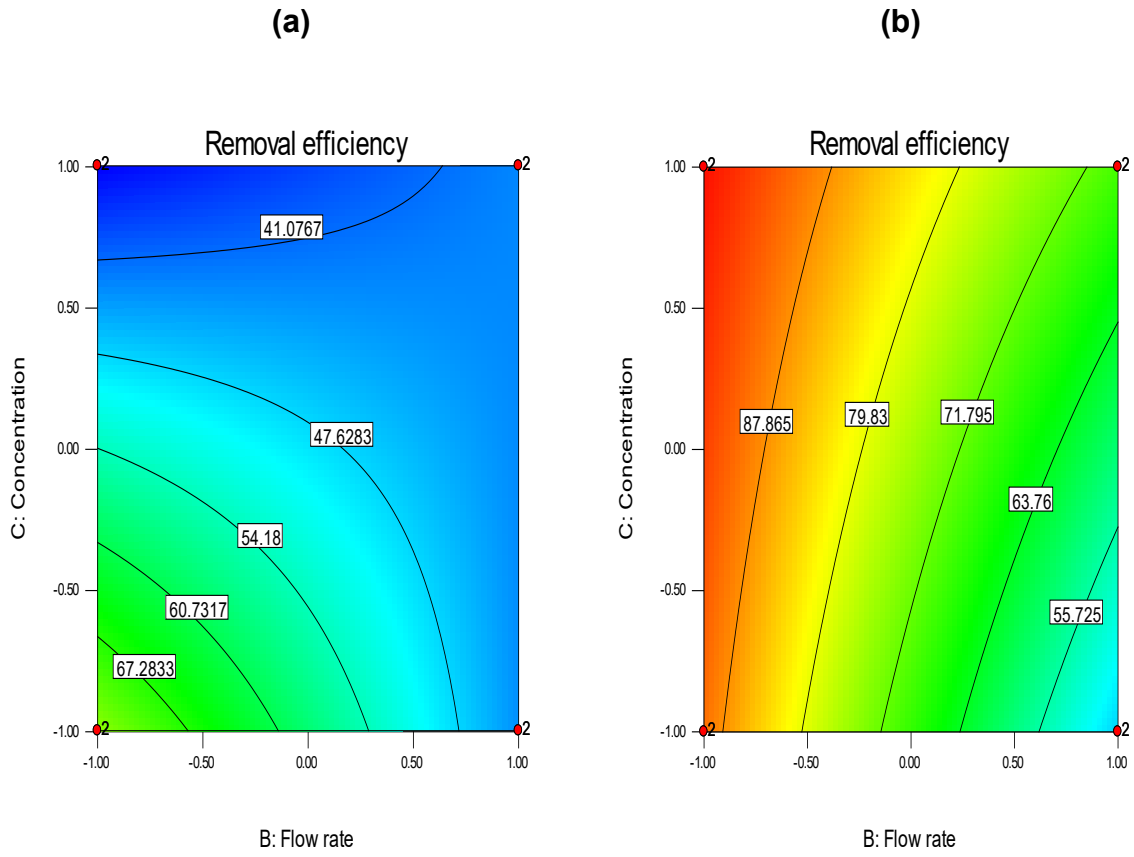

Figure 4.12 Effect of flow rate and concentration and their interaction on removal efficiency at **(a)** 0,25 A; **(b)** 0.45 A

Figure 4.12 show that an increase in the flow rate and initial concentration, individually or together, reduce the removal efficiency. The effect of the flow rate and initial concentration on removal efficiency is more marked for lower current setting (Figure 4.12 (a)).

4.7.3 Effect of Process parameters on energy consumption

The ANOVA results show the effect of the individual process parameters and p-values on energy consumption (see Table 4.9). The current and flow rate are significant factors as their p-values are below the critical value of 0.05. The current is the dominant factor affecting the energy efficiency of the plasma process with the highest F-value and lowest p-value. The discussion will only focus on the current and flowrate as they are the only two factors involved, and there are no interactions.

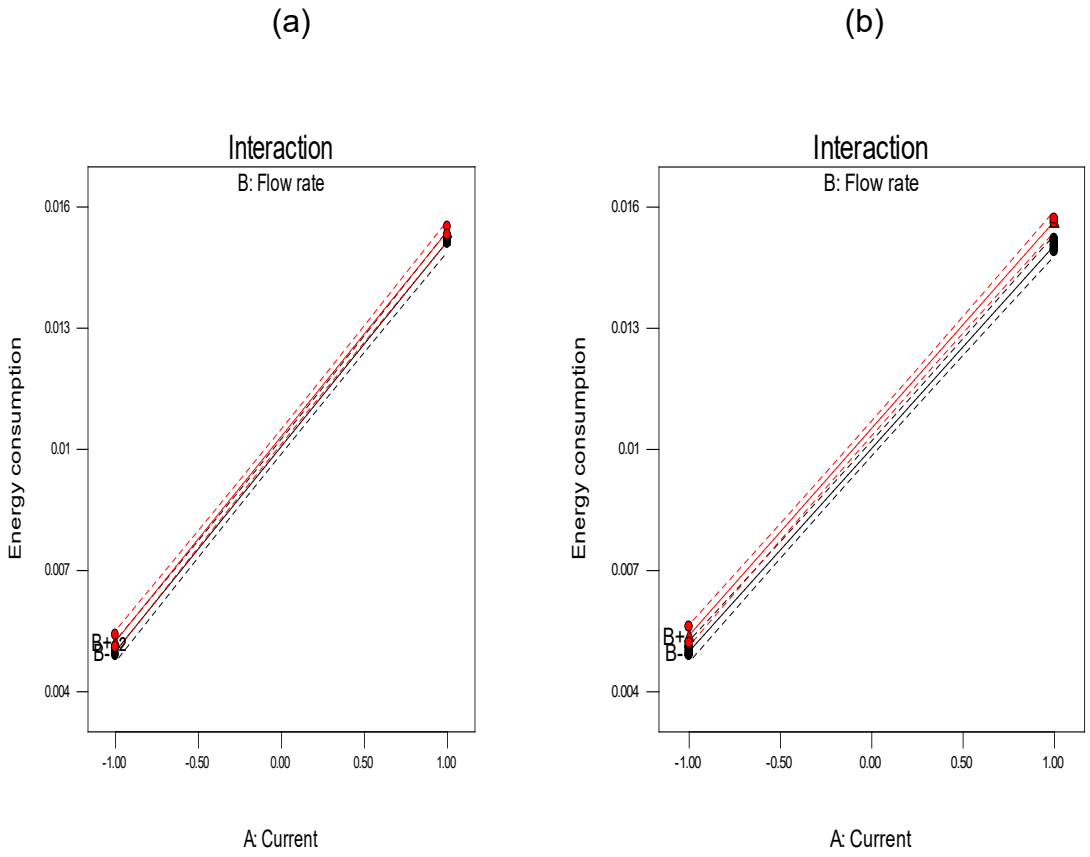

Figure 4.13 The effect of current and flow rate at **(a)** 10 mg/L and **(b)** 40 mg/L showing no interactions as demonstrated by the parallel red line and black lines.

Figure 4.13 show the direct relationship between the energy consumption and the current irrespective of the initial CBZ concentration or flowrate setting (the black line signifies air flow rate at 0 L/min and the red line shows the air flow rate at 3 L/min). While increasing the flow rate does result in increased energy consumption (the red line above the black line), the difference is minimal as the two lines are close together. The insignificance of the starting concentration for the 10 – 40 mg/L range is in agreement with the assertion that at initial starting concentrations below 100 mg/L, E_{EO} values are not affected by initial concentration (Bolton et al., 1996).

Figure 4.13, the current and energy consumption graph shows a straight line with a positive gradient at an approximately 45 ° angle for all current and flowrate variations and combinations. The observation is logical for DC as the power and eventually, energy consumption is directly proportional to the current (Equation 4.9).

The increase in energy consumption as a result of the increased flowrate may be due to the noted discharge instability at higher flow rate. Discharge instability results in the increase in voltage as electric

discharge ignition requires higher voltages (breakdown voltage) as compared to maintaining the discharge.

4.7.4 Constraint bound optimisation

Optimisation in this study is aimed at cost reduction as the process has very high operating costs. The most economic treatment involves reducing process costs (energy consumption and air flow rate and having the highest removal efficiency. Cost reduction involves setting the process parameters to the settings in Table 4.10.

Table 4.10 Optimisation constraints for economical operation

Constraint	Goal	Lower Limit	Upper Limit
Current	In range	-1	1
Flow rate	Minimise	-1	1
Concentration	Maximise	-1	1
Removal Efficiency	Maximise	33.9	99
Electricity consumption	Minimise	0.005	0.015

Optimisation focus is intuitive as it is trying to maximise output and minimise input. Costs related to the process include electricity and air hence the optimisation criteria were to reduce cost. The concentration was aimed at treating the highest CBZ concentration. The goal was to maximise CBZ removal efficiency and minimise electric energy consumption (reduce cost).

Numerical optimisation will be utilised as it searches the design space, using the models you created in the analysis, to find factor settings that meet the goals you define.

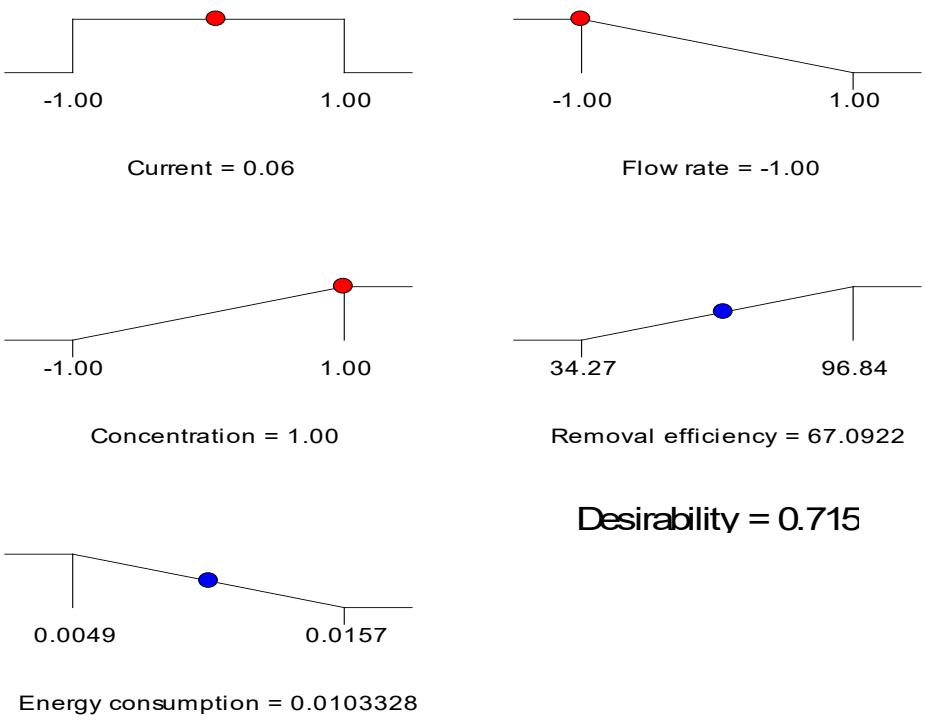

Figure 4.14 Sample numerical solution presented as a ramp (numerical solutions 1)

The set conditions produced 13 solutions. Figure 4.14 shows a sample solution and set values for the optimisation. It can be concluded that the removal efficiency and energy consumption of the plasma treatment process cannot reach the desirable values simultaneously, which results in the most economic runs. The set conditions and the outputs calculated had maximum desirability of 0.715. Desirability is an objective function that ranges from zero outside of the limits to one at the goal. The numerical optimisation finds a point that maximizes the desirability function (Table 4.11).

Table 4.11 Five sample solutions satisfying the optimisation criteria

Solution number	Current (A)	Flow rate (L/min)	Concentration mg/L	Removal Efficiency (%)	Electric energy consumption (kWh)	Desirability
1	0.06	-1.0	1	67.09	0.01033	0.715
2	0.04	-1.0	1	66.57	0.01024	0.714
3	0.03	-1.0	1	66.19	0.01018	0.714
4	0.12	-1	1	68.92	0.01063	0.714
5	0.07	-0.99	1	67.27	0.01037	0.714

4.8 System bench marking for CBZ degradation

It is imperative to compare the technology used in this work to other technologies that have been demonstrated to be able to treat concentrated CBZ wastewater. However, this poses a challenge on how to evaluate and benchmark the technologies in terms of i) operational costs (for example, energy consumption, chemical input), ii) sustainability (for example, resource use, carbon footprint, and iii) general feasibility (for example, physical footprint and oxidation byproduct formation).

To illustrate, Bolton et al. (1996) developed figures of merit (E_{EO}) based on electrical energy consumption only. However, the E_{EO} will not be used in the evaluation of the technologies. It should be noted that additional energy demand for chemicals or catalysts requirements is not reflected within this figure of merit hence the effectiveness of the EEO values lie only in electric energy assessment and will easily favour system which utilise electricity and chemicals, for example, UV/H_2O_2 as the chemical aspect is not considered.

4.8.1 Context of benchmarking

The context of this comparison is for the evaluation of small decentralized disinfection systems, which will be treating less than 200m^3/day. The basis for the comparison is 1 m^3 of wastewater. These systems will most likely be in the tertiary phase of wastewater treatment. Examples of these small volumes but high contaminated wastewaters are from hospitals, industries, and landfill leachate. An operation unit-based approach was used for the evaluation. Every attempt was made to use data and conditions from plants with similar contaminant levels. It is highly unreliable to make a comparison of wastewater treatment costs for different technologies if there is no data in the range of the water quality parameters.

For example, extrapolations from ng/L to mg/L and vice versa, giving rise to highly speculative results (Parsons, 2004).

4.8.2 Assumptions

The following assumptions are used in the evaluation are:

1. Only systems capable of degradation to a minimum of 90% CBZ degradation for wastewater with CBZ in the mg/L range are considered.
2. This is an evaluation of wastewater treatment systems only at the tertiary stage.
3. Operational costs are for the specified unit operation and auxiliary systems only.
4. The operational costs will be focused solely on the cost of chemicals (catalysts if applicable) and the process equipment and chemical delivery systems' electricity cost. Part replacement and cleaning costs are not included.
5. Electric power cost is 153.805 c/kWh (VAT included, excluding fixed monthly charges).
6. Water pumping costs are excluded as they are assumed to be equal for all systems.
7. Cost break down for the individual chemical and energy components is the basis for the costing methodology is used to quantify costs (see Appendix C)
8. South African Rand (ZAR) 14.8 to one United States of America Dollars ($) exchange rate is used for conversions (12 Nov 2019 exchange rate).
9. Historic prices in $ or ZAR are adjusted for inflation by an inflation calculator.

Although reverse osmosis and adsorption on activated carbon (AC) based system are effective in CBZ removal, however, these were not included in the evaluation as they pose an additional problem of what to do with the concentrated CBZ on the membranes or on the AC.

4.8.3 CBZ degradation benchmarking results

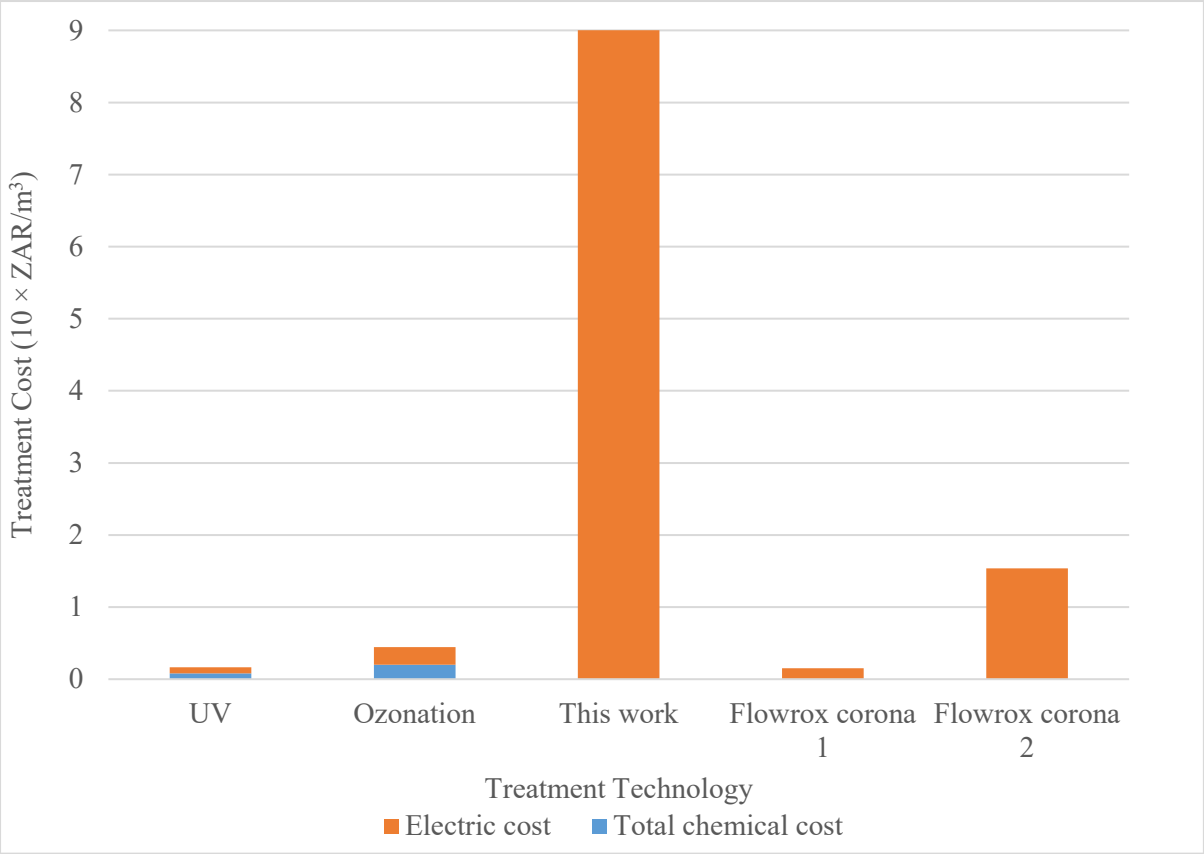

Figure 4.15 CBZ treatment operational cost comparison of technologies.

Figure 4.15 shows that all the systems show a common trend of electricity being the largest cost contributor. Thus, the type of power supply has a very significant impact on the treatment cost. All the other two systems except the reactor used in this work use AC power sources.

The reactor used in this work shows the highest treatment cost, with the cost being entirely made up of electricity cost. However, the result is for a process that has not been optimised and treated exceptionally high CBZ concentrations up to a maximum of 40 mg/L. Additionally, the result should be taken in the context of the 90% CBZ degradation as there are technologies that have less cost per cubic metre but cannot degrade CBZ in the mg/L range by up to 50%.

The Flowrox Corona is an AC powered commercial plasma-based unit rated at 2kW and a flow rate of 1-25 m^3/h depending on the condition of the water. The purpose of the Flowrox corona in Figure 4.15 is to illustrate the negative effect of increasing starting contaminant concentration hence low throughput on treatment cost for the Flowrox Corona system. Flowrox corona 1 is for 25 m^3/h through suitable for possibly CBZ in the ng/L range, while Flowrox corona 2 is for throughput due to dilute CBZ

concentrations, and Flowrox corona 2 shows the unit operating at l m^3/h throughput due to more treatment time required to treat a high mg/L CBZ concentrations.

Studies on AOPs show that pulsed DC or AC reduced energy consumption by more than 60 % (Hiolski, 2019); therefore, it can be theorised that the use of an AC power source may reduce the treatment cost of the NTP used in this study.

4.9 Conclusion

This study investigated the degradation of CBZ by a plasma discharge produced under reactor conditions.

The plasma reactor utilised in this study was capable of CBZ degradation of 93% ± 4% for 10 mg/L and 40 mg/L at 0.45A and 0 L/min. In this study, the qualitative analysis of the CBZ spiked wastewater showed that plasma treatment mostly degrades the CBZ into heavier compound as demonstrated by the m/z of the fragments.

Regression models developed to describe the relationships between the plasma discharge process parameters and responses verified by the analysis of variance. Discharge current and flow rate are the most significant parameter influencing CBZ degradation. The results show that CBZ degradation increases with increasing current and a combination of current and concentration but decreases with the increase of flow rate, concentration, current-flowrate combination, flowrate-concentration combination. Energy consumption is described by a simple model with current and flowrate as the only significant terms. The results show that electricity consumption increases with increasing current and flowrate. Optimisation shows a minimum of 67% removal which is higher than most technologies and good as it degrades the CBZ. Energy consumption of on average 0.01 kWh is calculated by the optimisation constraints.

The high energy consumption noted in some of the experimental runs, may be feasible if the reactor is used for treating pre-concentrated wastewater streams, for example, hospital or industrial wastewater However, this is subject to further study.

Chapter Five

Escherichia coli (ATCC 25922) results and discussion

5.1 Introduction

Electrohydraulic discharges generate intense shockwaves, UV radiation, high energy particles, and reactive radicals. In this study, it is proposed that the synergy of the physical phenomena and chemical species are responsible for the inactivation of *E. coli*.

This chapter fulfils research objectives three and focuses on the results and discussion of *E. coli* results. An attempt to ascertain the individual contribution of the various chemical species and physical phenomena towards the *E. coli* inactivation is made and discussed based on the reactor geometry and imaging of inactivated cells. Non-thermal plasma literature on bacterial inactivation rarely attempts to investigate the contribution of the metal electrode wear towards inactivation. Therefore, a section of the chapter documents the results of a preliminary investigation into the effect of the electrode metal ions deposited in solution during plasma treatment.

5.2 Electrode gap determination

The first step in the *E. coli* inactivation study was the determination of the suitable electrode gap. The electrode gap is a critical aspect of the NTP discharge. The power supply and power supply polarity determine the maximum electrode gap as it should be able to supply the breakdown voltage to initiate the electric discharge.

The ESSWW utilised in this study is a matrix of the bacterial cells and the broth, which impacts the water's physical and chemical properties in a complicated way. It was essential first to determine the suitable electrode gap. The electrode gap was varied between 2 mm and 4 mm. The electrode gap should be as large as possible to generate the largest plasma volume yet sustaining a stable discharge. CBZ degradation work in chapter four demonstrated the 2 mm gap as a suitable electrode gap, so it was used as the minimum electrode gap.

The electrode gap determination was a qualitative process involving the analyses of selected characteristics of the discharge as well as the effects of the discharge, as shown in Table 5.1.

Table 5.1 Discharge characteristics used in electrode gap determination

Discharge characteristic	Electrode Gap (mm) 2	4
Ignition of an electric discharge	Consistent visible electric discharge.	Dynamic discharge properties as some time there was no visible discharge.
Discharge stability	The discharge was visibly stable and consistent with minimum interruptions	The discharge was not stable as it was characterised by an on and off characteristics
Brightness of UV	Dull UV	Dull UV
Temperature Increase	A temperature increase of less than 5 °C	A marked temperature increase of up to10 °C
Electrode wear	Noticeable electrode wear as shown by a change of colour to a light brown colour.	Marked electrode wear as demonstrated by the darker brown colour and visibly noticeable electrode wear

The **ignition of an electric discharge** is characterised by numerous physical process to ensure that there are ample charged carriers to maintain the discharge between the static electrodes (Höft and Huiskamp, 2018, Schoenbach et al., 2008). The ignition of an electric discharge is a function of the electrical architecture of the power supply and the water properties between the two electrodes. In both the 2 mm and 4 mm gap, there is a discharge as shown by the change in voltage readings on the oscilloscope indicating the flow of current. However, for the 4 mm gap, there is a on and off visible discharge which could be a characteristic of spark discharge or a silent electric discharge. It is possible that a combination of the nutrient broth and the large4 mm gap could be acting as a dielectric between the electrodes.

In this study, **discharge stability** means a continuous stable discharge with a minimum number of transient phenomena from one type of discharge to another. A stable continuous discharge is preferred as it ensures a steady and consistent production of chemical species and propagation of shock waves to inactivate the pathogens. Transient phenomena as observed in the electric discharge produced by the 4 mm electrode gap introduces more variables into the treatment process as different types of discharges will be contributing to the discharge.

Temperature is critical in pathogen inactivation. The stock *E. coli* broth is maintained at 4 °C then diluted with distilled water at room temperature, so the starting temperature for the water used in the gap determination experiments was 19 ± 1.1 °C. For the 2 mm gap, the temperature increase was less than 5 °C, while for the 4 mm gap, the mean temperature increase of 10 °C was recorded. The premise

of conventional sterilisation is the utilisation of moist or dry heat. For instance, in autoclaving, moist heat under pressure in the form of steam at a temperature of 120 °C is contacted with items to be sterilised for 15 minutes or more (Gopal, 1978). However, heating wastewater for inactivation of pathogens is not economically feasible due to the high heat capacity of water and the volumes involved. However, most non-thermal plasmas operate at low temperatures (20 – 70 °C). It can be inferred that the contribution of the thermal effect of plasma on bacterial cells is not significant. Some non-thermal plasmas, for example, DBD discharges, can exhibit elevated temperatures in localised regions in the reactor hence for these electrical discharges, the effect of heat must be taken into consideration (Fridman, 2008). In this work, heat has no substantial contribution to the sterilisation effect of the plasma as the maximum temperature recorded is less than 30 °C and the treatment time is 3 minutes, sterilisation by heat requires higher temperatures for longer periods.

The electric discharge produced some **UV radiation**. However, in this setup, it could not be established which electrode gap produced brighter UV light due to the semi-opaque nature of the synthetic *E. coli* wastewater. UV pathogen inactivation is prone to water turbidity as it affects transmittance and delivered dose (Christensen and Linden, 2003, Shaban et al., 1997), thus favouring clear water for effectiveness. In this study, the UV may not significantly contribute to inactivation as the water has high turbidity.

Electrode wear in electrical discharges in a liquid application has been reported in both AC and DC power supply applications (Perinban et al., 2019). In wastewater application, electrode wear should be avoided as it deposits metal ions in the water which are strictly regulated. For wastewater, the copper stipulated discharge limit ranges from 40 µg/L to 3 mg/L depending on location, discharge volume etc. (Chang et al., 2002, Boulay and Edwards, 2000). In this study, the 4 mm gap resulted in more electrode wear as demonstrated by a darker brown colour, indicative of the copper in solution, after the end of a 180 seconds treatment period. Additionally, visual inspection of the electrode showed that the electrode with a 4 mm gap was damaged more by the treatment. Electrode wear should be avoided or at least minimised as the metal ions represent another pollutant which will require an additional unit operation to be removed/reduced from the treated wastewater before discharge into the aquatic environment.

After considered the effect the electrode gap has on parameters in Table 5.1, the 2 mm electrode gap was decided as the most suitable electrode gap to utilise in this study.

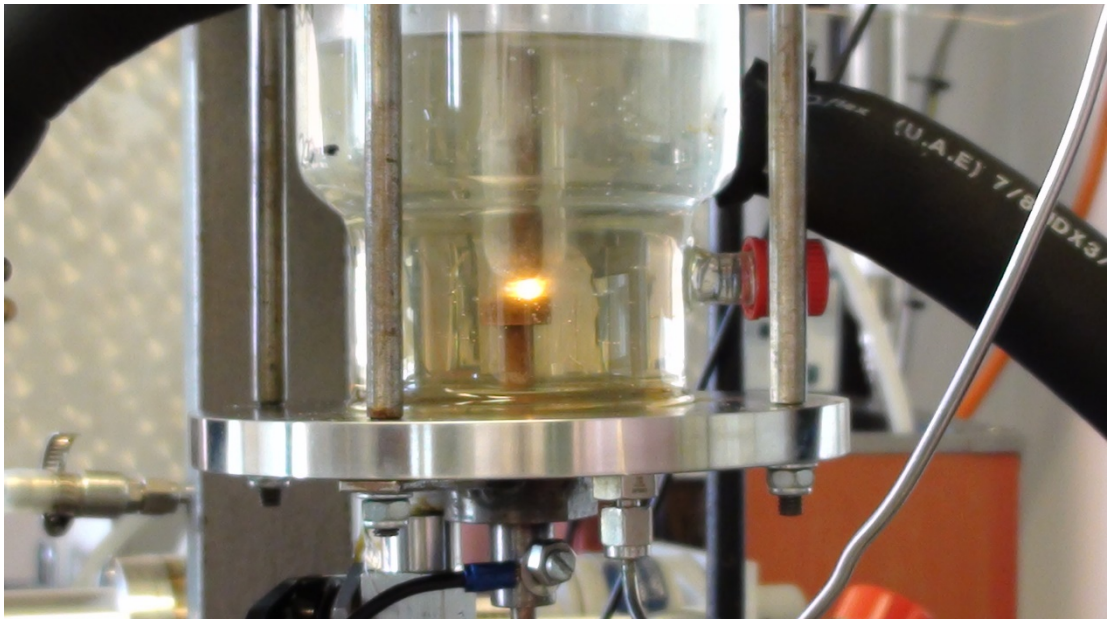

Figure 5.1 Stable electric discharge in ESSWW at 2 mm electrode gap, 0.45 A and 0 L/min (note the ESSWW was not clear)

5.3 Electrical characterisation

The electrical characterisation was intended to measure the power rating of the reactor at different current ratings as electrohydraulic discharges in ESSWW with nutrient broth and excretion by-products of the biological process metabolism of the cells in the water inherently more complicated as compared to discharges in gases (Höft and Huiskamp, 2018).

The power supply utilised in this study was DC, hence the power of the plasma discharge was determined by multiplying the voltage by the current as described in section 3.4.4. For *E. coli* inactivation experiments, the formula for calculating the voltage followed the methodology utilised in previous work which utilised the same power supply (Govender, 2016) and is the same as equation 4.6.

Figure 5.2 shows the electrical characterisation of the plasma reactor. The power was calculated using equation 4.7. The discharge voltage decreases with increasing current. A similar inverse current voltage characterisation is reported in literature (Fulcheri et al., 2010). The voltage current relationship depends on the physical characteristics of the environment which the plasma is generated. The voltage current characteristic observed in the ESSWW experiments could be a behaviour of a glow discharge.

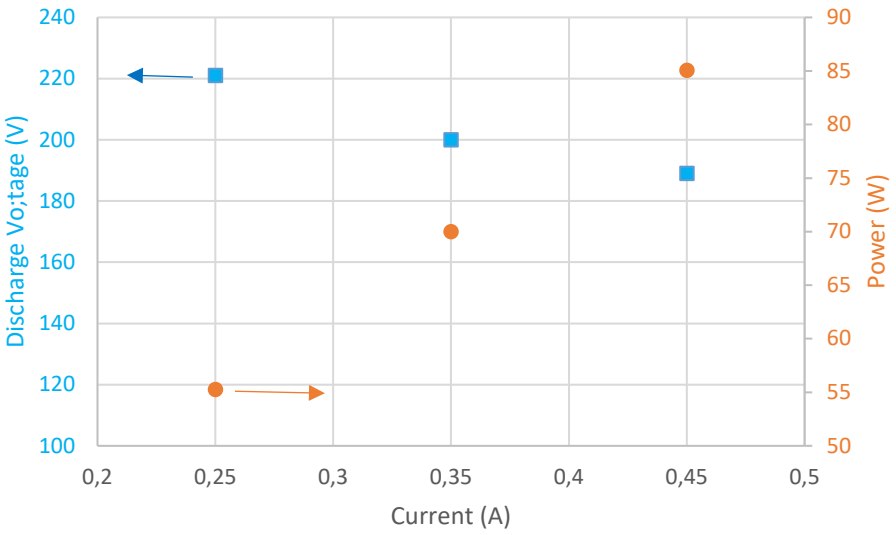

Figure 5.2 Power and Voltage as a function of operating current at atmospheric pressure for *E. coli* inactivation experiments

5.4 Water quality parameters

As previously noted, the plasma-liquid interactions are very complex, and understanding the system in terms of the chemical and physical processes is minimal. However, to gain insight into *E. coli* inactivation, experimental determination of the influence of the plasma treatment on pH and conductivity had to be done.

5.4.1 pH

The attention to pH is due to the possible synergy pH may infer to plasma effectiveness in waterborne pathogen inactivation. There are conflicting results on the effect that pH has on inactivation. Some researchers concluded that inactivation of *E. coli* in water with a pH of approximately 3.4 is not favourable as it required longer plasma treatment time than plasma treatment in non-acidic environments (Satoh et al., 2007). However, other researchers have confirmed that an acidic environment could not bring significant differences in the disinfection of microorganisms as compared to plasma treatment in non-acidic conditions (Oehmigen et al., 2010, Qian et al., 2019). Still, other researchers propose that a lower pH is beneficial as it promotes the penetration of the reactive species through the cell wall, and aiding in bacterial inactivation through cell wall disruptions (Ikawa et al., 2010, Bourke et al., 2017).

In all the experimental runs in this study, a decrease in the pH value, from the pre-plasma treatment value, was recorded in the water after 180 seconds exposure to plasma. The pH of the water dropped from an initial mean value of 7.5 ± 0.10 to 5.15 ± 0.1 at the end of plasma treatment.

It is interesting to note that the pH value change was minimal (a decrease of 2.35). Other researchers have also observed a small pH change after plasma treatment. Sterile water alone decreased to a pH of approximately 3.2, while it required significantly more time for the pH value to stabilise at 4.5 and 4.2 in water with nutrient broth culture and in sterile water with the bacteria suspension, respectively, using a low-frequency electric discharge (Laroussi and Leipold, 2004). The small pH changes may be due to the buffering capacity of the nutrient broth in the water. Additionally, the short plasma exposure of 180 seconds could be the reason for the small pH drop. Possibly longer treatment time may have resulted in more significant pH drops.

The change in pH may be due to the multistage reaction at the gas-phase interface and in the liquid bulk. These reactions involve the NO_x, O, O_3 species.

One source of variance on the reported effect of plasma on wastewater pH with waterborne pathogens is the time after plasma treatment when pH measurements are made. In this study, pH measurements were made within 5 hours of the plasma treatment. The same sample may show different pH value depending on the time after plasma treatment that the pH measurement is made. A decrease in pH after storage of plasma-treated wastewater has been reported by other researchers, a possible explanation for the pH drop may be the oxidation of NO_2 to NO_3 in the plasma-treated liquid over time (Rashmei et al., 2016).

5.4.2 Conductivity

Conductivity changes during plasma are a result of chemical species and the addition of metallic ions from electrode wear. Electrode erosion as a result of electrohydraulic discharge in liquids releases both metallic nanoparticles and metal ions in the bulk liquid (Potocký et al., 2009). The introduction of metal ions and nanoparticles is proposed to be a result of a series of physical and chemical phenomena which is initiated by current heating leading to electrode material melting (Goryachev et al., 1997, Lukes et al., 2012)

In addition to the pH measurements, also changes in solution conductivity were measured. The initial conductivity was 0.24± 0.06 µS/cm. The general trend is for the increase in the initial conductivity due to plasma treatment. which produced a final conductivity of 273 ± 7.2 µS/cm.

Together with the pH drop explained in the pH measurements (Section 5.3.1), the increase in conductivity delivers additional experimental evidence about the production of charged species in the treated solution. However, Equation 4.5 (Section 4.4.1), particularly in the case of synthetic bacterial wastewaters, does not exhaustively explain the increase in conductivity as there are other ions and biochemicals (nutrient broth, excretion) influencing the final conductivity value. The explanation of the conductivity measurements in this E. coli study is complicated as the wastewater has a nutrient broth

hence introducing a matrix effect. Additionally, the biological process of the cells and the by-products of the biological process may affect the conductivity more significantly. Also, electrode wear deposits metal ions which contribute to the conductivity.

5.5 Effect of initial E. coli population density

The operational limit of the *E. coli* population density that the reactor can treat had to be determined to ascertain if the reactor can inactivate *E. coli* population densities reported in wastewaters. *E. coli* cell density in sewage and the aquatic environment has been reported to vary over a wide range from as low as 100 CFU/mL (Omar and Barnard, 2010) to as high as approximately 2 $\times 10^7$ CFU/mL (Huijbers et al., 2020). The *E. coli* concentration was steadily increased to determine the limits of the system as shown in Table 3.5.

Table 5.2 shows the log reduction figures of Run 3 -5 with increase in treatment time and demonstrates that lower initial *E. coli* concentrations require less treatment time (Run 3 has total inactivation at 60 seconds while Run 5 which has a higher initial *E.coli* density requires 120 seconds for total inactivation)

Table 5.2 Results on the investigation of the effect of initial E. coli density

Treatment Time (sec)	Log reduction with treatment		
	Run 3	Run 4	Run 5
0	0	0	0
30	4.60	3.233	0.825
60	NG	3.427	1.879
90	NG	NG	2.210
120	NG	NG	NG
150	NG	NG	NG
180	NG	NG	NG

Note: NG represents no growth of the bacteria culture which implies total inactivation of E. coli

The study demonstrated that total E. coli inactivation for cell densities up to 2.5×10^7 CFU/mL is achieved by 180 seconds of plasma treatment using the reactor utilised in this study. Intuitively, higher E. coli densities required more treatment time and the result agrees as 3.96×10^4 and 2.5×10^7 CFU/mL initial cell densities required 60 seconds and 120 seconds treatment time respectively for total inactivation. The relationship between the initial cell density and the treatment time required for total

inactivation does not appear to be linear. Reported plasma treatment times in literature range from less than 1 minute to more than 10 minutes. Plasma treatment time is a function of the type of plasma. The power supplied to generate the plasma, the initial cell density and the cell culture composition. It should be noted that some cell cultures have a nutrient broth which consists of different nutrient sources that can interact with the plasma generated reactive species, so increasing or decreasing the inactivation effect of the plasma., depending on its composition. Nevertheless, the influence of the ager was beyond the scope of this study, and there is little literature on this subject.

The cause of bacterial inactivation of bacteria by plasma involves numerous plasma species, for example, high energy charged species, reactive neutral species and UV photons. This section of the discussion attempts to give insight into the contribution of the various plasma species in E. coli inactivation in the reactor utilised in this study. UV radiation and have already been discussed hence the section will major on charged particles and reactive species.

Several investigators have attributed a significant portion of the inactivation ability of plasma to reactive neutral species, for example, O, O_2*, O_3, OH, NO and NO2) (Laroussi, 2002, Fridman, 2008). In this work, the Reactive Oxidative Species (ROS) (OH and HO_2 radicals), due to their short lifetime after production and limited diffusivity in the liquid bulk, are expected to make minimal contributions to the inactivation as they are confined to the 2 mm region between the electrode gap where they are produced. In DBD, the contribution of the ROS may be significant as the plasma volume is significant as compared to the total reactor volume.

There has been a bias in literature towards the investigation and documentation of the of UV radiation and reactive species. The result is that the contribution of high energy electrons and ions has not been exhaustively investigated. The contribution of charged particles may be significant, especially in electrohydraulic discharges since the plasma is in direct contact with the bacteria as in this research (Fridman et al., 2007, Fridman, 2008). The exact effect of the charged particles may be due to their influencing the rupture of outer cell membranes (Guo et al., 2015). The contribution of the charged particles has been noted to be significant in gram-negative bacteria as their biological structure has a thin outer membrane and murein layer, which is similar to the *E. coli* in this study. According to studies by Laroussi (2002), charged particles likely have minimal contribution to the inactivation of Gram-positive bacteria, as it has no outer membrane but has thick and protective outer murein layer, which provides enhanced bacteria higher strength and rigidity.

The proposition that the charged particles were causing cell wall rapture was tested in this study by utilising SEM to try and determine if plasma treatment inactivation is associated with physical damage to the E. coli cells. Figures 5.3 (a) show a cell before plasma exposure and Figure 5.3 (b) after 90 seconds of plasma treatment. Figure 5.3 (c) the cell after 180 seconds of plasma treatment and shows

that the plasma exposure raptures/perforates the cell wall possibly leading to the exposure of the internal cell contents being exposed to the outside environment thus causing inactivation. However, Cell A in Figure 5.3 (c) does not show any visible cell wall damage, hence it could be inferred that cell wall damage may not be the only inactivation mechanism or possibly the cell wall damage is not visible.

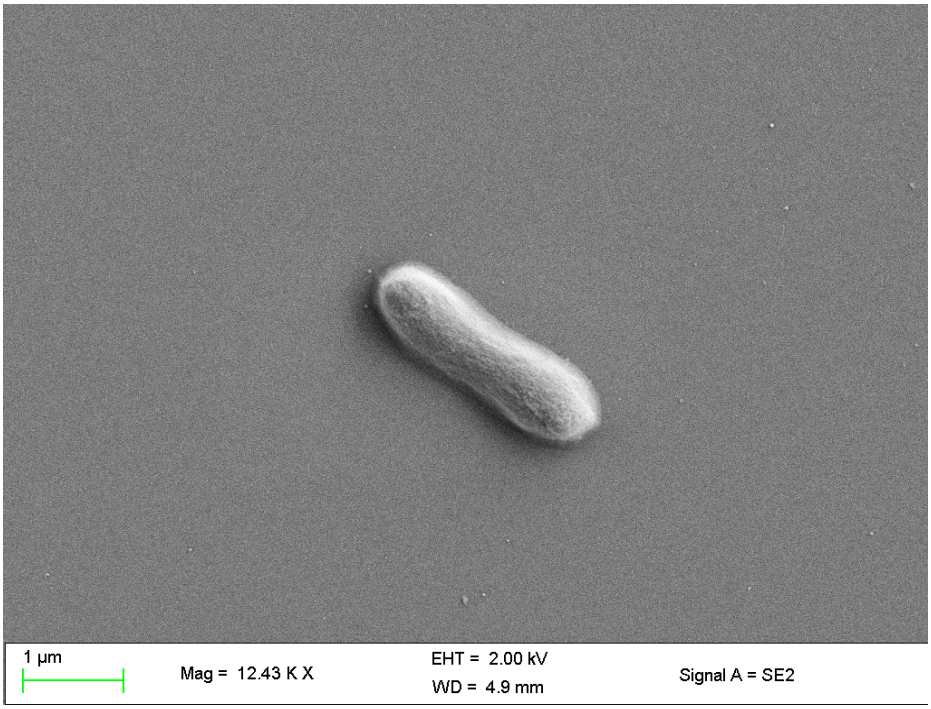

Figure 5.3 (a) *E. coli* cell before exposure to plasma treatment

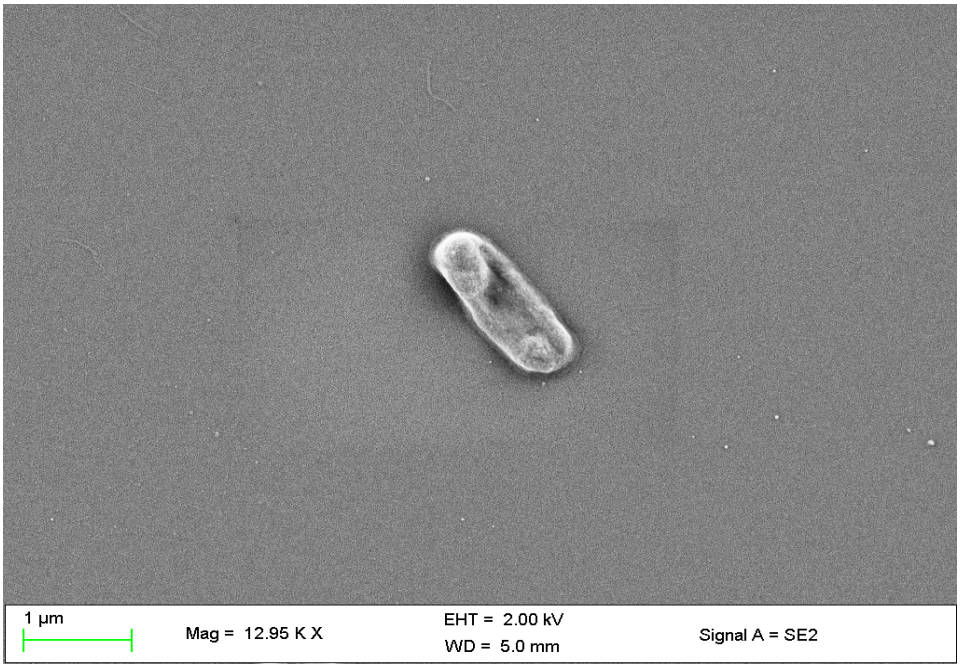

Figure 5.3 (b) Damaged *E. coli* cell after 90 seconds of plasma exposure

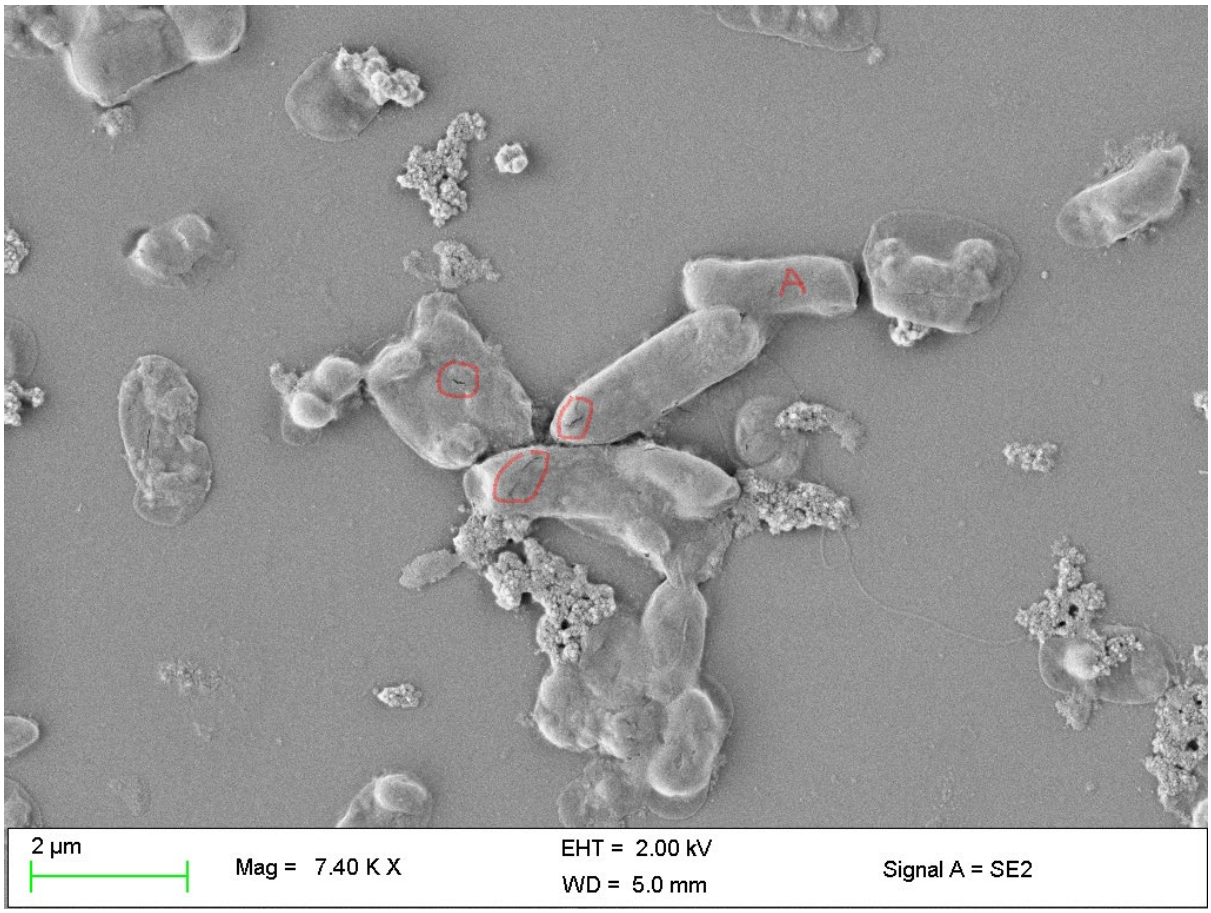

Figure 5.3 (c) E. coli cells after 180 seconds of plasma exposure (total inactivation)

The above discussion one can preliminarily propose that in the point to plane reactor utilised in this study, charged particles and reactive neutral species significantly contribute to *E. coli* inactivation. However, this interesting proposition will require further study in greater detail to be able to make conclusive deductions.

5.6 Contribution of copper to *E. coli* inactivation

There has been a significant effort by researchers to comprehend the mechanism of waterborne pathogens inactivation (reference). However, the best hypothesis is the combined effect of electrical, chemical and physical effects of plasma treatment. In this study, the complexity of pathogen inactivation in wastewater was further complicated by the addition of copper ions and nanoparticles into the copper solutions. The power supply was connected in negative polarity as it has a higher voltage gradient compared to positive polarity. However, the disadvantage is that negative polarity results in increased

electrode wear (Vukusic et al., 2016). Therefore, there is a need to establish if the inactivation is primarily due to plasma or the copper in solution as copper has antimicrobial effects.

After experiment three, four and five, the remaining treated wastewater in the reactor was drained, decontaminated in the autoclave set at 120 ºC for 30 minutes followed by the quantification of copper ions in the wastewater by ICP-OES. The concentration of copper released into solution was 0.55 mg/L ± 0.15 mg/L. Table 3.8 depicts the experimental runs for *E. coli* at the same starting concentration with exposure to plasma (Run 6) and non-exposure but with copper ions in solution at the lower limit (Run 7) and upper limit (Run 8) of the measured copper in solution from all the previous runs and the conditions of the experiments.

Figure 5.3 illustrates that in the absence of the plasma, copper ions at 0.4 mg/L in solution exhibited a negligible effect on the inactivation. 0.7 mg/L of copper ions shows a 0.7 log reduction in *E. coli* at 300 seconds of copper exposure. The inactivation by copper at 0.7 mg/L is significant, however, it has to be realised that the copper exposure is 2.5 times longer than the treatment time (120 seconds) required to have total inactivation by plasma treatment for a starting E. coli density of 2.5×10^7 CFU/mL. At the upper limit of the copper ion concentration (0.7 mg/L) there is significant inactivation but the contribution of the copper ions total inactivation at 180 seconds is very minimal.

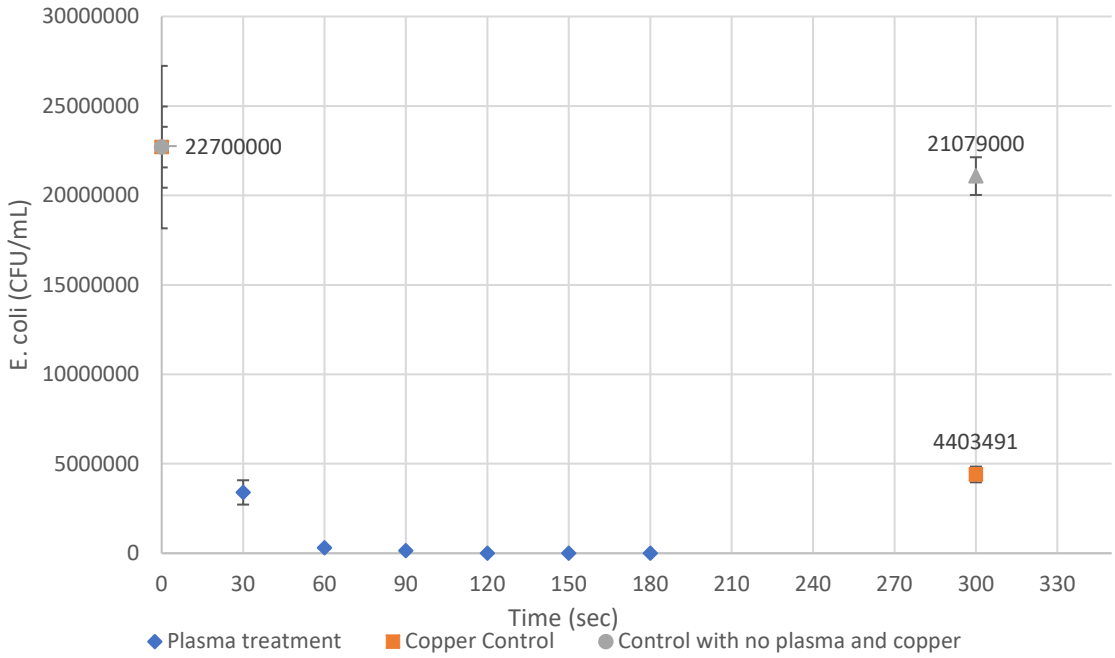

Figure 5.4 Treatment times of plasma and control experimental runs

While the result of the experimental runs 6 to 8 (shown in Figure 5.3) favour plasma treatment. However,

(i) there is literature which proposes that a continuous addition of copper ions shows improved antimicrobial properties than the addition a specific amount of copper ions at the start an experiment as was done in the control in this study (Liau et al., 1997);

(ii) copper ions generated as a result of electrical discharge inactivate microbes better than copper ions from copper-based compounds (Berger et al., 1976a, Berger et al., 1976b);

(iii) electrohydraulic discharge plasma, as discussed in Section 5.5, cause cell wall damage which allows the copper ions to penetrate the cells and amplify the antibacterial effect of the copper ions. All the three scenarios mentioned above could not be simulated to confirm them in this study and to the authors best knowledge, no such plasma related experiments have been conducted.

5.7 *E. coli* Plasma disinfection benchmarking

The context and assumptions for *E. coli* disinfection are similar to those stated in Section 4.8 with the exception that there are specifics applicable to *E. coli* disinfection, for example:

1. Treatment objective is total bacterial inactivation
2. For *E. coli*, a maximum count of 500 CFU/mL was assumed with a treatment goal
3. For operation conditions used in the benchmark, see Appendix D

5.7.1 *E. coli* Inactivation bench marking results

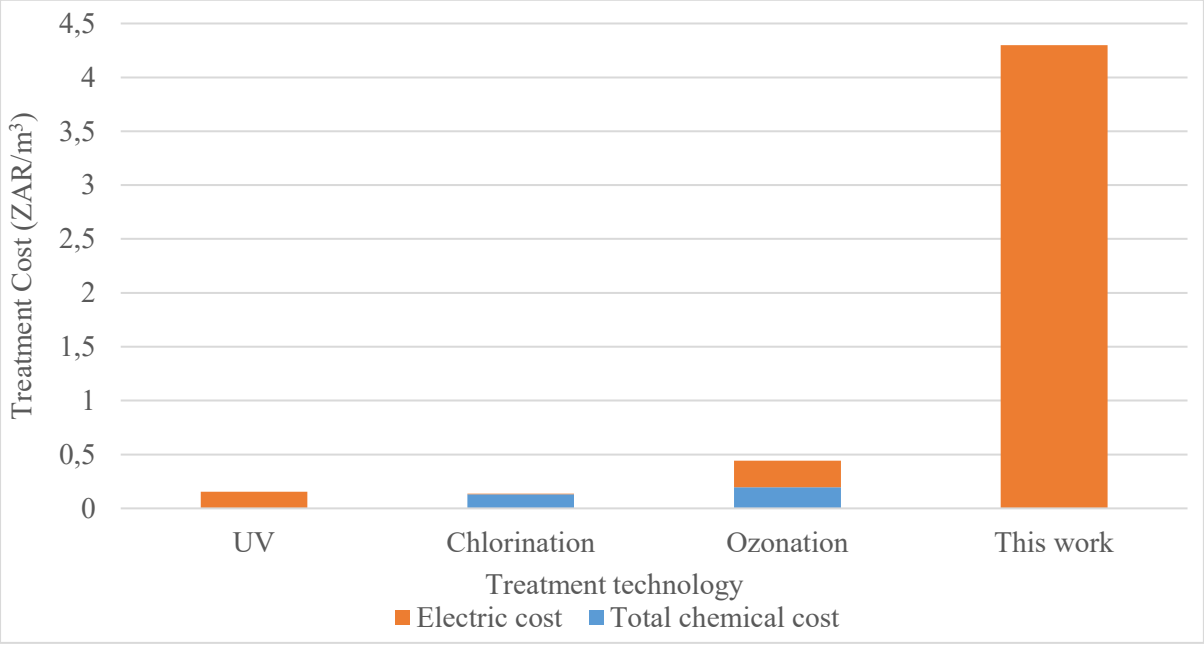

Figure 5.5 Water borne pathogen inactivation operational cost comparison of technologies

Figure 5.4 shows that the reactor used in this study shows a distinctly high treatment cost of 4.3 ZAR/m^3. This is still exorbitantly high, and the technology is not yet ready for commercialization and requires further research and development.

A positive aspect of this result is that the cost for *E. coli* treatment is significantly lower than the treatment cost of chemical contaminants, CBZ, as a case in point (see Figure 4.15).

5.6 Conclusion

This study has established that the point to plane electrohydraulic discharge is effective for E. coli as it has short inactivation times for high E. coli densities. The cause of inactivation, from SEM image analysis, appears to be cell wall damage caused by the charged particles generated by the plasma. However, this study has raised areas which require further study namely the effect of the composition of the cell culture on the efficacy of the plasma treatment process and a detailed evaluation of the influence of metallic ions which may have antimicrobial activities, for example, copper and silver.

Chapter Six

Conclusion and recommendations

This chapter concludes the work on the assessment of a newly setup atmospheric pressure NTP reactor for treatment of wastewater as reported for the following:

1. The degradation of carbamazepine at atmospheric pressure, current (0.25 – 0.45 A), air flow rate (0 – 3 L/min) and starting concentration (10 - 40 mg/L);
2. The inactivation of *E. coli* at atmospheric pressure and the contribution of copper ions from electrode wear to *E. coli* inactivation.

The modifications on the reactor were based on recommendations from work on phenolic compounds done in 2018 with the first prototype reactor. The primary design recommendation was the need for a stirrer for better mixing and wastewater homogeneity. The following design modifications were made on the reactor used in this work: i) moving the air inlet from the top to the bottom of the rector to utilise the air for mixing and to increase the air-water contact time ii) adjust the position of the electrode gap to the bottom half of the reactor to ensure better mixing and temperature control as water heated by the plasma would initial conventional current and move to the top thus ensuring enhancing mixing and preventing thermal hotspots and ensuring better temperature uniformity; iii) removal of the cathode quartz insulator to ensure better cleaning and modifying the anode quartz insulator to expose only the tip hence increasing the electric field intensity and iv) redesign the electrode holders so that they had fewer moving parts to ensure ease of maintenance and troubleshooting.

In the CBZ experiments, the plasma treatment resulted in reduction in pH and a corresponding increase in conductivity. The electrical characterisation showed that the discharge current was directly proportional to the discharge voltage and power usage of the reactor. At both 10 and 40 mg/L starting CBZ concentration, the highest current (0.45A) and no air flowrate (0 L/min) resulted in the highest removal efficiencies of 89.8% and 95.8 % respectively. 0.45 A resulted in the production of stronger electric fields hence the production of more plasma species while no air flowrate ensures a stable continuous plasma discharge. Optimisation for reactor energy consumption was positively influenced by current and flowrate while the starting concentrations investigated had no effect on reactor energy consumption. Optimisation for energy efficiency was more complex as it was positively influenced by current and current-concentration interactions while concentration and flowrate have negative influences. The reactor used in this work had high energy consumption but was effective in degrading high CBZ, thus this reactor setup may be feasible for the degradation of pre-concentrated wastewater streams, for example, hospital and industrial wastewater.

In the *E. coli* inactivation experiments, a 2 mm electrode gap was experimentally determined as the most suitable electrode gap for the treatment of ESSWW. The NTP reactor utilised in this work was effective in treating E. coli densities up to 2.5×10^7 CFU/mL in 180 seconds. Inactivation can be partly attributed to the charged species, which caused physical cell wall damage as demonstrated by SEM imaging. Control experiments with copper ions equal to the electrode copper deposited in the ESSWW, demonstrated that E. coli inactivation was dominantly due to the plasma treatment. Nevertheless, the copper ions' contribution to inactivation could not be conclusively established as the copper ions may have had been more effective in cells with damaged cell walls.

The experimental results confirm that the NTP reactor used in this experimental investigation was thus able to degrade a recalcitrant chemical pollutant (CBZ) to above 90% and achieve total inactivate of a waterborne bacterial organism (*E. coli*).

There is still room for further investigations. The study recommends the following:

1. The energy consumption per unit volume treated of the reactor(kWh/m^3), due to the utilisation of DC high voltage power supply, is still above the 5 kWh/m^3 economic feasibility benchmark for NTP wastewater treatment. Work on the use of a plug and play AC high voltage power supply would certainly be interesting as it will enhance economic feasibility of the process.
2. A detailed study on the contribution of the different electrode metals, with antimicrobial properties, to inactivation simulating the possible conditions which occur during plasma treatment.
3. There is a need to do a toxicology study of the possible CBZ degradation by-products. This is important as it ensures that the treatment does not produce by-products which are more dangerous to the toxic environment and human health.

References

ADNAN, M. 2019. *ANTIMICROBIAL PROPERTIES OF SILVER NANOPARTICLES.*

ALEXANDER, J. T., HAI, F. I. & AL-ABOUD, T. M. 2012. Chemical coagulation-based processes for trace organic contaminant removal: Current state and future potential. *Journal of environmental management,* 111**,** 195-207.

ALHARBI, S. K., KANG, J., NGHIEM, L. D., VAN DE MERWE, J. P., LEUSCH, F. D. & PRICE, W. E. 2017. Photolysis and UV/H2O2 of diclofenac, sulfamethoxazole, carbamazepine, and trimethoprim: identification of their major degradation products by ESI–LC–MS and assessment of the toxicity of reaction mixtures. *Process Safety and Environmental Protection,* 112**,** 222-234.

ALVARINO, T., SUAREZ, S., LEMA, J. & OMIL, F. 2014. Understanding the removal mechanisms of PPCPs and the influence of main technological parameters in anaerobic UASB and aerobic CAS reactors. *Journal of hazardous materials,* 278**,** 506-513.

ALVARINO, T., SUAREZ, S., LEMA, J. & OMIL, F. 2018. Understanding the sorption and biotransformation of organic micropollutants in innovative biological wastewater treatment technologies. *Science of the Total Environment,* 615**,** 297-306.

AMANO, R. & TEZUKA, M. 2006. Mineralization of alkylbenzenesulfonates in water by means of contact glow discharge electrolysis. *Water research,* 40**,** 1857-1863.

ARSHAD, B., IQBAL, T., AKRAM, S. & MUSHTAQ, M. 2017. An expedient reverse-phase high-performance chromatography (RP-HPLC) based method for high-throughput analysis of deferoxamine and ferrioxamine in urine. *Biomedical Chromatography,* 31**,** e3805.

ARYE, G., DROR, I. & BERKOWITZ, B. 2011. Fate and transport of carbamazepine in soil aquifer treatment (SAT) infiltration basin soils. *Chemosphere,* 82**,** 244-252.

ASIF, M. B., HAI, F. I., HOU, J., PRICE, W. E. & NGHIEM, L. D. 2017. Impact of wastewater derived dissolved interfering compounds on growth, enzymatic activity and trace organic contaminant removal of white rot fungi–a critical review. *Journal of environmental management,* 201**,** 89-109.

BAHLMANN, A., BRACK, W., SCHNEIDER, R. J. & KRAUSS, M. 2014. Carbamazepine and its metabolites in wastewater: Analytical pitfalls and occurrence in Germany and Portugal. *Water Res,* 57**,** 104-14.

BATMEN, C. 2010. SA facing water pollution crisis. *CME: Your SA Journal of CPD,* 28**,** 491-492.

BEIER, S., KÖSTER, S., VELTMANN, K., SCHRÖDER, H. & PINNEKAMP, J. 2010. Treatment of hospital wastewater effluent by nanofiltration and reverse osmosis. *Water Science and Technology,* 61**,** 1691-1698.

BÉLANGER, L., GARENAUX, A., HAREL, J., BOULIANNE, M., NADEAU, E. & DOZOIS, C. M. 2011. Escherichia coli from animal reservoirs as a potential source of human extraintestinal pathogenic E. coli. *FEMS Immunology & Medical Microbiology,* 62**,** 1-10.

BENETOLI, L. O. D. B., CADORIN, B. M., POSTIGLIONE, C. D. S., SOUZA, I. G. D. & DEBACHER, N. A. 2011. Effect of temperature on methylene blue decolorization in aqueous medium in electrical discharge plasma reactor. *Journal of the Brazilian Chemical Society,* 22**,** 1669-1678.

BERGER, T., SPADARO, J., BIERMAN, R., CHAPIN, S. & BECKER, R. 1976a. Antifungal properties of electrically generated metallic ions. *Antimicrobial agents and chemotherapy,* 10**,** 856-860.

BERGER, T., SPADARO, J., CHAPIN, S. & BECKER, R. 1976b. Electrically generated silver ions: quantitative effects on bacterial and mammalian cells. *Antimicrobial agents and chemotherapy,* 9**,** 357.

BHAVSAR, S. & KRILOV, L. 2015. Escherichia coli Infections. *Pediatrics in review / American Academy of Pediatrics,* 36**,** 167-71.

BI JEON, E., CHOI, M. S., KIM, J. Y. & PARK, S. Y. 2020. Synergistic Effects of Mild Heating and Dielectric Barrier Discharge Plasma on the Reduction of Bacillus Cereus in Red Pepper Powder. *Foods,* 9.

BÖGER, B., AMARAL, B. D., ESTEVÃO, P. L. D. S., WAGNER, R., PERALTA-ZAMORA, P. G. & GOMES, E. C. 2018. Determination of carbamazepine and diazepam by SPE-HPLC-DAD in Belém River water, Curitiba-PR/Brazil. *Revista Ambiente & Água,* 13.

BOKULICH, N. A. & BAMFORTH, C. W. 2013. The microbiology of malting and brewing. *Microbiol Mol Biol Rev,* 77**,** 157-72.

BOLONG, N., ISMAIL, A., SALIM, M. R. & MATSUURA, T. 2009. A review of the effects of emerging contaminants in wastewater and options for their removal. *Desalination,* 239**,** 229-246.

BOLTON, J. R., BIRCHER, K. G., TUMAS, W. & TOLMAN, C. A. 1996. Figures-of-merit for the technical development and application of advanced oxidation processes. *Journal of advanced oxidation technologies,* 1**,** 13-17.

BOLTON, J. R., BIRCHER, K. G., TUMAS, W. & TOLMAN, C. A. 2001. Figures-of-merit for the technical development and application of advanced oxidation technologies for both electric-and solar-driven systems (IUPAC Technical Report). *Pure and Applied Chemistry,* 73**,** 627-637.

BONDARCZUK, K. & PIOTROWSKA-SEGET, Z. 2019. Microbial diversity and antibiotic resistance in a final effluent-receiving lake. *Science of The Total Environment,* 650**,** 2951-2961.

BORISOVER, M., SELA, M. & CHEFETZ, B. 2011. Enhancement effect of water associated with natural organic matter (NOM) on organic compound–NOM interactions: A case study with carbamazepine. *Chemosphere,* 82**,** 1454-1460.

BOULAY, N. & EDWARDS, M. 2000. Copper in the urban water cycle. *Critical reviews in environmental science and technology,* 30**,** 297-326.

BOURKE, P., ZIUZINA, D., HAN, L., CULLEN, P. & GILMORE, B. 2017. Microbiological interactions with cold plasma. *Journal of applied microbiology,* 123**,** 308-324.

BRISSET, J.-L., MOUSSA, D., DOUBLA, A., HNATIUC, E., HNATIUC, B., KAMGANG YOUBI, G., HERRY, J.-M., NAITALI, M. & BELLON-FONTAINE, M.-N. 2008. Chemical reactivity of discharges and temporal post-discharges in plasma treatment of aqueous media: examples of gliding discharge treated solutions. *Industrial & Engineering Chemistry Research,* 47**,** 5761-5781.

BURLICA, R. & LOCKE, B. R. 2008. Pulsed plasma gliding-arc discharges with water spray. *IEEE transactions on industry applications,* 44**,** 482-489.

CHANG, Y.-K., CHANG, J.-E., LIN, T.-T. & HSU, Y.-M. 2002. Integrated copper-containing wastewater treatment using xanthate process. *Journal of hazardous materials,* 94**,** 89-99.

CHENG, H.-H., CHEN, S.-S., YOSHIZUKA, K. & CHEN, Y.-C. 2012. Degradation of phenolic compounds in water by non-thermal plasma treatment. *Journal of Water Chemistry and Technology,* 34.

CHO, M., KIM, J., KIM, J. Y., YOON, J. & KIM, J.-H. 2010. Mechanisms of Escherichia coli inactivation by several disinfectants. *Water Research,* 44**,** 3410-3418.

CHRISTENSEN, J. & LINDEN, K. G. 2003. How particles affect UV light in the UV disinfection of unfiltered drinking water. *Journal-American Water Works Association,* 95**,** 179-189.

CLARA, M., STRENN, B., GANS, O., MARTINEZ, E., KREUZINGER, N. & KROISS, H. 2005. Removal of selected pharmaceuticals, fragrances and endocrine disrupting compounds in a membrane bioreactor and conventional wastewater treatment plants. *Water research,* 39**,** 4797-4807.

CLARA, M., STRENN, B. & KREUZINGER, N. 2004. Carbamazepine as a possible anthropogenic marker in the aquatic environment: investigations on the behaviour of carbamazepine in wastewater treatment and during groundwater infiltration. *Water research,* 38**,** 947-954.

COMERTON, A. M., ANDREWS, R. C., BAGLEY, D. M. & HAO, C. 2008. The rejection of endocrine disrupting and pharmaceutically active compounds by NF and RO membranes as a function of compound and water matrix properties. *Journal of Membrane Science,* 313**,** 323-335.

CUI, Y., CHENG, J., CHEN, Q. & YIN, Z. 2018. The Types of Plasma Reactors in Wastewater Treatment. *IOP Conference Series: Earth and Environmental Science,* 208.

DAI, C.-M., ZHOU, X.-F., ZHANG, Y.-L., DUAN, Y.-P., QIANG, Z.-M. & ZHANG, T. C. 2012. Comparative study of the degradation of carbamazepine in water by advanced oxidation processes. *Environmental technology,* 33**,** 1101-1109.

DAUGHTON, C. G. 2001. Pharmaceuticals and Personal Care Products in the Environment: Overarching Issues and Overview. *Pharmaceuticals and Care Products in the Environment.*

DEBLONDE, T., COSSU-LEGUILLE, C. & HARTEMANN, P. 2011. Emerging pollutants in wastewater: a review of the literature. *International journal of hygiene and environmental health,* 214**,** 442-448.

DEPARTMENT OF WATER AFFAIRS 2013. Revision of general authorisations in terms of Section 39 of the National Water Act, 1998 (Act No. 36 of 1998), No. 665. *Government Gazette*.

DURÁN-ALVAREZ, J. C., BECERRIL-BRAVO, E., CASTRO, V. S., JIMÉNEZ, B. & GIBSON, R. 2009. The analysis of a group of acidic pharmaceuticals, carbamazepine, and potential endocrine disrupting compounds in wastewater irrigated soils by gas chromatography–mass spectrometry. *Talanta,* 78**,** 1159-1166.

ELIASSON, B., HIRTH, M. & KOGELSCHATZ, U. 1987. Ozone synthesis from oxygen in dielectric barrier discharges. *Journal of Physics D: Applied Physics,* 20**,** 1421-1437.

ERSHOV, B. & MOROZOV, P. 2009. The kinetics of ozone decomposition in water, the influence of pH and temperature. *Russian Journal of Physical Chemistry A,* 83**,** 1295-1299.

ESTIFAEE, P., SU, X., YANNAM, S. K., ROGERS, S. & THAGARD, S. M. 2019. Mechanism of E. coli Inactivation by Direct-in-liquid Electrical Discharge Plasma in Low Conductivity Solutions. *Sci Rep,* 9**,** 2326.

FARKAS-HIMSLEY, H. 1964. Killing of chlorine-resistant bacteria by chlorine-bromine solutions. *Appl. Environ. Microbiol.,* 12**,** 1-6.

FOSTER, J., SOMMERS, B. S., GUCKER, S. N., BLANKSON, I. M. & ADAMOVSKY, G. 2012. Perspectives on the Interaction of Plasmas With Liquid Water for Water Purification. *IEEE Transactions on Plasma Science,* 40**,** 1311-1323.

FOSTER, J. E. 2017. Plasma-based water purification: Challenges and prospects for the future. *Physics of Plasmas,* 24.

FRIDMAN, A. 2008. *Plasma chemistry*, Cambridge university press.

FRIDMAN, G., BROOKS, A. D., BALASUBRAMANIAN, M., FRIDMAN, A., GUTSOL, A., VASILETS, V. N., AYAN, H. & FRIEDMAN, G. 2007. Comparison of direct and indirect effects of non-thermal atmospheric-pressure plasma on bacteria. *Plasma Processes and Polymers,* 4**,** 370-375.

FULCHERI, L., ROHANI, V., FABRY, F. & TRAISNEL, N. 2010. Experimental electrical characterization of a low-current tip–tip arc discharge in helium atmosphere at very high pressure. *Plasma Sources Science and Technology,* 19**,** 045010.

GAO, J. 2006. A Novel Technique for Wastewater Treatment by Contact Glow-discharge Electrolysis. *Parkistand Journal of Biological Science,* 9**,** 323-329.

GAO, X., WANG, J., GAO, Y., YAN, H., XUE, K., DENG, X. & YANG, X. 2020. Underwater pulsed spark discharge influenced by the relative position between the top of a pin electrode and an insulating tube. *Plasma Science and Technology,* 22.

GHARAGOZALIAN, M., DORRANIAN, D. & GHORANNEVISS, M. 2017. Water treatment by the AC gliding arc air plasma. *Journal of Theoretical and Applied Physics,* 11**,** 171-180.

GOLAN-ROZEN, N., CHEFETZ, B., BEN-ARI, J., GEVA, J. & HADAR, Y. 2011. Transformation of the recalcitrant pharmaceutical compound carbamazepine by Pleurotus ostreatus: role of cytochrome P450 monooxygenase and manganese peroxidase. *Environmental science & technology,* 45**,** 6800-6805.

GOPAL, N. 1978. Radiation sterilization of pharmaceuticals and polymers. *Radiation Physics and Chemistry (1977),* 12**,** 35-50.

GORYACHEV, V., UFIMTSEV, A. & KHODAKOVSKII, A. 1997. Mechanism of electrode erosion in pulsed discharges in water with a pulse energy of∼ 1 J. *Technical Physics Letters,* 23**,** 386-387.

GOVENDER, B. B. 2016. *The application of non-thermal plasma-catalysis in Fischer-Tropsch synthesis at high pressure.*

GREKHOV, I., KOROTKOV, S., ANDREEV, A., KOZLOV, A., ROL'NIK, I. & STEPANYANTS, A. 1997. High-power reverse switch-on dynistor-based generators for electric-discharge water purification. *Instruments and Experimental Techniques,* 40**,** 705-707.

GUAN, Y., JIA, J., WU, L., XUE, X., ZHANG, G. & WANG, Z. 2018. Analysis of Bacterial Community Characteristics, Abundance of Antibiotics and Antibiotic Resistance Genes Along a Pollution Gradient of Ba River in Xi'an, China. *Front Microbiol,* 9**,** 3191.

GUIDELINE, I. H. T. 2005. Validation of analytical procedures: text and methodology. *Q2 (R1),* 1**,** 1-15.

GUO, J., HUANG, K. & WANG, J. 2015. Bactericidal effect of various non-thermal plasma agents and the influence of experimental conditions in microbial inactivation: A review. *Food Control,* 50**,** 482-490.

GUPPY, L. & ANDERSON, K. 2017. Water Crisis Report. Hamilton, Canada.: United Nations University Institute for Water, Environment and Health.

GUPTA, S. K. S. 2017. Contact glow discharge electrolysis: a novel tool for manifold applications. *Plasma Chemistry and Plasma Processing,* 37**,** 897-945.

GUR-REZNIK, S., KOREN-MENASHE, I., HELLER-GROSSMAN, L., RUFEL, O. & DOSORETZ, C. G. 2011. Influence of seasonal and operating conditions on the rejection of pharmaceutical active compounds by RO and NF membranes. *Desalination,* 277**,** 250-256.

HAI, F., YANG, S., ASIF, M., SENCADAS, V., SHAWKAT, S., SANDERSON-SMITH, M., GORMAN, J., XU, Z.-Q. & YAMAMOTO, K. 2018. Carbamazepine as a Possible Anthropogenic Marker in Water: Occurrences, Toxicological Effects, Regulations and Removal by Wastewater Treatment Technologies. *Water,* 10.

HAI, F. I., LI, X., PRICE, W. E. & NGHIEM, L. D. 2011. Removal of carbamazepine and sulfamethoxazole by MBR under anoxic and aerobic conditions. *Bioresource technology,* 102**,** 10386-10390.

HAI, F. I., YAMAMOTO, K. & FUKUSHI, K. 2006. Development of a submerged membrane fungi reactor for textile wastewater treatment. *Desalination,* 192**,** 315-322.

HERBIG, F. J. W. & MEISSNER, R. 2019. Talking dirty - effluent and sewage irreverence in South Africa: A conservation crime perspective. *Cogent Social Sciences,* 5**,** 1701359.

HIJOSA-VALSERO, M., MOLINA, R., MONTRÀS, A., MÜLLER, M. & BAYONA, J. M. 2014. Decontamination of waterborne chemical pollutants by using atmospheric pressure nonthermal plasma: a review. *Environmental Technology Reviews,* 3**,** 71-91.

HIOLSKI, E. 2019. The toilet gets a makeover. ACS Publications.

HÖFT, H. & HUISKAMP, T. 2018. Direct comparison of pulsed spark discharges in air and water by synchronized electrical and optical diagnostics. *The European Physical Journal D,* 72**,** 217.

HUERTA-FONTELA, M., GALCERAN, M. T. & VENTURA, F. 2011. Occurrence and removal of pharmaceuticals and hormones through drinking water treatment. *Water research,* 45**,** 1432-1442.

HUIJBERS, P. M., LARSSON, D. J. & FLACH, C.-F. 2020. Surveillance of antibiotic resistant Escherichia coli in human populations through urban wastewater in ten European countries. *Environmental Pollution,* 261**,** 114200.

IJAH, U. J., AUTA, H. S., ADULOJU, M. O. & ARANSIOLA, S. A. 2014. Microbiological, Nutritional, and Sensory Quality of Bread Produced from Wheat and Potato Flour Blends. *Int J Food Sci,* 2014**,** 671701.

IKAWA, S., KITANO, K. & HAMAGUCHI, S. 2010. Effects of pH on bacterial inactivation in aqueous solutions due to low-temperature atmospheric pressure plasma application. *Plasma Processes and Polymers,* 7**,** 33-42.

IM, J.-K., CHO, I.-H., KIM, S.-K. & ZOH, K.-D. 2012. Optimization of carbamazepine removal in O3/UV/H2O2 system using a response surface methodology with central composite design. *Desalination,* 285**,** 306-314.

JELIĆ, A., GROS, M., PETROVIĆ, M., GINEBREDA, A. & BARCELÓ, D. 2012. Occurrence and elimination of pharmaceuticals during conventional wastewater treatment. *Emerging and priority pollutants in rivers.* Springer.

JIANG, B., ZHENG, J., QIU, S., WU, M., ZHANG, Q., YAN, Z. & XUE, Q. 2014. Review on electrical discharge plasma technology for wastewater remediation. *Chemical Engineering Journal,* 236**,** 348-368.

JOSHI, A. A., LOCKE, B. R., ARCE, P. & FINNEY, W. C. 1995. Formation of hydroxyl radicals, hydrogen peroxide and aqueous electrons by pulsed streamer corona discharge in aqueous solution. *Journal of hazardous materials,* 41**,** 3-30.

JUHLER, R. K. & FELDING, G. 2003. Monitoring methyl tertiary butyl ether (MTBE) and other organic micropollutants in groundwater: results from the Danish National Monitoring Program. *Water, Air, and Soil Pollution,* 149**,** 145-161.

KADIOGLU, Y. & DEMIRKAYA, F. 2007. Determination of carbamazepine in pharmaceutical dosage form using GC-FID. *Chromatographia,* 66**,** 169-172.

KHLYUSTOVA, A., KHOMYAKOVA, N., SIROTKIN, N. & MARFIN, Y. 2016. The effect of pH on OH radical generation in aqueous solutions by atmospheric pressure glow discharge. *Plasma Chemistry and Plasma Processing,* 36**,** 1229-1238.

KOGELSCHATZ, U., ELIASSON, B. & EGLI, W. 2003. Plasma Chem. Plasma Process.

KONG, L., KADOKAMI, K., DUONG, H. T. & CHAU, H. T. C. 2016. Screening of 1300 organic micro-pollutants in groundwater from Beijing and Tianjin, North China. *Chemosphere,* 165**,** 221-230.

KORZENIEWSKA, E., KORZENIEWSKA, A. & HARNISZ, M. 2013. Antibiotic resistant Escherichia coli in hospital and municipal sewage and their emission to the environment. *Ecotoxicol Environ Saf,* 91**,** 96-102.

KOSJEK, T., ANDERSEN, H. R., KOMPARE, B., LEDIN, A. & HEATH, E. 2009. Fate of carbamazepine during water treatment. *Environmental science & technology,* 43**,** 6256-6261.

KRAUSE, H., SCHWEIGER, B., PRINZ, E., KIM, J. & STEINFELD, U. 2011. Degradation of persistent pharmaceuticals in aqueous solutions by a positive dielectric barrier discharge treatment. *Journal of Electrostatics,* 69**,** 333-338.

LAPWORTH, D., BARAN, N., STUART, M. & WARD, R. 2012. Emerging organic contaminants in groundwater: a review of sources, fate and occurrence. *Environmental pollution,* 163**,** 287-303.

LAROUSSI, M. 2002. Nonthermal decontamination of biological media by atmospheric-pressure plasmas: review, analysis, and prospects. *IEEE Transactions on plasma science,* 30**,** 1409-1415.

LAROUSSI, M. & LEIPOLD, F. 2004. Evaluation of the roles of reactive species, heat, and UV radiation in the inactivation of bacterial cells by air plasmas at atmospheric pressure. *International Journal of Mass Spectrometry,* 233**,** 81-86.

LECLERCQ, M., MATHIEU, O., GOMEZ, E., CASELLAS, C., FENET, H. & HILLAIRE-BUYS, D. 2009. Presence and fate of carbamazepine, oxcarbazepine, and seven of their metabolites at wastewater treatment plants. *Archives of environmental contamination and toxicology,* 56**,** 408.

LERTRATANANGKOON, K. & HORNING, M. 1982. Metabolism of carbamazepine. *Drug Metabolism and Disposition,* 10**,** 1-10.

LEWIS, R. J., ANGIER, M. K. & JOHNSON, R. D. 2014. False Carbamazepine Positives Due to 10, 11-Dihydro-10-Hydroxycarbamazepine Breakdown in the GC–MS Injector Port. *Journal of analytical toxicology,* 38**,** 519-523.

LI, S., JIANG, Y., CAO, X., DONG, Y., DONG, M. & XU, J. 2013. Degradation of nitenpyram pesticide in aqueous solution by low-temperature plasma. *Environmental technology,* 34**,** 1609-1616.

LI, Z., FENET, H., GOMEZ, E. & CHIRON, S. 2011. Transformation of the antiepileptic drug oxcarbazepine upon different water disinfection processes. *Water research,* 45**,** 1587-1596.

LIAU, S., READ, D., PUGH, W., FURR, J. & RUSSELL, A. 1997. Interaction of silver nitrate with readily identifiable groups: relationship to the antibacterialaction of silver ions. *Letters in applied microbiology,* 25**,** 279-283.

LIU, Y., MEI, S., IYA-SOU, D., CAVADIAS, S. & OGNIER, S. 2012. Carbamazepine removal from water by dielectric barrier discharge: comparison of ex situ and in situ discharge on water. *Chemical Engineering and Processing: Process Intensification,* 56**,** 10-18.

LOCKE, B., SATO, M., SUNKA, P., HOFFMANN, M. & CHANG, J.-S. 2006. Electrohydraulic discharge and nonthermal plasma for water treatment. *Industrial & engineering chemistry research,* 45**,** 882-905.

LOCKE, B. R. & THAGARD, S. M. 2012. Analysis and review of chemical reactions and transport processes in pulsed electrical discharge plasma formed directly in liquid water. *Plasma Chemistry and Plasma Processing,* 32**,** 875-917.

LÓPEZ, M., CALVO, T., PRIETO, M., MÚGICA-VIDAL, R., MURO-FRAGUAS, I., ALBA-ELÍAS, F. & ALVAREZ-ORDÓÑEZ, A. 2019. A Review on Non-thermal Atmospheric Plasma for Food Preservation: Mode of Action, Determinants of Effectiveness, and Applications. *Frontiers in Microbiology,* 10.

LUKES, P., LOCKE, B. R. & BRISSET, J.-L. 2012. Aqueous-phase chemistry of electrical discharge plasma in water and in gas-liquid environments. *Plasma chemistry and catalysis in gases and liquids,* 1**,** 243-308.

LUO, Y., GUO, W., NGO, H. H., NGHIEM, L. D., HAI, F. I., ZHANG, J., LIANG, S. & WANG, X. C. 2014. A review on the occurrence of micropollutants in the aquatic environment and their fate and removal during wastewater treatment. *Sci Total Environ,* 473-474**,** 619-41.

MAGUREANU, M., MANDACHE, N. B. & PARVULESCU, V. I. 2015. Degradation of pharmaceutical compounds in water by non-thermal plasma treatment. *Water research,* 81**,** 124-136.

MAGUREANU, M., PIROI, D., MANDACHE, N., DAVID, V., MEDVEDOVICI, A., BRADU, C. & PARVULESCU, V. 2011. Degradation of antibiotics in water by non-thermal plasma treatment. *Water research,* 45**,** 3407-3416.

MALIK, M. A., GHAFFAR, A. & MALIK, S. A. 2001a. Water purification by electrical discharges. *Plasma Sources Science and Technology,* 10**,** 82.

MALIK, M. A., GHAFFAR, A. & MALIK, S. A. 2001b. Water purification by electrical discharges. *Plasma Sources Science and Technology,* 10**,** 82-91.

MARGOT, J., MAILLARD, J., ROSSI, L., BARRY, D. A. & HOLLIGER, C. 2013. Influence of treatment conditions on the oxidation of micropollutants by Trametes versicolor laccase. *New biotechnology,* 30**,** 803-813.

MARKOVIĆ, M., JOVIĆ, M., STANKOVIĆ, D., KOVAČEVIĆ, V., ROGLIĆ, G., GOJGIĆ-CVIJOVIĆ, G. & MANOJLOVIĆ, D. 2015. Application of non-thermal plasma reactor and Fenton reaction for degradation of ibuprofen. *Science of the Total Environment,* 505**,** 1148-1155.

MCDOWELL, D. C., HUBER, M. M., WAGNER, M., VON GUNTEN, U. & TERNES, T. A. 2005. Ozonation of carbamazepine in drinking water: identification and kinetic study of major oxidation products. *Environmental science & technology,* 39**,** 8014-8022.

MECHSNER, J., SCHMIDT, M., SCHNEIDER, R. & WAGNER, H. 2013. *Nonthermal Plasma Chemistry and Physics*, CRC Press.

MEMA, V. 2010. Impact of poorly maintained waste water and sewage treatment plants: Lessons from South Africa. *ReSource,* 12**,** 60-61.

MIAO, X.-S. & METCALFE, C. D. 2003. Determination of carbamazepine and its metabolites in aqueous samples using liquid chromatography− electrospray tandem mass spectrometry. *Analytical chemistry,* 75**,** 3731-3738.

MIKLOS, D. B., REMY, C., JEKEL, M., LINDEN, K. G., DREWES, J. E. & HUBNER, U. 2018. Evaluation of advanced oxidation processes for water and wastewater treatment - A critical review. *Water Res,* 139**,** 118-131.

MOHAN, B. 2018a. Degradation of Phenolic Aqueous solutions in an atmospheric pressure Electric Discharge in air. *In:* IWARERE, D. (ed.). University of KwaZulu Natal.

MOHAN, B. 2018b. DEGRADATION OF PHENOLIC AQUEOUS SOLUTIONS IN AN ATMOSPHERIC PRESSURE ELECTRICAL ARC DISCHARGE IN AIR. University of KwaZulu Natal.

MOHAPATRA, D. P., BRAR, S. K., TYAGI, R. D., PICARD, P. & SURAMPALLI, R. Y. 2013. A comparative study of ultrasonication, Fenton's oxidation and ferro-sonication treatment for degradation of carbamazepine from wastewater and toxicity test by Yeast Estrogen Screen (YES) assay. *Science of the total environment,* 447**,** 280-285.

MOOSAVI, S. & GHASSABIAN, S. 2018. A Sampling of Current Approaches *Linearity of Calibration Curves for Analytical Methods: A Review of Criteria for Assessment of Method Reliability. Calibration and Validation of Analytical Methods.*

MOTYKA, A., DZIMITROWICZ, A., JAMROZ, P., LOJKOWSKA, E., SLEDZ, W. & POHL, P. 2018. Rapid eradication of bacterial phytopathogens by atmospheric pressure glow discharge generated in contact with a flowing liquid cathode. *Biotechnology and bioengineering,* 115**,** 1581-1593.

MOUELE, E. S. M., TIJANI, J. O., FATOBA, O. O. & PETRIK, L. F. 2015. Degradation of organic pollutants and microorganisms from wastewater using different dielectric barrier discharge configurations—a critical review. *Environmental Science and Pollution Research,* 22**,** 18345-18362.

MOZGINA, O., KOUTSOSPYROS, A., GERSHMAN, S., BELKIND, A., CHRISTODOULATOS, C. & BECKER, K. 2009. Decomposition of energetic materials by pulsed electrical discharges in gas-bubbled aqueous solutions. *IEEE transactions on plasma science,* 37**,** 905-910.

MURPHY, D., RODRıGUEZ-CINTRÓN, F., LANGEVIN, B., KELLY, R. & RODRıGUEZ-HORNEDO, N. 2002. Solution-mediated phase transformation of anhydrous to dihydrate carbamazepine and the effect of lattice disorder. *International journal of pharmaceutics,* 246**,** 121-134.

NGUYEN, L. N., HAI, F. I., PRICE, W. E., KANG, J., LEUSCH, F. D., RODDICK, F., VAN DE MERWE, J. P., MAGRAM, S. F. & NGHIEM, L. D. 2015. Degradation of a broad spectrum of trace organic contaminants by an enzymatic membrane reactor: complementary role of membrane retention and enzymatic degradation. *International Biodeterioration & Biodegradation,* 99**,** 115-122.

NGUYEN, L. N., HAI, F. I., YANG, S., KANG, J., LEUSCH, F. D., RODDICK, F., PRICE, W. E. & NGHIEM, L. D. 2014. Removal of pharmaceuticals, steroid hormones, phytoestrogens, UV-filters, industrial chemicals and pesticides by Trametes versicolor: role of biosorption and biodegradation. *International Biodeterioration & Biodegradation,* 88**,** 169-175.

OEHMIGEN, K., HÄHNEL, M., BRANDENBURG, R., WILKE, C., WELTMANN, K. D. & VON WOEDTKE, T. 2010. The role of acidification for antimicrobial activity of atmospheric pressure plasma in liquids. *Plasma Processes and Polymers,* 7**,** 250-257.

OMAR, K. & BARNARD, T. 2010. The occurrence of pathogenic Escherichia coli in South African wastewater treatment plants as detected by multiplex PCR. *Water SA,* 36**,** 172-176.

OMAR, K. B. & BERNARD, T. G. 2010. The occurrence of pathogenic Escherichia coli in South African wastewater treatment plants as detected by multiplex PCR. *Southern African Young Water Professionals Conference.* Pretoria.

OSIŃSKA, A., KORZENIEWSKA, E., HARNISZ, M., FELIS, E., BAJKACZ, S., JACHIMOWICZ, P., NIESTĘPSKI, S. & KONOPKA, I. 2020. Small-scale wastewater treatment plants as a source of the dissemination of antibiotic resistance genes in the aquatic environment. *Journal of Hazardous Materials,* 381**,** 121221.

PANG, Y., HUANG, J., XI, J., HU, H. & ZHU, Y. 2016. Effect of ultraviolet irradiation and chlorination on ampicillin-resistant Escherichia coli and its ampicillin resistance gene. *Frontiers of Environmental Science & Engineering,* 10**,** 522-530.

PARSONS, S. 2004. *Advanced oxidation processes for water and wastewater treatment*, IWA publishing.

PERINBAN, S., ORSAT, V. & RAGHAVAN, V. 2019. Nonthermal Plasma–Liquid Interactions in Food Processing: A Review. *Comprehensive Reviews in Food Science and Food Safety,* 18**,** 1985-2008.

PETRIK, L., FATOBA, O., MOUELE, E. & TOTITO, T. 2015. Advanced oxidative water treatment process for water disinfection using an electrohydraulic discharge reactor and titanium oxide immobilized on nanofibres. University of Western Cape.

PETROVIC, M., DE ALDA, M. J. L., DIAZ-CRUZ, S., POSTIGO, C., RADJENOVIC, J., GROS, M. & BARCELO, D. 2009. Fate and removal of pharmaceuticals and illicit drugs in conventional and membrane bioreactor wastewater treatment plants and by riverbank filtration. *Philosophical Transactions of the Royal Society A: Mathematical, Physical and Engineering Sciences,* 367**,** 3979-4003.

PIEL, A. 2017. *Plasma Physics: An introduction to Labaratory, Space, and Fusion Plasmas*, Springer International Publishing AG.

POTOCKÝ, Š., SAITO, N. & TAKAI, O. 2009. Needle electrode erosion in water plasma discharge. *Thin Solid Films,* 518**,** 918-923.

QIAN, J., ZHUANG, H., NASIRU, M. M., MUHAMMAD, U., ZHANG, J. & YAN, W. 2019. Action of plasma-activated lactic acid on the inactivation of inoculated Salmonella Enteritidis and quality of beef. *Innovative Food Science & Emerging Technologies,* 57**,** 102196.

RADJENOVIĆ, J., PETROVIĆ, M., VENTURA, F. & BARCELÓ, D. 2008. Rejection of pharmaceuticals in nanofiltration and reverse osmosis membrane drinking water treatment. *Water research,* 42**,** 3601-3610.

RAKIĆ, T., KASAGIĆ-VUJANOVIĆ, I., JOVANOVIĆ, M., JANČIĆ-STOJANOVIĆ, B. & IVANOVIĆ, D. 2014. Comparison of full factorial design, central composite design, and box-behnken design in chromatographic method development for the determination of fluconazole and its impurities. *Analytical letters,* 47**,** 1334-1347.

RASHMEI, Z., BORNASI, H. & GHORANNEVISS, M. 2016. Evaluation of treatment and disinfection of water using cold atmospheric plasma. *Journal of water and health,* 14**,** 609-616.

REINTHALER, F. F., POSCH, J., FEIERL, G., WÜST, G., HAAS, D., RUCKENBAUER, G., MASCHER, F. & MARTH, E. 2003. Antibiotic resistance of E. coli in sewage and sludge. *Water Research,* 37**,** 1685-1690.

RIZZO, L., MANAIA, C., MERLIN, C., SCHWARTZ, T., DAGOT, C., PLOY, M. C., MICHAEL, I. & FATTA-KASSINOS, D. 2013. Urban wastewater treatment plants as hotspots for antibiotic resistant bacteria and genes spread into the environment: A review. *Science of The Total Environment,* 447**,** 345-360.

RYU, J. H. & BEUCHAT, L. R. 2005. Biofilm formation by Escherichia coli O157:H7 on stainless steel: effect of exopolysaccharide and Curli production on its resistance to chlorine. *Appl Environ Microbiol,* 71**,** 247-54.

SATOH, H., NAKAMURA, Y. & OKABE, S. 2007. Influences of infaunal burrows on the community structure and activity of ammonia-oxidizing bacteria in intertidal sediments. *Applied and Environmental Microbiology,* 73**,** 1341-1348.

SCHMID-HEMPEL, P. & FRANK, S. A. 2007. Pathogenesis, virulence, and infective dose. *PLoS Pathog,* 3**,** 1372-3.

SCHOENBACH, K., KOLB, J., XIAO, S., KATSUKI, S., MINAMITANI, Y. & JOSHI, R. 2008. Electrical breakdown of water in microgaps. *Plasma Sources Science and Technology,* 17**,** 024010.

SCHWARZENBACH, R. P., ESCHER, B. I., FENNER, K., HOFSTETTER, T. B., JOHNSON, C. A., VON GUNTEN, U. & WEHRLI, B. 2006. The challenge of micropollutants in aquatic systems. *Science,* 313**,** 1072-1077.

SCHWERING, M., SONG, J., LOUIE, M., TURNER, R. J. & CERI, H. 2013. Multi-species biofilms defined from drinking water microorganisms provide increased protection against chlorine disinfection. *Biofouling,* 29**,** 917-28.

SHABAN, A., EL-TAWEEL, G. & ALI, G. 1997. UV ability to inactivate microorganisms combined with factors affecting radiation. *Water science and technology,* 35**,** 107-112.

SHAINSKY, N., DOBRYNIN, D., ERCAN, U., JOSHI, S. G., JI, H., BROOKS, A., FRIDMAN, G., CHO, Y., FRIDMAN, A. & FRIEDMAN, G. 2012. Plasma acid: water treated by dielectric barrier discharge. *Plasma processes and Polymers,* 9**,** 1-6.

SHIRAZI, E., TORABIAN, A. & NABI-BIDHENDI, G. 2013. Carbamazepine Removal from Groundwater: Effectiveness of the TiO2/UV, Nanoparticulate Zero-Valent Iron, and Fenton (NZVI/H2O2) Processes. *CLEAN–Soil, Air, Water,* 41**,** 1062-1072.

SIEGRIST, H. & JOSS, A. 2012. Review on the fate of organic micropollutants in wastewater treatment and water reuse with membranes. *Water Science and Technology,* 66**,** 1369-1376.

SMULDERS, E. H., VAN HEESCH, B. E. & VAN PAASEN, S. S. 1998. Pulsed power corona discharges for air pollution control. *IEEE Transactions on Plasma Science,* 26**,** 1476-1484.

STATISTICAL SUBCOMMITTEE OF THE ANALYTICAL METHODS COMMITTEE 2004. The amazing Horwitz function, AMC Technical Brief No. M. Thompson. Royal Society of Chemistry.

SUBEDI, B. & KANNAN, K. 2015. Occurrence and fate of select psychoactive pharmaceuticals and antihypertensives in two wastewater treatment plants in New York State, USA. *Science of the Total Environment,* 514**,** 273-280.

SUN, B., SATO, M. & CLEMENTS, J. 1999. Use of a pulsed high-voltage discharge for removal of organic compounds in aqueous solution. *Journal of Physics D: Applied Physics,* 32**,** 1908.

SUN, B., SATO, M. & CLEMENTS, J. 2000. Oxidative processes occurring when pulsed high voltage discharges degrade phenol in aqueous solution. *Environmental science & technology,* 34**,** 509-513.

SUN, B., SATO, M. & CLEMENTS, J. S. 1997. Optical study of active species produced by a pulsed streamer corona discharge in water. *Journal of Electrostatics,* 39**,** 189-202.

SUNKA, P., BABICKÝ, V., CLUPEK, M., LUKES, P., SIMEK, M., SCHMIDT, J. & CERNAK, M. 1999. Generation of chemically active species by electrical discharges in water. *Plasma Sources Science and Technology,* 8**,** 258.

TADKAEW, N., HAI, F. I., MCDONALD, J. A., KHAN, S. J. & NGHIEM, L. D. 2011. Removal of trace organics by MBR treatment: the role of molecular properties. *Water research,* 45**,** 2439-2451.

TERNES, T. A., MEISENHEIMER, M., MCDOWELL, D., SACHER, F., BRAUCH, H.-J., HAIST-GULDE, B., PREUSS, G., WILME, U. & ZULEI-SEIBERT, N. 2002. Removal of pharmaceuticals during drinking water treatment. *Environmental science & technology,* 36**,** 3855-3863.

TEZUKA, M. & IWASAKI, M. 1997. Oxidative degradation of phenols by contact glow discharge electrolysis. *Denki Kagaku Oyobi Kogyo Butsuri Kagaku,* 65**,** 1057-1060.

TEZUKA, M. & IWASAKI, M. 1999. Liquid-phase reactions induced by gaseous plasma. Decomposition of benzoic acids in aqueous solution. *Plasmas & Ions,* 2**,** 23-26.

VERLICCHI, P., AL AUKIDY, M. & ZAMBELLO, E. 2012. Occurrence of pharmaceutical compounds in urban wastewater: removal, mass load and environmental risk after a secondary treatment—a review. *Science of the total environment,* 429**,** 123-155.

VERLICCHI, P., GALLETTI, A., PETROVIC, M. & BARCELÓ, D. 2010. Hospital effluents as a source of emerging pollutants: An overview of micropollutants and sustainable treatment options. *Journal of Hydrology,* 389**,** 416-428.

VIENO, N., TUHKANEN, T. & KRONBERG, L. 2007. Elimination of pharmaceuticals in sewage treatment plants in Finland. *Water research,* 41**,** 1001-1012.

VOGNA, D., MAROTTA, R., ANDREOZZI, R., NAPOLITANO, A. & D'ISCHIA, M. 2004. Kinetic and chemical assessment of the UV/H2O2 treatment of antiepileptic drug carbamazepine. *Chemosphere,* 54**,** 497-505.

VOM EYSER, C., BÖRGERS, A., RICHARD, J., DOPP, E., JANZEN, N., BESTER, K. & TUERK, J. 2013. Chemical and toxicological evaluation of transformation products during advanced oxidation processes. *Water science and technology,* 68**,** 1976-1983.

VUKUSIC, T., SHI, M., HERCEG, Z., ROGERS, S., ESTIFAEE, P. & THAGARD, S. M. 2016. Liquid-phase electrical discharge plasmas with a silver electrode for inactivation of a pure culture of Escherichia coli in water. *Innovative food science & emerging technologies,* 38**,** 407-413.

WANDA, E. M., NYONI, H., MAMBA, B. B. & MSAGATI, T. A. 2017. Occurrence of Emerging Micropollutants in Water Systems in Gauteng, Mpumalanga, and North West Provinces, South Africa. *Int J Environ Res Public Health,* 14.

WANG, B. 2017. A Novel Dielectric-Barrier-Discharge Loop Reactor for Cyanide Water Treatment. *Plasma Chemistry and Plasma Processing,* 37**,** 1121-1131.

WARDENIER, N., DUMOULIN, A. P. & VAN HULLE, S. P. 2016. Non-equilibrium plasma in contact with water as advanced oxidation process for decomposition of micropollutants. 2016.

WARDENIER, N., VANRAES, P., NIKIFOROV, A., VAN HULLE, S. W. & LEYS, C. 2019. Removal of micropollutants from water in a continuous-flow electrical discharge reactor. *Journal of hazardous materials,* 362**,** 238-245.

WATKINSON, A. J., MICALIZZI, G. B., GRAHAM, G. M., BATES, J. B. & COSTANZO, S. D. 2007. Antibiotic-resistant Escherichia coli in wastewaters, surface waters, and oysters from an urban riverine system. *Appl Environ Microbiol,* 73**,** 5667-70.

WERSCHKUN, B., SOMMER, Y. & BANERJI, S. 2012. Disinfection by-products in ballast water treatment: An evaluation of regulatory data. *Water Research,* 46**,** 4884-4901.

WICK, A., FINK, G., JOSS, A., SIEGRIST, H. & TERNES, T. A. 2009. Fate of beta blockers and psycho-active drugs in conventional wastewater treatment. *Water research,* 43**,** 1060-1074.

WIEGMAN, S., BARRANGUET, C., SPIJKERMAN, E., KRAAK, M. H. S. & ADMIRAAL, W. 2003. The role of ultraviolet-adaptation of a marine diatom in photoenhanced toxicity of acridine. *Environmental Toxicology and Chemistry: An International Journal,* 22**,** 591-598.

WIJEKOON, K. C., HAI, F. I., KANG, J., PRICE, W. E., GUO, W., NGO, H. H. & NGHIEM, L. D. 2013. The fate of pharmaceuticals, steroid hormones, phytoestrogens, UV-filters and pesticides during MBR treatment. *Bioresource technology,* 144**,** 247-254.

WOODWARD, S. 2015. E. coli bacteraemia: an overview. *British Journal of Nursing,* 24**,** 159-160.

WU, H., SUN, P., FENG, H., ZHOU, H., WANG, R., LIANG, Y., LU, J., ZHU, W., ZHANG, J. & FANG, J. 2012. Reactive oxygen species in a non-thermal plasma microjet and water system: generation, conversion, and contributions to bacteria inactivation—an analysis by electron spin resonance spectroscopy. *Plasma Processes and Polymers,* 9**,** 417-424.

XIAO, D., CHENG, C., LAN, Y., NI, G., SHEN, J., MENG, Y. & CHU, P. 2016. Effects of Atmospheric-Pressure Nonthermal Nitrogen and Air Plasma on Bacteria Inactivation. *IEEE Transactions on Plasma Science,* 44.

XIAO, S., HU, S., ZHANG, Y., ZHAO, X. & PAN, W. 2018. Influence of sewage treatment plant effluent discharge into multipurpose river on its water quality: A quantitative health risk assessment of Cryptosporidium and Giardia. *Environ Pollut,* 233**,** 797-805.

YAN, Q., GAO, X., CHEN, Y.-P., PENG, X.-Y., ZHANG, Y.-X., GAN, X.-M., ZI, C.-F. & GUO, J.-S. 2014. Occurrence, fate and ecotoxicological assessment of pharmaceutically active compounds in wastewater and sludge from wastewater treatment plants in Chongqing, the Three Gorges Reservoir Area. *Science of the Total Environment,* 470**,** 618-630.

YANG, S., HAI, F. I., NGHIEM, L. D., PRICE, W. E., RODDICK, F., MOREIRA, M. T. & MAGRAM, S. F. 2013. Understanding the factors controlling the removal of trace organic contaminants by white-rot fungi and their lignin modifying enzymes: a critical review. *Bioresource technology,* 141**,** 97-108.

YEHIA, A. 2016. The electrical characteristics of the dielectric barrier discharges. *Physics of Plasmas,* 23.

YU, Z., PELDSZUS, S. & HUCK, P. M. 2008. Adsorption characteristics of selected pharmaceuticals and an endocrine disrupting compound—Naproxen, carbamazepine and nonylphenol—on activated carbon. *Water research,* 42**,** 2873-2882.

ZENG, F., CAO, S., JIN, W., ZHOU, X., DING, W., TU, R., HAN, S.-F., WANG, C., JIANG, Q. & HUANG, H. 2020. Inactivation of chlorine-resistant bacterial spores in drinking water using UV irradiation, UV/Hydrogen peroxide and UV/Peroxymonosulfate: Efficiency and mechanism. *Journal of Cleaner Production,* 243**,** 118666.

ZHANG, Y., GEIßEN, S.-U. & GAL, C. 2008. Carbamazepine and diclofenac: Removal in wastewater treatment plants and occurrence in water bodies. *Chemosphere,* 73**,** 1151-1161.

ZHAO, Y.-B., LV, X.-D. & NI, H.-G. 2018. Solvent-based separation and recycling of waste plastics: A review. *Chemosphere,* 209**,** 707-720.

ZHONG, X., CUI, C. & YU, S. 2017. Seasonal evaluation of disinfection by-products throughout two full-scale drinking water treatment plants. *Chemosphere,* 179**,** 290-297.

ZHOU, S., XIA, Y., LI, T., YAO, T., SHI, Z., ZHU, S. & GAO, N. 2016. Degradation of carbamazepine by UV/chlorine advanced oxidation process and formation of disinfection by-products. *Environmental Science and Pollution Research,* 23**,** 16448-16455.

ZIMMER, J. L. & SLAWSON, R. M. 2002. Potential repair of Escherichia coli DNA following exposure to UV radiation from both medium- and low-pressure UV sources used in drinking water treatment. *Appl Environ Microbiol,* 68**,** 3293-9.

ZUEHLKE, S., DUENNBIER, U. & HEBERER, T. 2004. Determination of Polar Drug Residues in Sewageand Surface Water Applying LiquidChromatography-Tandem Mass Spectrometry. *Analytical Chemistry,* 76**,** 6548-6554.

ZUMSTEIN, M. T. & HELBLING, D. E. 2019. Biotransformation of antibiotics: Exploring the activity of extracellular and intracellular enzymes derived from wastewater microbial communities. *Water Research,* 155**,** 115-123.

ZYARA, A., TORVINEN, E., VEIJALAINEN, A.-M. & HEINONEN-TANSKI, H. 2016. The Effect of UV and Combined Chlorine/UV Treatment on Coliphages in Drinking Water Disinfection. *Water,* 8.

APPENDICES

APPENDIX A: Calibration data

Appendix A1: CBZ calibration curve for 1 – 50 mg/L

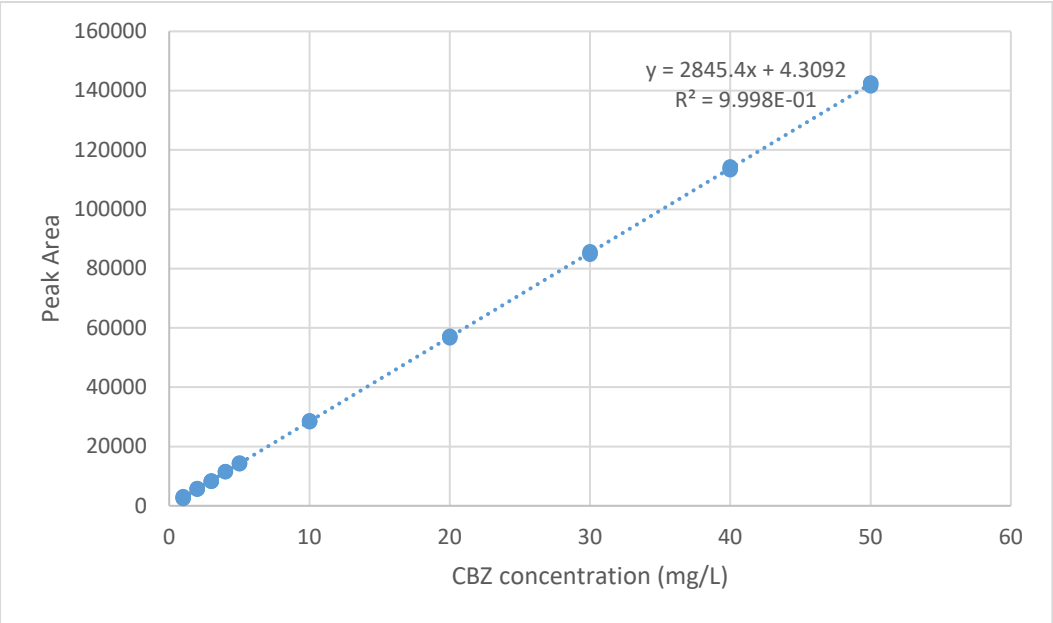

Appendix A2: Calibration residuals

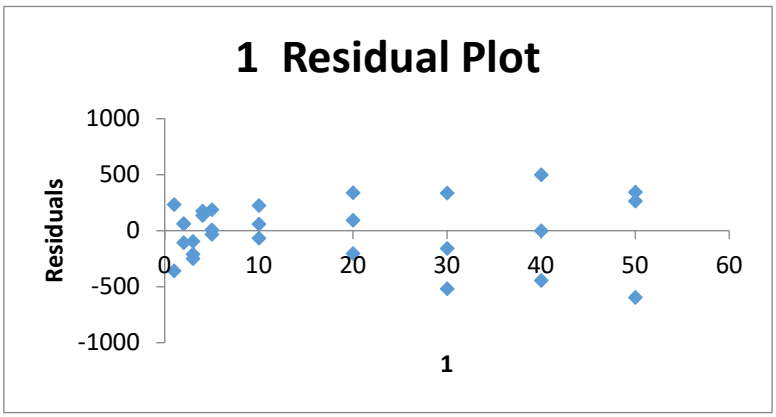

Appendix A3: Sample chromatogram of standards (1 – 30 mg/L) showing stable baseline

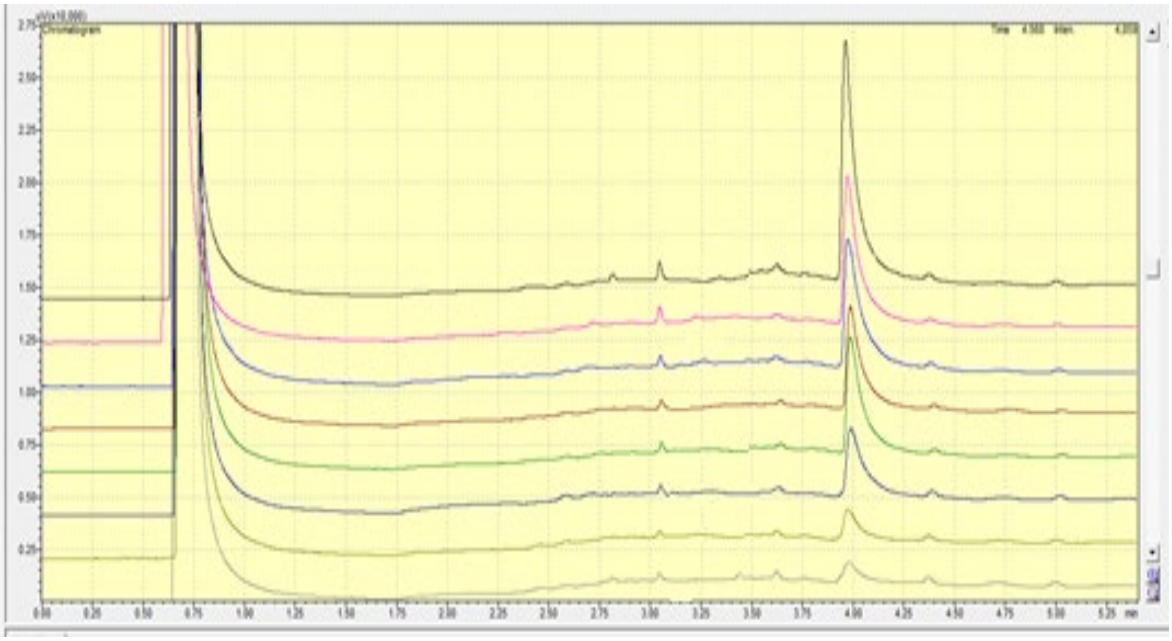

Colour legend (from the bottom up) 1 mg/L, 2 mg/L, 3mg/L, 4mg/L, 5 mg/L, 10 mg/L, 20 mg/L and 30 mg/L. Solvent peak at 0.7 minutes and CBZ peak at 3.9 minutes. (the software can only show 7 chromatograms stacked hence only the 1- 30 mg/L representive chromatograms are shown)

APPENDIX B: Photographs

Appendix B1: Electrode orientation and quartz cathode cover exposing the tip of the cathode

Appendix B2: Quartz tube wear due to continuous plasma discharge

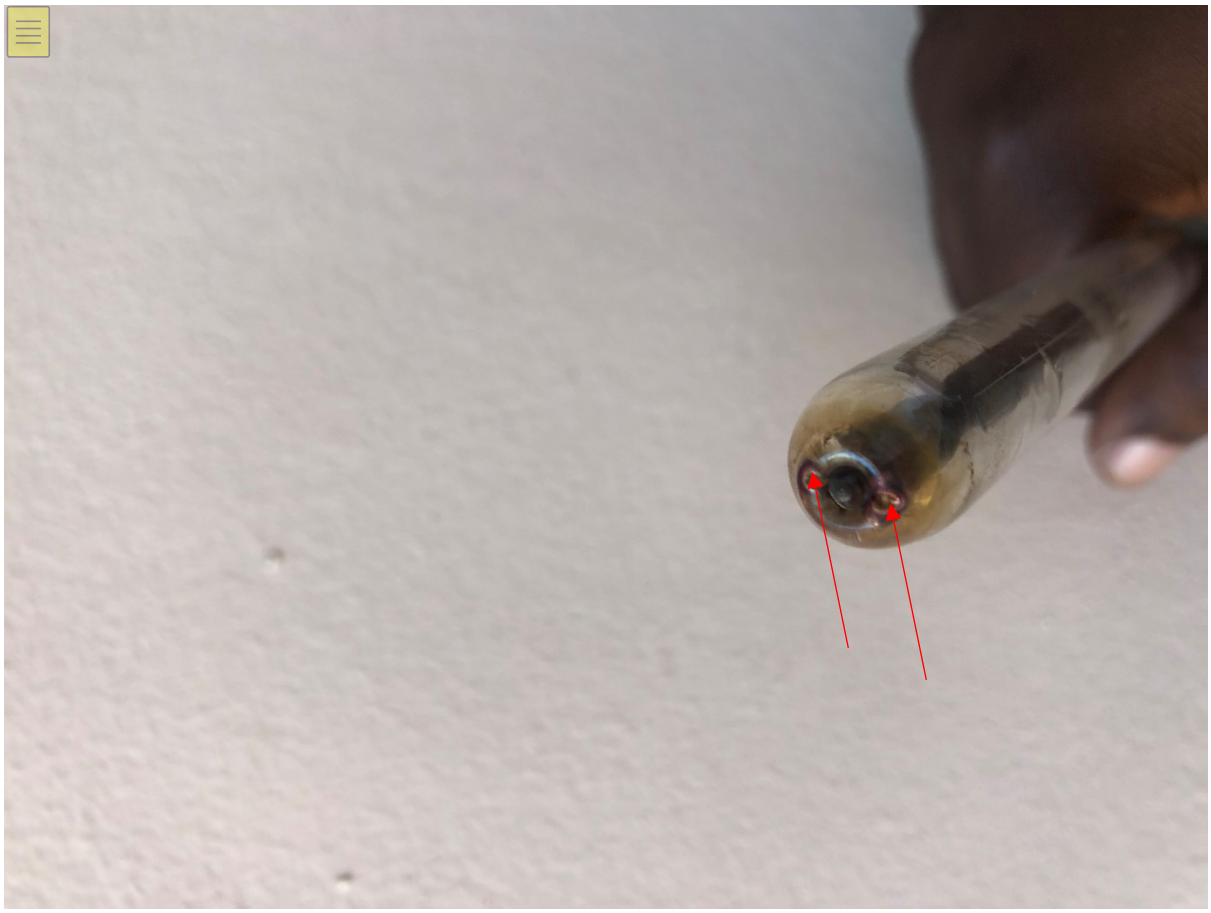

APPENDIX C: CBZ benchmarking cost estimation specifications

Ozone Cost estimation

For CBZ degradation, ozone dosage of 10 mg/L and 3.5 mg/L of 50% hydrogen peroxide re required for 90% degradation (Pisarenko et. Al., 2012)

In developing a baseline ozone costing, the ozone generator electricity cost to liquid oxygen cost ratio of 0.8 as shown by Mundy (2018), this give comparable results to values by Freese, Bailey and Nozaic, 2003 (2009). Liquid oxygen (LOX) is used as air or PSA oxygen sources system require 15% more maintenance and complicate operations (Freese, Bailey and Nozaic, 2003). The production cost of 50% hydrogen peroxide is R13.32/kg, 1 g of Ozone requires 0.016 kWh and LOX cost R 2151.77/ton (Rosenfeldt et al., 2006). The oxygen will be delivered to the ozone generator by a passive system due to pressure build up in the oxygen gas tank. H_2O_2 will be dosed using a 10 W peristaltic pump with adjustable flow rate from 0-160 mL/min, though pumping costs are negligible.

This work Cost estimation

The operating conditions for the reactor was an operating volume of 0.3 L, DC current of 0.25 A, operating voltage of 206 V with no air flow rate. There is no chemical addition, the operational costs are based on the electric energy to generate and sustain the plasma only. Treatment time is 10 minutes to archieve 90% CBZ degradation.

UV Cost Estimation

Generally, CBZ is not susceptible to UV alone, so hydrogen peroxide is added to improve the degradation kinetics. For 90% degradation, UV lamp rated at 0.056 kWh/m3 was used and 6 mg/L of hydrogen peroxide (Sichel et al., 2011; Kruithoff at al., 2005).

APPENDIX D: *E. coli* benchmarking cost estimation specifications

Ozone Cost estimation

For E. coli, ozone dosage of 10 mg/L is assumed (Freese, Bailey and Nozaic, 2003, 2003).

In developing a baseline ozone costing, the ozone generator electricity cost to liquid oxygen cost ratio of 0.8 as shown by Mundy (2018), this give comparable results to values by Freese, Bailey and Nozaic, 2003 (2009). Liquid oxygen (LOX) is used as air or PSA oxygen sources system require 15% more maintenance and complicate operations (Freese, Bailey and Nozaic, 2003). The production cost of 50% hydrogen peroxide is R13.32/kg, 1 g of Ozone requires 0.016 kWh and LOX cost R 2151.77/ton (Rosenfeldt et al., 2006). The oxygen will be delivered to the ozone generator by a passive system due to pressure build up in the oxygen gas tank. H_2O_2 will be dosed using a 10 W peristaltic pump with adjustable flow rate from 0-160 mL/min, though pumping costs are negligible.

This work Cost estimation

The operating conditions for the reactor was an operating volume of 0.3 L, DC current of 0.45 A, operating voltage of 189 V. There is no chemical addition, the operational costs are based on the electric energy to generate and sustain the plasma only. Operation time is assumed to be 30 seconds for the synthetic wastewater. However, note that treatment time can be less than 30 seconds, 30 seconds as it is a reasonable sampling time for batch operations.

Chlorination Cost estimation

Chlorination was based on a dose of 100 % chlorine gas at 5 mg/L (FREESE, BAILEY AND NOZAIC, 2003), The high chlorine dose was in line with a very high E.coli CFU/ml. SO_2 was used for dechlorination, Residual chlorine is assumed at 0.25 mg/L. Dechlorination is based on a 1:1 mass ratio of chlorine to SO_2. The energy cost for the chlorine and SO_2 feed system was based on the ratio of the chlorine cost to the electricity of 0.045 for chlorination at 5 mg/L (Freese, Bailey and Nozaic, 2003).

UV Cost Estimation

For E.coli total inactivation, 0.1 Kwh/m^3 rated lamp was used with no chemical addition. The wastewater is assumed to be clear hence there is maximum delivery of the UV radiation.